Synthesis of Some Piperazine Containing Scaffolds as Potential MAO Inhibitors

Thesis submitted to the Central University of Punjab

For the award of

Master of Pharmacy

in

Medicinal Chemistry

by

Sheetal

Supervisor : Dr. Vinod Kumar

Co-Supervisor : Dr. Anil K. Mantha

Centre for Chemical and Pharmaceutical Sciences

School of Basic and Applied Sciences Central

University of Punjab, Bathinda

DECLARATION

I declare that the thesis entitled “Synthesis of Some Piperazine Containing Scaffolds as Potential MAO Inhibitors” has been prepared by me under the guidance of Dr. Vinod Kumar, Assistant Professor, Centre for Chemical and Pharmaceutical Sciences; and Dr. Anil K. Mantha, Assistant Professor, Centre for Bioscience, School of Basic and Applied Sciences, Central University of Punjab, Bathinda. No part of this thesis has formed the basis for the award of any degree or fellowship previously**.**

(Sheetal)
Centre for Chemical and Pharmaceutical Sciences,
School of Basic and Applied Sciences,
Central University of Punjab,
Bathinda - 151001.

Date:

CERTIFICATE

We certify that Ms. Sheetal has prepared her thesis entitled “Synthesis of Some Piperazine Containing Scaffolds as Potential MAO Inhibitors” for the award of M. Pharm (Medicinal Chemistry) degree of the Central University of Punjab, under our guidance. She has carried out this work at the Centre for Chemical and Pharmaceutical Sciences and Centre for Biosciences, School of Basic and Applied Sciences, Central University of Punjab, Bathinda.

Dr. Vinod Kumar
Supervisor
Assistant Professor
Centre for Chemical and Pharmaceutical Sciences

Dr. Anil. K. Mantha
Co-supervisor
Assistant Professor
Centre for Biosciences

School of Basic and Applied Sciences, Central University of Punjab,
Bathinda - 151001.

Date

ABSTRACT

"Synthesis of Some Piperazine Containing Scaffolds as Potential MAO Inhibitors"

Name of student : Sheetal

Registration Number : CUPB/M.Pharm-MC-/SBAS/CPS/2012-13/07

Degree for which submitted : Master of Pharmacy (Medicinal Chemistry)

Supervisor : Dr. Vinod Kumar

Co-Supervisor : Dr. Anil K. Mantha

Centers : Chemical and Pharmaceutical Sciences

Biosciences

School of Studies : Basic and Applied Sciences

Key words: Piperazine, Docking, MAO-A, MAO-B Neurodegenerative diseases, Parkinson's disease, MAO inhibition assay.

Monoamine oxidase (MAO) is the flavoenzyme which is present on the outer membrane of the mitochondria. The two isoforms of the enzyme are MAO-A and MAO-B that have sequence similarity of 73% but differ in substrate specificity, inhibitor selectivity and tissue distribution and their crystal structure is well explored. MAOs play major role in Parkinson's, Alzheimer's and depression and also involved in other disease states like anxiety, anorexia, bulimia, dysmorphic disorder. Recently *para*-substituted 4-phenylpiperidines and 4-phenylpiperazine have been reported as MAO inhibitors and results suggested that *p*-substituent's with low dipole moment increases affinity to MAO-A, while substituent with high dipole moment have weak MAO-B. We have designed some phenyl piperazine derivatives with the help of molecular docking studies and explored various interactions of the ligands with reported crystal structure of both isoforms of MAO. Docking studies reveals that the proposed compounds shows significant binding interactions with the enzyme. A series of 10 compounds **(VS-1 to 10)** synthesized and evaluated for their MAO inhibitory potency. The results suggested that the synthesized compounds **VS-1** showed 57% to 46% inhibition in total MAO activity as

compared to the control whereas **VS-2, VS-3, VS-4, VS-6** and **VS-10** compounds also displayed inhibitory response. While, **VS-3** was found to be less active with increase in the concentration. The compounds **VS-5, VS-7, VS-8** and **VS-9** displayed constant inhibitory response at all concentrations as compared to the untreated control. It is pertinent to mention that the standard inhibitor used in the experiment i.e. clorgyline (MAO-A) and pargyline (MAO-B) displayed 36% and 52% inhibitory activity respectively. The current synthesis strategy employed here a scope for generation of a library of compounds and their evaluation against selective MAO-A and MAO-B enzyme.

Sheetal **Dr. Vinod Kumar** **Dr. Anil K. Mantha**

ACKNOWLEDGEMENTS

I would like to thank the following people and affiliations that played a role in helping me complete my Master's study:

- Firstly to my **Lord** and Saviour for His grace, guidance and patience
- My supervisor, **Dr. Vinod Pathania** for his support, wisdom and always being there when needed most.
- My co-supervisor, **Dr. Anil K. Mantha** for all his help and guidance in biological studies.
- **Dr. Raj Kumar** and **Dr. Vikas Jaitak** for their support and guidance.
- **Prof. P. Ramarao** for his wisdom and guidance.
- **Prof. R.G Saini** for his guidance and improving our presentation skills by his comments and tips.
- A special thanks to **Ashish (ashi)** and **Vijayinder (khamba)** for helping me throughout my thesis and gave me the possibility to complete this research work. Thank you guys for always being there whenever needed.
- A big thanks to Mr. **Ravi Cholia** for helping me in biological studies.
- My fellow students' (**Gaurav, Anil, Gagan (gaggu), Akanksha** and **Mayank)** support has been continuous fuel during my journey in finishing this thesis program. My deepest thanks to my seniors **(Monika, Ramit, Arvind negi, Jimi, Prakriti, and yashika)** who supported and helped me throughout my work.
- A deepest thanks to **Mr. Rajesh Tiwari, Vishal and Roshan** for helping me and providing me all the Lab facilities.

Life would not have been as colorful without the many good friends, a very special thanks to all my caring, loving, supportive and Special friends **(Shifali, Shiny, Deepika, Rekha, Manpreet, Rajandeep, Hilal, Mudasir,**

Sameer, Raoof) for sharing good times throughout my research work and making me happy.

- Last but not least, I want to thank my loving and caring family (Meenia Family). Thanks to my father Subhash chander and my mother Sandhya Devi for teaching me to be curious and sincere to life, and for always being there for me. **Anamika meenia**, for being such a sweet and uplifting little sister. Words cannot express my appreciation and love for my other brothers and sisters **(Pratima, Abhishek, Pamela, Ranjeet, Pawan, Monika, Seema, Vikas, Sonika,)**.

"I WOULD LIKE TO DEDICATE THIS THESIS TO MY WHOLE FAMILY AND WOULD LIKE TO EXPRESS MY LOVE AND THANKS FOR GIVING ME THE OPPORTUNITY FOR HIGHER STUDIES AND SUPPORTING ME EVEN IN THEIR HARD TIMES. LOVE U ALL."

- **Sheetal**

TABLE OF CONTENTS

LIST OF TABLES

LIST OF FIGURES

LIST OF ABBREVIATIONS

S. No.	Full Form	Abbreviation
1.	Monoamine oxidase	MAO
2.	Flavin Adenine Dinucleotide	FAD
3.	Parkinson's Disease	PD
4.	Alzheimer's Disease	AD
5.	Hydrogen peroxide	H_2O_2
6.	Amyotrophic Lateral Sclerosis	ALS
7.	Tyrosine	TYR
8.	Acetylcholinesterase	AChE
9.	Butyrylcholinesterase	BuChE
10.	Blood Brain Barrier	BBB
11.	Protein Data Bank	PDB
12.	Root Mean Square Deviation	RMSD
13.	Molecular Operating Environment	MOE
14.	Reactive oxygen species	ROS
15.	Dopamine	DA
16.	Nerve Growth Factor	NGF
17.	Glial cell line derived neurotropic factor	GDNF
18.	Brain derived neurotropic factor	BDNF
19.	Glyceraldehydes-3-phosphate dehydrogenase	GADPH
20.	Superoxide dismutase	SOD
21.	B-cell leukemia/lymphoma	BCL
22.	5-Hydroxytryptamine	5-HT
23.	Structure activity relationship	SAR
24.	Dimethyl sulfoxide	DMSO

25.	Fourier transform Infrared spectroscopy	FT-IR
26.	Nuclear magnetic resonance	NMR
27.	Gas chromatography-Mass spectrometry	GC-MS
28.	Thin layer chromatography	TLC
29.	Dimethyl formamide	DMF
30.	Cuprous iodide	CuI
31.	Cesium carbonate	Cs_2CO_3
32.	Dichloromethane	DCM
33.	Round bottom flask	RBF
35.	Dulbecco's modified Eagle's medium	DMEM
36.	(3-[4,5-dimethylthiazol-2-yl]-2,5-diphenyl tetrazolium bromide	MTT
37.	Bovine serum albumin	BSA
38.	Coomassie Brilliant Blue G-50	CBB G-50
39.	Sodium hydride	NaH

CHAPTER 1

INTRODUCTION

1.1 Monoamine oxidase

Monoamine oxidase (MAO) is an enzyme existing in all living cells and bound to the outer membrane of the mitochondria. The enzyme contain a flavin adenine dinucleotide (FAD) cofactor vital for its activity (Youdim *et al.*, 2006). FAD co-factor covalently bind to MAO at cysteine residue by an 8-alpha (s-cysteinyl) riboflavin linkage. MAO acts as a catalytic agent in the oxidative deamination of various monoamines, comprising 5-hydroxytryptamine (serotonin), dopamine, histamine, adrenaline and noradrenaline.

1.2 Pharmacological significance

1.2.1 Substrates and inhibitors similarities and specificities

MAO was not a single enzyme but might exist in at least two forms that had different pH optima and sensitivity to heat inactivation's (Blaschko *et al.*, 1937). MAO exists in two isoforms (Carradori *et al.*, 2013): MAO-A and MAO-B. These two isoforms have sequence similarity of around 73% but vary in their *substrate specificity* and *inhibitor selectivity*. MAO-B deaminates benzylamine and 2-phenylethylamine (aryl/ alkylamines) and is inhibited by (R)-deprenyl whereas MAO-A deaminates 5-hydroxytryptamine (serotonin) and is inhibited by clorgyline (Novaroli *et al.*, 2006). Both isoforms oxidizes tyramine and dopamine as substrates. MAO-A is expressed first but the expression level of MAO-B inside the brain is increased intensely after birth (Nicotra *et al.*, 2004). Although the two isoforms of MAO are preferentially inhibited by different inhibitors, they show similar susceptibility to some inhibitors, such as iproniazid, phenylzine, tranylcypromine and propargylamines. Iproniazid, a common drug to treat tuberculosis patients, was found to produce mood elevation in patients, so this hydrazine derived inhibitor was an initial MAO inhibitor to treat depression (Ganrot *et al.*, 1962).

1.2.2 Tissue distribution

The sources of the enzyme are human placenta (MAO-A and B), blood platelets (MAO-B), bovine liver (MAO-B), and baboon liver (MAO-B) and recently human MAO-B reported from yeast cells (Weyler *et al.*, 1990). MAO enzyme activity is different among various regions of human brain, hypothalamus and basal ganglia show the highest activity while cerebellum and neocortex show the lowest activity (O'Carroll *et al.*,

1983). To identify the distribution of MAO isozymes throughout the brain, radio labeled inhibitors were used and it was found that basal ganglia contains mainly MAO-B (Fowler *et al.*, 1987).

1.3 Reaction mechanism of MAO

In the MAO catalytic reaction, there are two half-reactions: reduction and oxidation, and molecular O_2 assists as the electron acceptor. The amine substrates are first oxidized by the covalent flavin cofactor to produce an imine intermediate in the reductive half-reaction, and flavin cofactor is correspondingly reduced to the hydroquinone. The reduced flavin is then reoxidized by O_2 in oxidative half reaction to form H_2O_2, and H_2O non-enzymatically hydrolyzes the dissociated imine product to aldehyde and NH_4^+ as shown in **Fig.1.1** (Edmondson *et al.*, 1993).

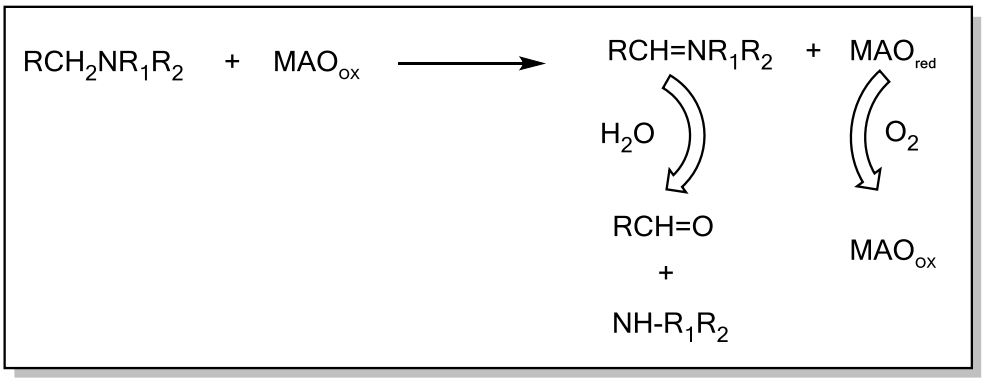

Fig.1.1 General Catalytic Reaction of MAO Enzyme

MAO enzyme catalyzes the oxidative deamination of biogenic monoamines to the corresponding hydrogen peroxides, aldehydes, ammonia and substituted amines that may causes neurodegeneration (Salach & Weyler, 1987). It is reported that the oxidation of the amine occurs when it is in the free base form (Silverman *et al.*, 1980).

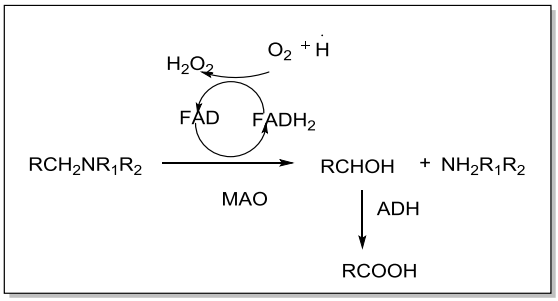

Fig.1.2 Oxidation of monoamine into aldehyde using FAD as Cofactor.

Metabolism of monoamines by MAO is major source of H_2O_2 in the brain in **Fig.1.2**. Normally the H_2O_2 is inactivated by glutathione peroxidase (GPO) but it can be converted chemically by Fe^{2+} ions (Fenton reaction) into highly reactive hydroxyl radical. This radical has widespread deleterious effects which can cause neuronal damage and death. So the inhibition of MAO decreases the formation of H_2O_2 and iron chelation removes the Fe^{2+} ions, both decreasing the formation of hydroxyl radical and the levels of oxidative stress as shown in **Fig.1.3**

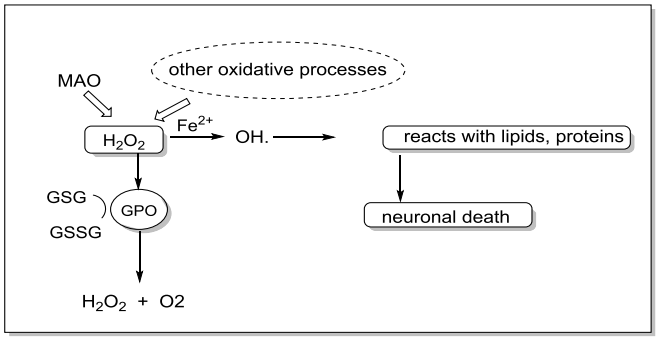

Fig. 1.3 Mechanism of neurotoxicity induced by Fe^{2+}ions due to Fenton reaction

1.4 **Physiological role of MAO enzyme in different disease states**

MAO in peripheral tissues, such as the intestine, liver, lungs and placenta, seems to protect the body by oxidizing amines from the blood or by preventing their entry into the circulation. MAO-B in the micro-vessels of the blood–brain barrier (BBB) apparently has a similar protective function, acting as a metabolic barrier. It has been proposed that in the peripheral nervous system (PNS) and central nervous system (CNS) MAO-A and MAO-B protect neurons from exogenous amines, terminate the actions of amine neurotransmitters and regulate the contents of intracellular amine stores. Noradrenergic neurons contain both MAO-A and MAO-B (O'Carroll *et al*., 1983), and NA is a reasonably good substrate for both forms of the enzyme. MAO regulates concentrations of important neurotransmitters in brain, such as dopamine and serotonin, as well as protects the body by oxidizing xenobiotic and dietary amines in peripheral tissues which could function as false neurotransmitters. A wide range of MAO inhibitors that includes reversible and irreversible inhibitors of MAO-A, MAO-B, or both are now available. These are ascertaining to have therapeutic value in several diverse

conditions, including affective disorders, neurodegenerative diseases, stroke and ageing. The therapeutic use of MAO inhibitors in these conditions is discussed below in **Fig. 1.4** -

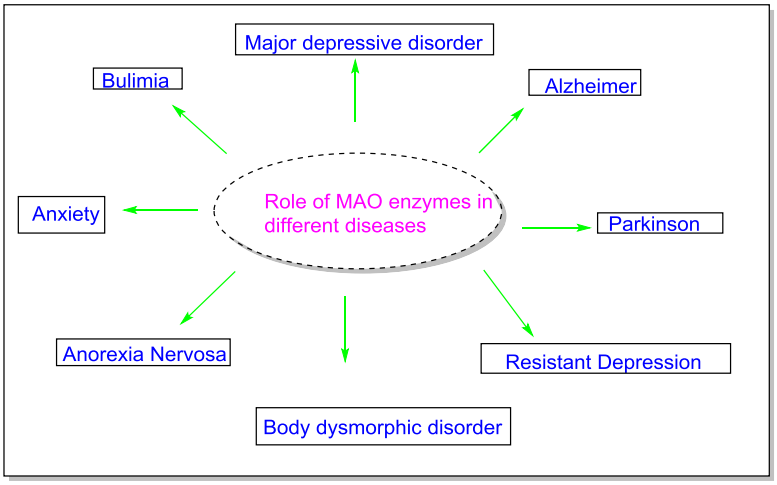

Fig. 1.4 Role of MAO enzyme in different disease states

1.4.1 MAO enzyme in depression

MAO inhibitors showed antidepressant properties by selectively inhibit MAO-A enzyme which leads to increased brain levels of dopamine, noradrenaline and 5-HT. Some of the non-selective irreversible inhibitors including phenelzine and tranylcypromine, are still in clinical use along with the reversible MAO inhibitors moclobemide, befloxatone and toloxatone. The reversible MAO-A inhibitors have been reported to be particularly effective in the treatment of depression in elderly patients (Da Prada *et al.*, 1987). MAO-A and non-selective MAO inhibitors seem to be particularly valuable in the treatment of phobic anxiety and atypical depressions, such as those involving hysterical traits, hypersomnia, bulimia, tiredness and impression of rejection, for which they are superior to amine-uptake inhibitors (Stahl & Felker, 2008). Interestingly, phenelzine has been shown to increase corticosterone levels associated with hypothalamic–pituitary–adrenocortical axis activity (Kier *et al.*, 2005), which is hypoactive in atypical depression, but hyperactive in major depressive conditions. MAO-B inhibitors are devoid of antidepressant activity and do not promote the cheese reaction unless administered at concentrations high enough to inhibit MAO-A.

1.4.2 MAO enzyme in alzheimer's disease

Alzheimer's disease (AD) is measured as extreme loss in memory and intellectual ability convoyed by behavioral disturbances & declining ability to perform basic activities of daily life (Zhang, 2005). Depressive symptoms occur in patients with AD and these may be associated with decrease in serotonergic and noradrenergic transmission in the limbic system (Cummings *et al.*, 1995; Garcia-Alloza *et al.*, 2005). Although the cause of progressive neuronal degeneration in AD is not known but there are evidences like: presence of oxidative stress mediated by increased levels of iron, breakdown of peroxynitrite and nitration of tyrosine residues in the cell membrane proteins has been reported (Christen, 2000) and MAO-B activity also increases in association with gliosis which can result in higher levels of H_2O_2 and oxidative free radicals (Markesbery, 1997; Sterling *et al.*, 2002). MAO is another target to be considered for the treatment of AD as it catalyzes the oxidative deamination of variety of biogenic and xenobiotic amines with the production of H_2O_2. MAO inhibitor deprenyl is an anti-Parkinson drug used to inhibit dopamine degradation in the brain. Also as a neuroprotective agent, deprenyl has been used to slow the progress of neurodegenerative diseases such as AD for many years. It is reported that the major depressive symptoms by a lack of noradrenaline and serotonin. MAO inhibitors increase the intracellular concentration of endogenous amines by inhibiting their deamination, which seems to be the cause of their antidepressant action (Stahl & Felker, 2008).

1.4.3 MAO enzyme in parkinson's disease

Both MAO-A and MAO-B are the major enzymes that catalyze the oxidative deamination of monoamine neurotransmitters such as dopamine (DA), noradrenaline, and serotonin in the central and peripheral nervous systems. MAO-B is mainly localized in glial cells. MAO B also oxidizes the xenobiotic 1-methyl-4-phenyl- 1, 2, 3,6-tetrahydropyridine (MPTP) to a parkinsonism-producing neurotoxin, 1-methyl-4-phenyl-pyridinium (MPP+). MAO-B may be closely related to the pathogenesis of PD, in which neuromelanin containing DA neurons in the substantia nigra projecting to the striatum in the brain selectively degenerate. MAO-B degrades the neurotransmitter DA that is

deficient in the nigro-striatal region in PD, and forms $H_2O_2$and toxic aldehyde metabolites of DA. H_2O_2 produces highly toxic reactive oxygen species (ROS) by Fenton reaction that is catalyzed by iron and neuromelanin. MAO-B inhibitors such as L-(−)-deprenyl (selegiline) and rasagiline are effective for the treatment of PD. Concerning the mechanism of the clinical efficacy of MAO-B inhibitors in PD, the inhibition of DA degradation (a symptomatic effect) and also the prevention of the formation of neurotoxic DA metabolites, i.e., ROS and dopamine derived aldehydes have been speculated. As another mechanism of clinical efficacy, MAO-B inhibitors such as selegiline are speculated to have neuroprotective effects to prevent progress of PD. The possible mechanism of neuroprotection of MAO B inhibitors may be related not only to MAO B inhibition but also to induction and activation of multiple factors for anti-oxidative stress and anti-apoptosis: i.e., catalase, superoxide dismutase (SOD) 1 and 2, thioredoxin, Bcl-2, the cellular poly(ADP-ribosyl)ation, and binding to glyceraldehydes-3-phosphate dehydrogenase (GAPDH). Furthermore, it should be noted that selegiline increases production of neurotrophins such as nerve growth factor (NGF), brain-derived neurotropic factor (BDNF), and glial cell line-derived neurotropic factor (GDNF), possibly from glial cells, to protect neurons from inflammatory process. PD is one of the common neurological disorders in that elevated level of MAO-B is found (Fowler *et. al.*1980). This disease may be associated with the effect of MAO-B activity by increasing the levels of toxic H_2O_2 and by bio activating exogenous or endogenous neurotoxins which lead to degradation of dopamine-producing neurons. PD occurs as a result of affected basal ganglia region where MAO-B isoform seems to be significantly responsible for the metabolism of dopamine, therefore inhibitors of MAO-B have been used in the therapy of PD (Thokozile *et al.*, 2012). In PD therapy, MAO-B inhibitors are frequently combined with levodopa, the metabolic precursor of dopamine. The inhibition of the MAO-B catalyzed oxidation of dopamine in the brain may elevate the levels of dopamine derived from levodopa and may allow for a reduction of the levodopa dose required for a therapeutic effect. In addition MAOs act as major source of H_2O_2 in cells which may causes oxidative stress and promote the neurodegenerative processes associated with PD (Manley-King *et al.*, 2011).

1.4.4 Other neurodegenerative diseases.

Neurodegenerative diseases such as Huntington's disease and amyotrophic lateral sclerosis (ALS) shows similar pathological features of PD and AD, such as oxidative stress, iron accumulation, excitotoxicity, inflammatory processes and the toxic proteins that cannot be degraded after ubiquitination. l-Deprenyl treatment has not been successful in the treatment of ALS (Lange *et al.*, 1998). However, rasagiline and CGP 3466 have been reported to be effective in mouse models of ALS (Kragten *et al.*, 1998; Waibel *et al.*, 2004). A single-patient study has reported beneficial effects of l-deprenyl, in combination with the 5-HT reuptake inhibitor fluoxetine, in Huntington's disease.

1.4.5 Cerebral ischaemia

l-Deprenyl declines the peripheral tissue damage that results from cardiac failure (Qin *et al.*, 2003), and that arising in the brain from cerebral ischaemia in animal models (Simon *et al.*, 2001). This protective effect has been credited to a decrease in H_2O_2generated by MAO during ischaemia-reperfusion, together with an increased ratio of B-cell leukaemia/lymphoma 2 (BCL2) to BCL2-associated protein X (BAX) it is reported that phase 2 clinical trials confirmed that the recovery after cerebral infarction enhances by selegiline [l-deprenyl] (Youdim *et al.*, 2006).

1.5 X-ray crystal structure of MAO-A and MAO-B

Mammalian MAOs are bound to outer mitochondrial membrane and have a FAD molecule covalently bound to protein via an 8α-thioether linkage to a cysteinyl residue. The two isoforms MAO-A and MAO-B share a high sequence identity (~70%) but different in their substrate specificities. MAO B mainly acts on small exogenous amines, whereas MAO-A carries out the degradation of bulkier endogenous amine neurotransmitters, such as serotonin.

1.5.1 Structure of hMAO-A

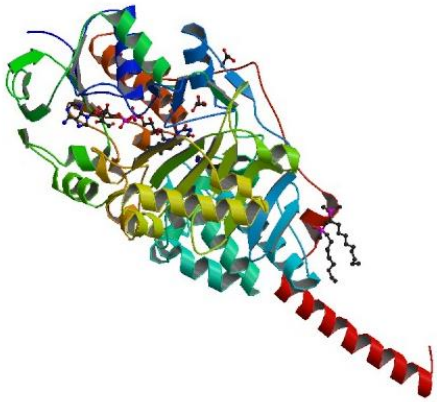

Fig. 1.5 Crystal structure of human MAO-A with harmine. PDB ID (2Z5X) (Son *et al.*, 2008)

Crystal structure of human MAO–A shown in **Fig. 1.5**, Human MAO-A contains 527 amino acid residues and it consists of a single cavity that extends from flavin ring to cavity-shaping loop consisting of residues 210-216.The volume of this cavity is predicted to be ~ 550$Å^3$ which is shorter in length and wider and is lined by 11 aliphatic and 5 aromatic residues which reveal that this cavity is quite hydrophobic.

1.5.2 Structure of human MAO-B

MAO-B consists of 520 amino acids. The crystal structure of MAO-B **(Fig. 1.6)** shows that the enzyme is a dimer and each monomer consists of a globular structure (residues 1-488) .The protein contains substrate-binding domain and FAD binding domain. The enzyme is attached to the outer mitochondrial membrane through its C-terminal amino acids (residues 461-520).The volume of MAO-B cavity as ~ 700 $Å^3$.Moreover, the MAO-B cavity was found to be bipartite containing two separate spaces -the substrate cavity (~400 $Å^3$) & the entrance cavity (~300 $Å^3$) (Milczek *et al.*, 2011). The position of FAD-cofactor with respect to the overall structure is highly conserved and the substrate binding sites consist of elongated cavities (Son *et al.*, 2008). Separating the “entrance cavity” from

the similarly hydrophobic “substrate cavity” (volume = 400 $Å^3$) is an isoleucine199 (Ile-199) side chain which serves as a “gate” between the two cavities.

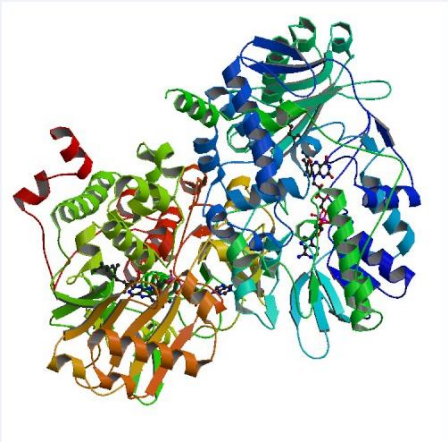

Fig.1.6 A ribbon crystal structure of MAO (dimeric) with Farnesol PDB (2BK3) (Hubalek *et al.*, 2005)

The two cavities are hydrophobic involving two nearly parallel tyrosyl (398 and 435) residues which forms an “aromatic cage (Edmonson et al., 2007). Substrate cavity and entrance cavity are separated by four amino acid side chains which are Tyr-326, Ile-199, Leu-171 and Phe-168. The hydrophilic section is near the flavin and is essential for recognition and directionality of the substrate amine functionality. This hydrophilic region is located between Tyr-398 and Tyr-435 which together with the flavin, form an aromatic cage for amine recognition. Structural data analysis of MAO-B enzyme has revealed that FAD coenzyme is situated in a solvent-inaccessible hydrophobic environment and forms several hydrogen bonds and peptide bonds with the enzyme (Edmondson *et al.*, 2004). Only one electrostatic interaction is present between FAD and MAO-B shows an electrostatic interaction between positively charge guanidine group of Arg42 and negatively charged pyrophosphate of the FAD, and mutation of Arg42 into alanine resulted in an enzyme that is incapable of incorporating FAD; thus data suggest that this electrostatic interaction is essential for FAD incorporation into MAO-B enzyme (Kirksey *et al.*, 1998). The ribose ring of the FAD adenosine moiety is bound to the carboxylate group of Glu34, to a H_2O molecule and to the guanidino group of Arg36 through hydrogen bonds, and mutation of Glu34 into Ala, Glu or Asp resulted in more than 90% loss in enzymatic

activity of MAO-B (Edmondson *et al.*, 2004). These data demonstrate that hydrogen bond between carboxyl group of Glu-34 and ribose ring of the FAD is essential for FAD binding to MAO-B.

1.5.3 Structural comparisons of hMAO-A with hMAO-B

As discussed above human MAO-A exhibits 72% sequence identity with human MAO-B. Both human MAO-A and human MAO-B are bound to the outer mitochondrial membrane as dimer. The substrate binding site in human MAO -B is smaller than that of human MAO-A and this can explain the greater affinity of human MAO-A to the bulkier monoamines such as 5-hydroxytryptamine. Aromatic cage in the human MAO-A is identical to that of human MAO-B. The conserved structure of aromatic cage in both isozymes of human MAO supports the concept that the principal role of aromatic cage is in the process of amine oxidation rather than determining substrate specificity. shows the three dimensional structure of human MAO-A (De Colibus *et al.*, 2005).The difference in the structure of active site of human MAO-A as compared with human MAO-B is due to change in 7 out of the 20 amino acids residues that line the active site in human MAO and also due to change in cavity shaping loop 210-216 .The most important amino acids replacements in human MAO-A are: Phenyalanine-208 (Isoleucine-199 in human MAO-B) and Isoleucine-335 (Tyrosine-326 in human MAO-B) shown in **Fig. 1.7**. These amino acids replacements have an important role in determining the substrate/inhibitor specifity of MAO-A and MAO-B.

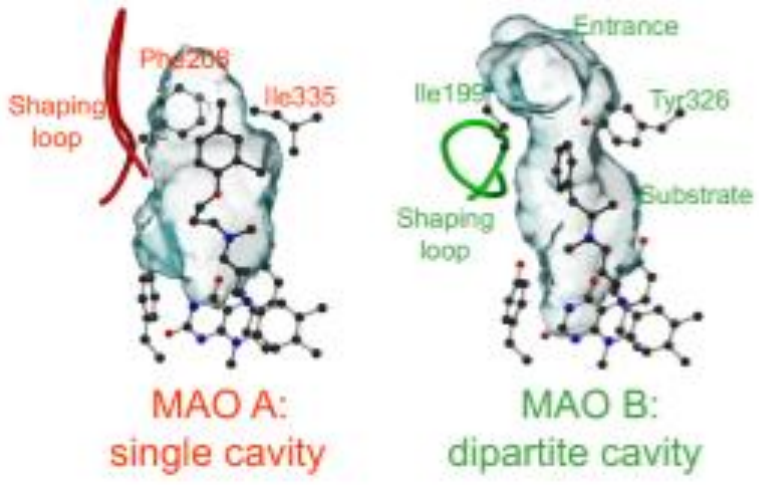

Fig. 1.7 Active site mutations and cavities of MAO-A and MAO-B (Son *et. al.,* 2008)

1.4 Monoamine oxidase inhibitors

MAO inhibitors were the first drugs indicated for treatment of depression. Though, they were used extensively from the 1950's and followed for the next two decades but their use declined because of the reported side effects in addition to their significant food and drug interactions i.e. Cheese effect. Various MAO Inhibitors are shown in **Fig. 1.8**

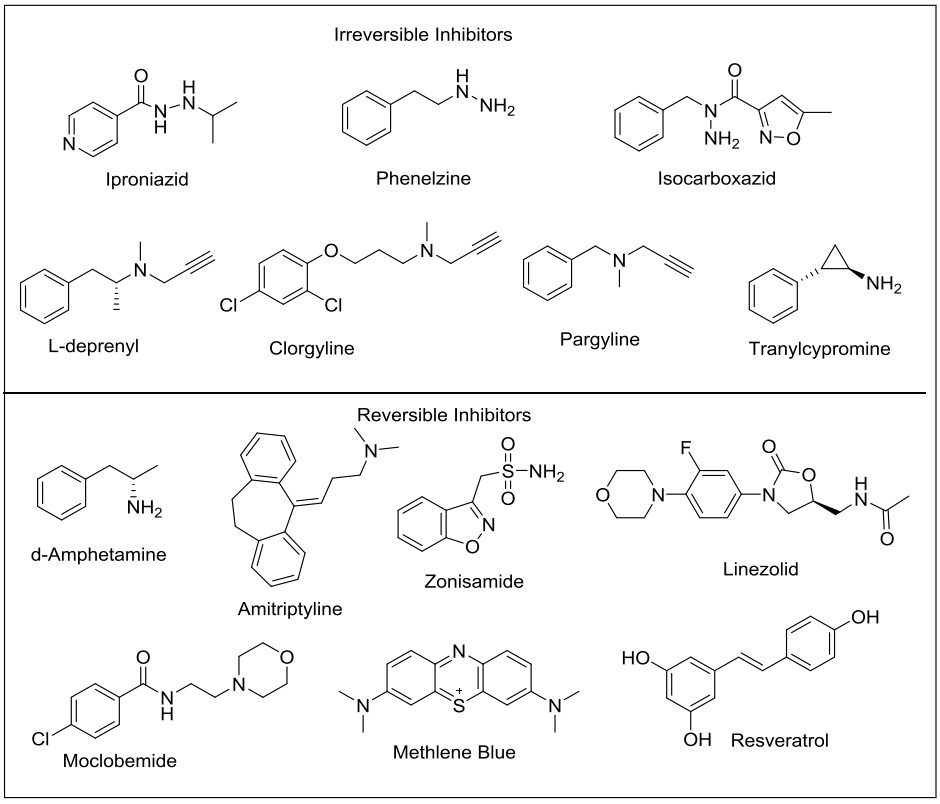

Fig.1.8 MAO Inhibitors(Ramsay, 2012).

CHAPTER-2

REVIEW OF LITERATURE

2.1 Problems associated with MAO inhibitors

Isoniazid and Iproniazid was withdrawn from the market due to the high incidence of hepatitis whereas isocarboxazid was found to be less toxic. The biggest disadvantage of the MAO inhibitors was their interaction with tyramine containing foods, like old cheese and wine, as a consequence of inhibition of the iso-enzyme MAO-B (Leonetti *et al.*, 2007). Tyramine was not only found to be involved with depression but also with blood pressure (Rao & Yeragani, 2009). Normally, the MAO enzyme also wipes tyramine out of the body, but in presence of MAO inhibitor, MAO is blocked from monitoring tyramine levels as well as levels of the neurotransmitters associated with depression (Blackwell & Mabbitt, 1965). Excess amount of tyramine causes increase in blood pressure resulting in hypertension. It has been seen that a dramatic rise in the tyramine level resulted possibly in a fatal spike in blood pressure, termed as hypertensive crisis(Tripathi, 2003).In order to address various issues related to the irreversible inhibitors, a number of MAO-A inhibitors (e.g. moclobemide) were developed (Da Prada *et al.*, 1987).The main advantage was the conspicuous absence of the 'cheese-effect' (Ramsay, 2013).

Table 2.1 MAO inhibitors under clinical trials

MAO inhibitor	Selectivity	Binding	Applications
Phenelzine	MAO-A/ MAO-B	Irreversible, covalent.	Antidepressant and anxiolytic
Tranylcypromine	MAO-A/ MAO-B	Irreversible, covalent.	Antidepressant and anxiolytic
Selegiline	MAO-B	Irreversible, covalent.	Antiparkinsonian
Rasagaline	MAO-B	Irreversible, covalent.	Antiparkinsonian
Lazabemide	MAO-B	Reversible, covalent.	Development as antiparkinsonian was discontinued due to toxicity issues
Safinamide	MAO-B	Reversible,	Currently undergo

		non-covalent.	phaseIIIclinical trials asantiparkinsonian
Zonisamide	MAO-B	Reversible, non-covalent.	Antiepileptic and it is approved in Japan as antiparkinsonian

(Shubbar, 2013)

The recent developments in the designing and synthesis of MAO inhibitors are given below:

2.2 Pyrazoline derivatives as MAO inhibitors

In 3,5-Diaryl pyrazolines compounds the 4-hydroxy substitution in ring A escalates the potency towards MAO-A at the same time reducing the cytotoxicity, substitution of thiophen-2-yl/furan-2-yl group as ring B and various substituents in phenyl group of ring C and explored their MAO-A inhibitory potency. The substitution of five membered hetero aromatic groups on ring B resulted in enhanced potency with substitution on ring C an essential factor for the selectivity towards MAO-A as in compounds (**1), (2)** and (**3)**as shown in **Fig. 2.1** (Karuppasamy *et al.*, 2010)**.** The N-substituted-3-[(2'-hydroxy-4'-prenyloxy)-phenyl]-5-phenyl-4,5-dihydro-(1H)-pyrazolines were synthesized **(4)** and **(5)**. The compounds exhibited significant inhibitory activity selectively towards MAO-B The compounds having benzyloxy group in the para position at C5 and those bearing chlorine substitution at the same position were essential for the greater potency(Fioravanti *et al.*, 2010)**.** Novel 3,5-diaryl pyrazolines were synthesized and evaluated as selective inhibitor of either one of the isoform. the compound **(6)** was found to be selective inhibitor of MAO-B while **(7)** portrayed MAO-A inhibitory property (Sahoo *et al.*, 2010). A series of ethyl and phenyl carbamate derivatives of pyrazolineand screened them for their MAO inhibitory activity. Structure activity relationship (SAR) studies suggested that the phenyl carbamate derivatives were more potent than ethyl carbamates with greater selectivity index. The compound **(8)** was found out to be the most potent inhibitor with best selectivity index. Molecular docking studies of individual enantiomer (R&S) of the lead compound indicates that the S-enantiomer is better than R-enantiomer.

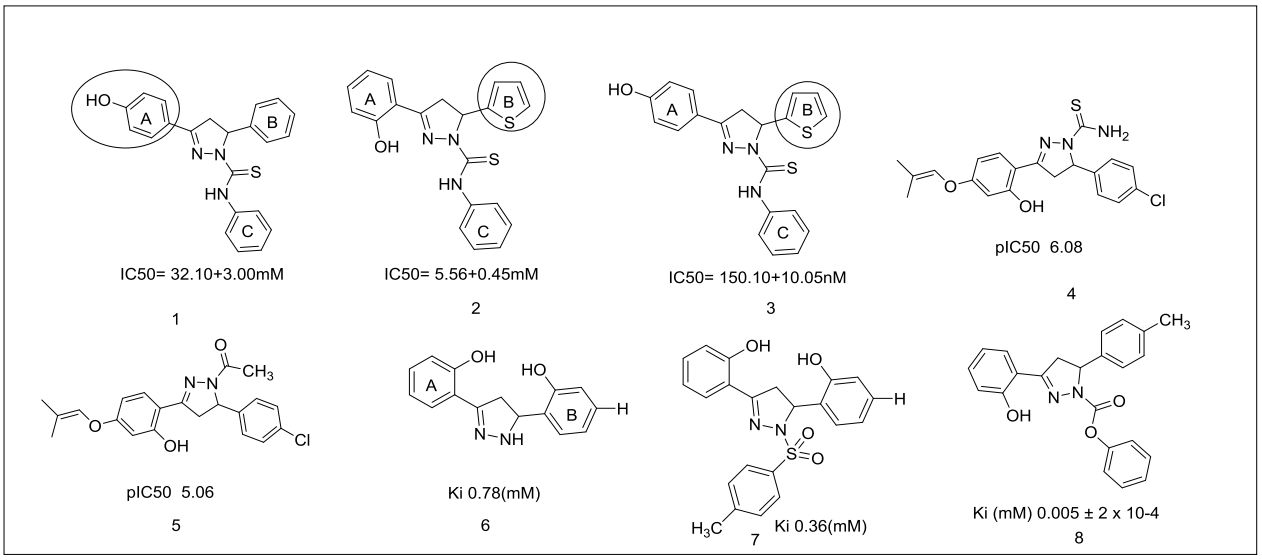

Fig. 2.1 Pyrazoline derivatives as MAO inhibitors

2.3 Coumarin derivatives

The bromo-6-methyl-3-phenylcoumarin derivatives were synthesized and the SAR studies suggested that the substitution of halogen in the coumarin moiety improved the inhibitory activity of MAO-B and substitution of bromo atom at 8th position of 3-phenyl coumarin **(9)** (shown in **Fig. 2.2**) improved the activity. The substitution of p-methoxy group in the phenyl ring improved the activity (Matos *et al.*, 2010). The compounds showed significant inhibitory activity towards hMAO-B. SAR studies revealed that the number and position of methoxy groups on the (1H)-benzopyran structure is crucial for the activity especially methoxy group at position 7 of benzopyran ring **(10)** & **(11)** increased the MAO-B inhibitory activity (Delogu *et al.*, 2011)**.** The 7‑Oxycoumarin designed, synthesized and performed molecular simulations on the series of 4-methyl and 3,4-dimethyl-7-oxycoumarin derivatives including oxadiazoles, thiadiazoles, triazoles, and thiazolidinones. They manifested their high affinity and selectivity toward MAO-A isoenzyme, compared to clorgyline and Moclobemide through *in vitro* investigations. In particular, the acetohydrazide derivative (**12)** (Ki (MAO-A) = 5.01 pM, and SI = 9.66 × 10 ^{4}) and the diethylaminoethylthio-1,3,4-thiadiazole compound (**13)** Ki(MAO-A) = 5.18 pM, and SI = 9.58×10^{4}) are exceptionally the most potent and selective MAO-A inhibitors (Abdelhafez *et al.*, 2012). Abdelhafez et al. in 2013 have

synthesized a series of 7-oxycoumarin derivatives and evaluated for their MAO-A and MAO-B inhibitory activities. The *in vitro* studies indicated that all the synthesized compounds were potent and selective MAO–A inhibitors. The *in vivo* results revealed that most of the compounds were more active than iproniazid. The most potent inhibitors reported in vitro and in vivo studies were 2-(3,4-dimethylcoumarin-7-yloxy)acetohydrazide **(14)** with in vitro Ki values (5.01 pM for MAO-A and 0.484 µM for MAO-B) and in vivo ED_{50} = 0.009143 µM and 2-(3,4-dimethylcoumarin-7-yloxy)-N-(2,5-dioxopyrrolidin-1-yl)acetamide **(15)** with in vitro Ki values (6.34 pM for MAO-A and 0.575 µM for MAO-B) and *in vivo* ED_{50} = 0.00915 µM. The molecular docking studies indicated direct correlation between binding affinities and percentage inhibition of MAO-A and MAO-B (Abdelhafez *et al.*, 2013). A series of new 3-aryl coumarins derivatives was synthesized by introducing hydroxyl group in the position 4 of ring B of coumarin skeleton. The synthesized compounds were evaluated for their potency towards inhibition of MAO-B. SAR studies revealed that the substitution of methoxy and chloro groups in the *para* and *meta* position of the 3-phenyl ring were crucial for inhibitory activities. Iproniazid was used as a reference and it was found that the compound with chloro substituent at the six position (**16)** was most potent in the series with better inhibitory activity and selectivity against MAO-B isoform (Serra *et al.*, 2012)**.**

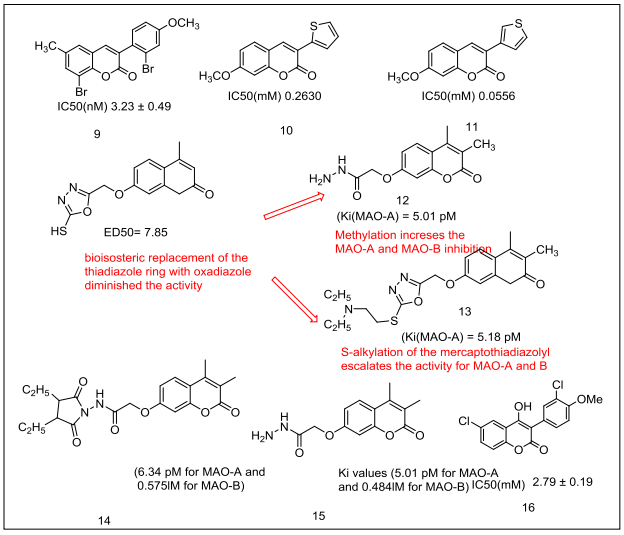

Fig. 2.2 Coumarin derivatives as MAO inhibitor

2.4 Chromone derivatives:

Chromone moiety plays a vital role in various medicinal and biological activities such as anti-inflammatory, antitumor and antimicrobial. The MAO inhibitory activity of chromone moiety were evaluated by Alcaro *et.al.* Wherein two chromone isomers were screened for their affinity towards MAO-A and MAO-B. The results suggested that the substitution of acidic group in position 3 of the heterocyclic scaffold significantly increased the inhibitory activity towards MAO-B whereas acid moiety at position 2 shows no inhibition. Thus, the chromone-3-carboxylic acid **(17)** (shown in **Fig. 2.3**) was found to be the most potent and selective MAO-B inhibitor. Molecular docking studies reveals that the hydrogen donor moiety should be placed in position 3 of the pyrone ring for favorable energy and selectivity towards MAO-B isoform (Alcaro *et al.*, 2010). Legoabe and group synthesized a series of chromone derivatives substituted at C-6 position with alkyloxy substituents and evaluated the resulting compounds as inhibitors of recombinant human MAO-A & B. It was reported that the C6-substituted chromones were potent reversible MAO-B inhibitors with IC_{50} values in sub nM range. The chromones were also found to bind reversibly to MAO-A, but with less affinities compared to MAO-B and hence it was concluded that the synthesized compounds were MAO-B selective inhibitors. The docking study of the lead compound **(18)** was performed for the analysis of potential binding orientation with MAO-A & B isoenzymes. The lead compound exhibited differing interactions and orientation within the two enzymes. Thus the C-6 substituted chromone derivatives possessed potency against MAO-B isoform and can be used as promising lead for the development of therapy against Parkinson's disease (Legoabe *et al.*, 2012a)**.** Same research group further carried out the modification at C-7 position of the chromone resulting in the synthesis of series of C-7 substituted chromone (1-benzopyran-4-one) derivatives. The synthesized compounds were evaluated for their potential to inhibit recombinant human MAO-A &B and were found to have IC_{50} values ranging from 0.008 to 0.370 μM. These compounds also displayed affinities for MAO-A with IC_{50} values ranging from 0.495 to 8.03 μM. Structure activity relationship studies suggested that 7-benzyloxy substitution of chromone is crucial for MAO-B inhibition and concluded that 7-benzyloxychromones **(19)** are appropriate lead compounds for the design of reversible and selective MAO-B inhibitors (Legoabe *et al.*, 2012b).

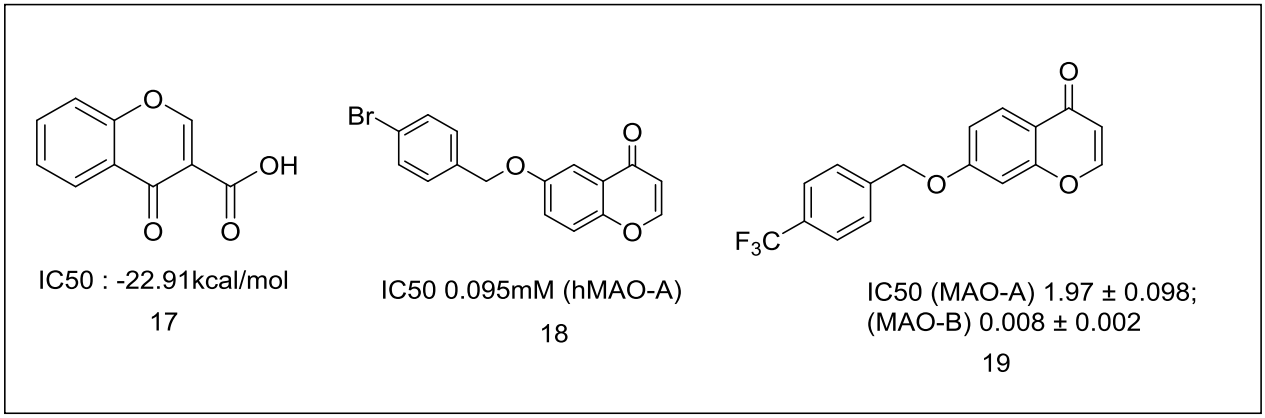

Fig. 2.3 Chromone derivatives as MAO inhibitors

Secci and co-workers recently established and evaluated a series of arylidene-(4-substituted-thiazol-2-yl) hydrazines as selective MAO-B inhibitors. They demonstrated that smaller heterocyclic moieties on the N1-hydrazine is essential for selective MAO-B inhibitory activity whereas substituent on the-carbon to the N1-hydrazine moiety was also indispensable for activity. Further a methyl group instead of a hydrogen in this position showed an escalated hMAO-B inhibition. 4-fluorophenyl substituted C-4 has been found to be most active and selective derivatives (**20)** (shown in **Fig. 2.4**), and progressively decreased for 2,4-difluorophenyl and 4-nitrophenyl derivatives. The substitution of aromatic ring has been linked to the FAD coenzyme via interaction with the structural “aromatic cage” of hMAOs (Secci *et al.*, 2012). Distinto and research group reported synthesis and biological evaluation of halogenated derivatives of a series of 1-arylidene-2-(4-phenylthiazol-2-yl)hydrazines. In this series of compounds, the effect of 4-chloro- or 4-fluoro-phenyl substituents in the position four of the thiazole ring was explored. It was concluded that the fluorine as a substituent played pivotal role both in activity and selectivity of ligands towards MAO-B isoform. In addition, to understand the possible binding mode and rationalizing the activity, docking simulations of the synthesized compounds were also performed. In the computational studies it was observed that fluorine substituent interacted with the water molecule close to cofactor and the understanding about these interactions with arylidene moiety further helped in designing ligand with more selectivity for MAO-B isoform. The 4-fluorophenyl derivative **(21)**, and the homologous 4-chlorophenyl **(22)**, were reported as most potent MAO-B inhibitors in the series (Distinto *et al.*, 2012). Park and group designed and synthesized

the oxazolopyridine and thiazolopyridine derivatives and evaluated these against MAO-B. Initially a series of 2-phenyloxazolopyridine derivatives was synthesized with various amino substituents and compounds were tested against hMAO-B isoform. The structure–activity relationship studies showed that the piperidino group at R_1 position was essential for the activity. In addition phenyl ring was also substituted with halogen group which improved the inhibitory activity of the ligands. It was concluded that by replacing the basic structure from oxazolopyridine to thiazolopyridine, the activities were dramatically improved and the compound **(23)** was found to be most potent in the series displaying IC_{50} value of 26.5 nM (Park *et al.,* 2013). Carradori and team designed hydrazothiazoles derivatives by combining the hydrazine moiety of iproniazid and the thiazole nucleus of glitazones. The compounds were screened for their affinity towards MAO isoforms and it was found that all the compounds displayed selective hMAO-B inhibitory activity. The SAR studies suggested that the presence of the less hindered substituent at C4 (ethyl ester) was essential for inhibitory activity and lead compounds obtained in the series (**24)** & (**25)** were found to be even more selective towards MAO-B than the reference drugs iproniazid and isatin. It was concluded that the hydrathiazole scaffold could be explored for the treatment of neurodegenerative diseases (Carradori *et al.*, 2013). D'Ascenzio and group synthesised a series of 4-aryl-2-cycloalkylidenhydrazinylthiazoles and studied the stereochemical property essential for the MAO inhibitory activity. The results showed that the 2- and 3-methylcyclohexylidene derivatives showed good inhibitory activity ,high selectivity towards MAO-B and biological assay studies specified that the compound **(26)** is the most active and selective MAO-B inhibitor (D'Ascenzio *et al.*, 2014).

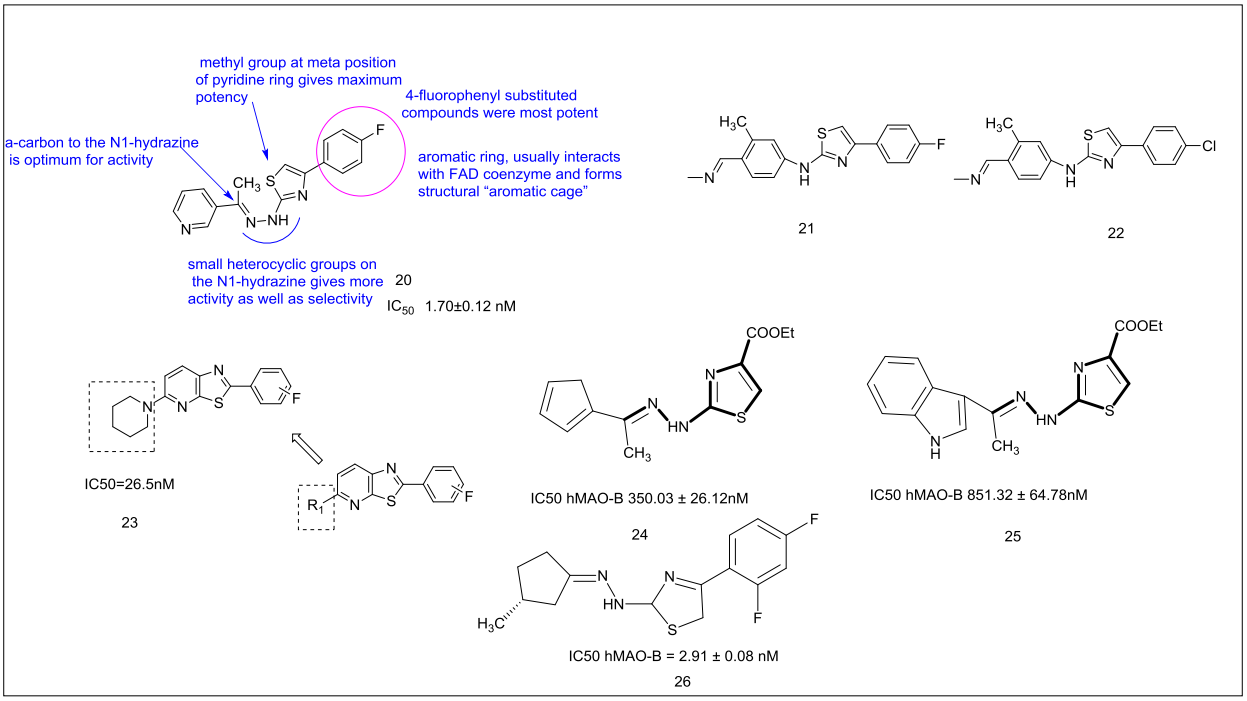

Fig. 2.4 Hydrazine derivatives as MAO inhibitors

2.5 Hybrid molecules as MAO inhibitors:

Samadiet.al. reported synthesis, pharmacological evaluation andmolecular modeling studies of two different series of compounds which simultaneously inhibit MAO as well as acetylcholinesterase (AChE) and butyrylcholinesterase (BuChE). Series I compounds were prepared from reaction of 2,6-dichloro-4-phenylpyridine-3,5-dicarbonitrile or 2,6-dichloropyridine-3,5-dicarbonitrile with prop-2-yn-1-amine and 2-(1-benzylpiperidin-4-yl)alkylamines. Similarly, series II compounds were prepared by reaction of 6-amino-5-formyl-2-(methyl(prop-2-yn-1-yl)amino)nicotinonitriles with 4-(1-benzylpiperidin-4-yl)butan-2-one. The screening of compounds help in the identification of lead compounds that act as multipotent drugs showing strong and selective AChE inhibitory activity (IC_{50} =37±4 nM)], and moderate, but selective MAO-A inhibitory profile (IC_{50} =41±7 μM). Molecular modeling investigation confirmed its dual AChE inhibitory profile, binding simultaneously at the catalytic active site and at the peripheric anionic site. The lead compound **(27)** as shown in **(Fig. 2.5)** was reported as a potent and selective dual AChEI, showing a moderate and selective MAO-A inhibitory profile, could be considered as an attractive multipotent drug for further development on two key

pharmacological targets playing key roles in the therapy of Alzheimer's disease (Samadi *et al.*, 2011)**.**The same research group reported synthesis, pharmacological evaluation and molecular modeling studies of heterocyclic substituted alkyl and cycloalkylpropargyl amine. These compounds were designed as multipotent inhibitors which were able to simultaneously inhibit monoamine oxidases (MAO-A & MAO-B) as well as cholinesterase (AChE/BuChE). The lead compound obtained in the series I, an indole derivative **(28)** has been reported as a multipotent compound being able to selectively inhibit MAO-B (IC_{50} =31 nM) and eqBuChE (IC_{50} =7 μM). The molecular docking studies indicated that the high MAO-B inhibitory activity of the lead compound **(29)** may be ascribed to the position of the methylpropargyl group, which is closer to N5 of FAD in MAO-B than in MAO-A. Similarly the series II compounds, i.e. 5-amino-7-(prop-2-yn-1-yl)-6,7,8,9-tetrahydropyrido[2,3-b][1,6]naphthyridine derivatives were reported as poor MAO inhibitors, but showed selective AChE inhibition activity. It was concluded that N-[(5-(benzyloxy)-1H-indol-2-yl)methyl]-N-methylbut-2-yn-1-amine (**29)** showed a multipotent pharmacological profile on BuChE and MAO-B, and it was proposed to be the starting point for the design of new and more efficient multipotent cholinesterase and MAO inhibitors for the treatment of AD(Samadi *et al.*, 2012).Boleaand group synthesized a series of new compounds using hybrid approach by combining the benzylpiperidine moiety of the AChE inhibitor donepezil and the indolylpropargylamino moiety of the MAO inhibitor N-[(5-benzyloxy-1-methyl-1H-indol-2-yl)methyl]-N-methylprop-2-yn-1-amine, connected through an oligomethylene linker. The molecular docking studies and kinetic studies have been performed and the results displayed that the most promising hybrid was found to be the inhibitor of both MAO-A and MAO-B isoforms that also exhibited potency towards AChE and BuChE. These enzymes play major role in neurodegenerative diseases and were proposed as a promising lead for the treatment of AD (Bolea *et al.*, 2011)**.**Lu and Co-workers synthesized and evaluated a series of tacrine-selegiline hybrids as multi-functional anti-AD agents with cholinesterase and MAO inhibition activities. They reported that the synthesized compounds have high inhibitory affinity for MAO-A &B. From their study on all the compounds they found that the compound **(30)** have good activity towards all targets (with IC_{50} values of 22.6 nM, 9.37 nM, 0.3724mM, and 0.1810mM for AChE, BuChE,

MAO-A and MAO-B, respectively). Their study revealed that the hybrids could improve patient cognition by increasing levels of acetylcholine and protect neurons by possessing the activities of Selegiline. Thus should be considered as “one compound multitarget drug targets” for the treatment of AD (Lu *et al.*, 2013).

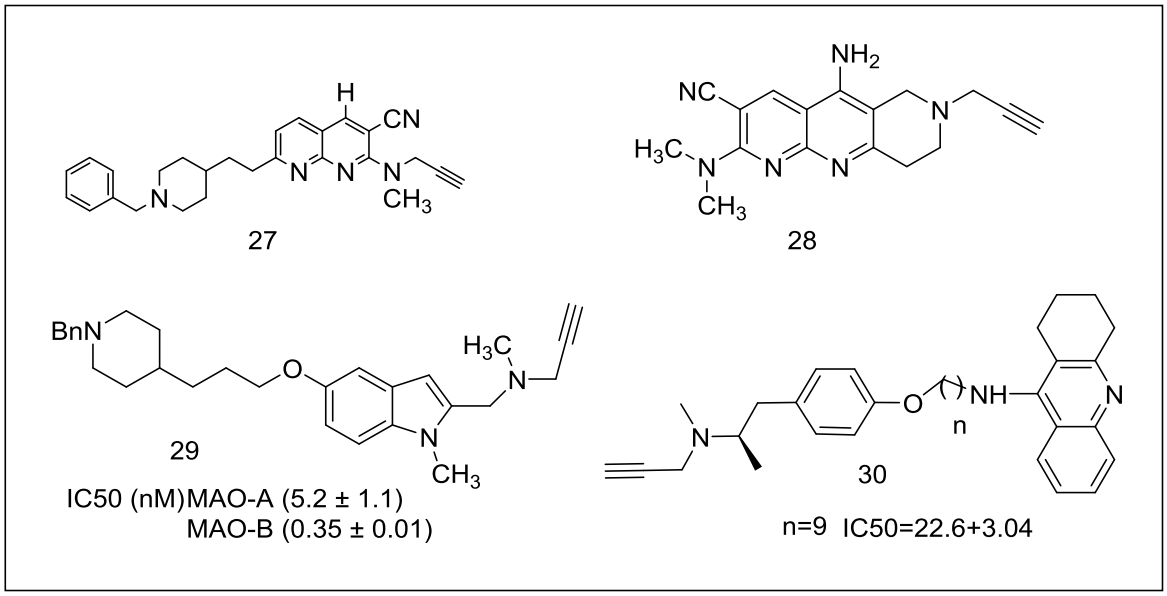

Fig. 2.5 Hybrid molecules as MAO inhibitors

Desideri and team reported a series of homoisoflavonoids [(E)-3-benzylidenechroman-4-ones, 3-benzyl-4H-chromen-4-ones, and 3-benzylchroman-4-ones and screened the synthesized compounds for their MAO inhibitory activity. It was found that the (E)-3-benzylidenechroman-4-ones derivatives exhibited higher selectivity and activity in nanomolar range towards hMAO-B isoform. The compounds (E)-3-(4-(Dimethylamino) benzylidene) chroman-4-one **(31)** and (E)-5,7-dihydroxy-3-(4-hydroxybenzylidene)chroman-4-one **(32)** were found to be most potent MAO-B inhibitor in the series and were found even more potent than the selegiline. The compounds were proposed as a good drug candidate for PD shown in **Fig.2.6** (Desideri *et al.*, 2011) .

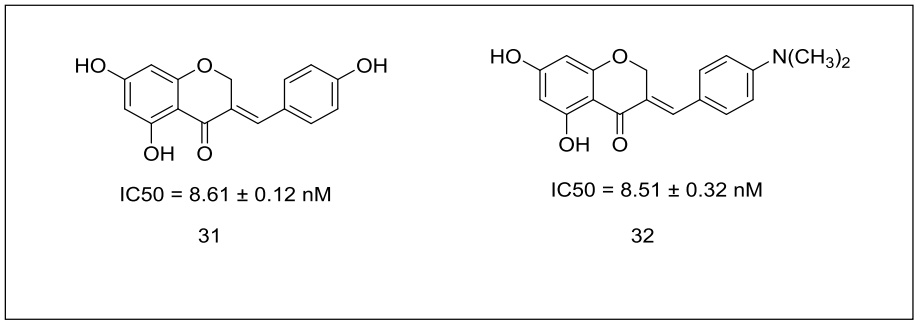

Fig. 2.6 Chroman analogues as MAO inhibitors

Prins and group synthesized a series of **indole and benzofuran derivatives (Fig. 2.7)**and evaluated their MAO inhibitory activity. The compounds were found to show significant MAO-B inhibitory activity. SAR studies suggested that the chlorine substitution at the C5 phenyl side chain of the indoles and benzofuranes improved both MAO-A and -B inhibition potencies. Molecular modelling studies demonstrated that the compound **(33)** is stabilized in active site of MAO B and showed hydrogen bonding with Tyr-435 and the waters in the vicinity of the FAD co-factor and found to be most potent MAO-B inhibitor. It was concluded that the indole and benzofuranes derivatives were selective inhibitor of MAO-B and could be used as promising therapeutic agent for treatment of PD (Prins *et al.*, 2010).

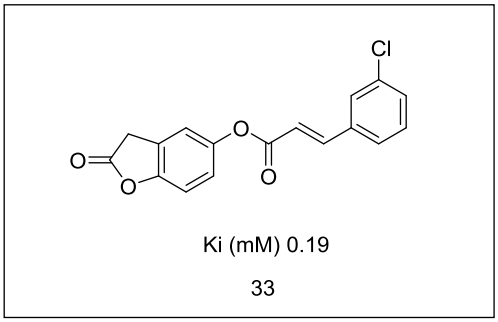

Fig. 2.7 Benzofuran derivative as MAO inhibitors

Legoabe and team synthesized a series of **anilide** derivatives to determine a lead for the design of reveals a potential MAO inhibitors. Amongst various synthesized compounds, the N,3-diphenylpropenamides were found to be promising MAO-B inhibitors. Different phenolic and bezonitrile derivatives were designed and the molecular docking studies were performed which suggested that the homologues

containing phenolic hydroxyl functional groups on the para position of the C-3 phenyl ring increases the potency of (2E)-N-(3-chlorophenyl)-3-phenylprop-2-enamide and (2E)-N-(3-bromophenyl)-3-phenylprop-2-enamide (2d) towards MAO-B and also that contains nitrile functional group on the meta position of C-3 ring exhibited more potency than the (2E)-N- (3-chlorophenyl)-3-phenylprop-2-enamide and (2E)-N-(3-bromophenyl)-3-phenylprop-2-enamide**.**The lead compounds obtained in the series (2E)-N- (3-chlorophenyl)-3-phenylprop-2-enamide (**34)** and (2E)-N-(3-bromophenyl)-3-phenylprop-2-enamide (**35)** were found to be most potent, reversible and selective MAO-B inhibitors. The SAR studies suggested that the substitution of chlorine and bromine at C-3 of phenyl ring of the anilide moiety improved the binding affinity with the active site of MAO-B enzyme. It was concluded that the N,3-diphenylpropenamides was suitable scaffold for the design of potent MAO-B inhibitors (Legoabe *et al.*, 2011).

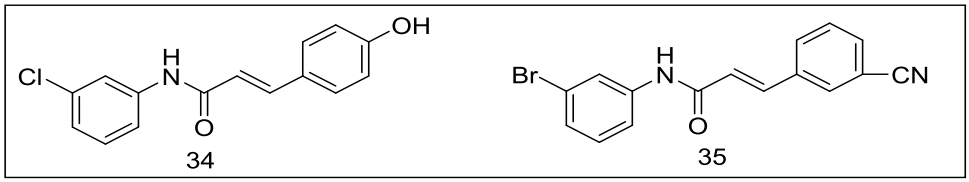

Fig. 2.8 Diphenylpropenamides as MAO inhibitors

Legoabe et al. synthesized a series of fifteen **α-tetralone (3,4-dihydro-2H-naphthalen-1-one)** derivatives as shown in fig. 2.14 and calculated their MAO inhibitory activity. 6-(3-iodobenzyloxy)-3,4-dihydro-2H-naphthalen-1-one was found to be the most potent MAO-B inhibitor **(36)**while 6-(3-cyanobenzyloxy)-3,4-dihydro-2H-naphthalen-1-one**(37)** exhibits greater potency and selectivity towards MAO-A. The SAR studies showed that the substitution at C-6 position is essential for MAO inhibitory activity. It was observed that benzyloxy substitution increases the MAO-A inhibitory activity and an alkyl and halogen substitution at the meta and para position of benzyloxy, increases the MAO-B inhibitory activity. It was proposed that these compounds could be used as a lead for the treatment of PD and depression (Legoabe *et al.*, `2014).

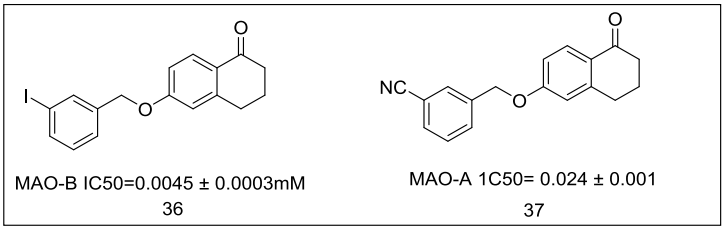

Fig. 2.9 α-tetralone derivatives as MAO inhibitors

Song and co-workers synthesized a series of 8-substituted **benzamido-phenylxanthine derivatives** and screened them *in vitro* for their potential as potent MAO-B inhibitors. Most of the compounds displayed promising activities and it was found that the *para*-substituted derivatives **(38 & 39)** shown in **Fig. 2.10** were more potent than the *meta*-substituted derivatives possibly due to steric interaction of the substituents at the binding pocket. It was concluded that caffeine scaffold may be favorable for designing potent MAO-B inhibitors and the compounds with smaller groups holds more potency as MAO-B inhibitors (Song *et al.*, 2012).

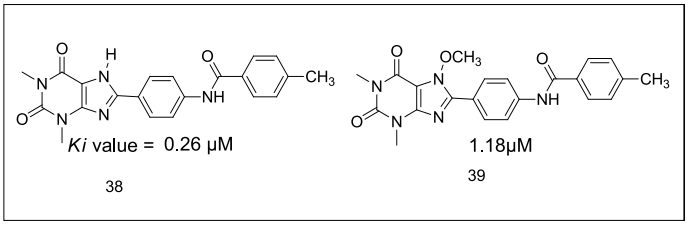

Fig. 2.10 Benzamido-phenylxanthine derivatives as MAO inhibitors

Al-Baghdadi and team designed and synthesized a series of **piperine and antiepilepsirine** derivatives and screened the synthesized compounds in MAO-A & B assays. The compounds tested were found to be selective for MAO-B and the most potent compound **(40)** shown in **Fig. 2.11** in the series displayed an IC_{50} of 498 nM. The BBB permeability of the compounds was confirmed through PAMPA assays. It was noticed through SAR studies that presence of nitrogen atom in the ring reduces MAO-B inhibition. In addition docking studies of the synthesized compounds were performed to understand various binding interaction of ligands with the receptor site. The lead compound **(40)** was found to dock in a similar orientation to MAO-B as the parent compound piperine (Al-Baghdadi *et al.*, 2012).

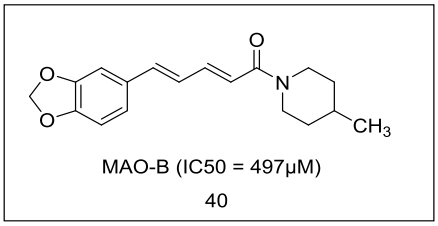

Fig. 2.11 Piperine derivatives as MAO inhibitors

Van der Walt et al. synthesized a series of **5-sulphanylpthalimide** analogues and screened these compounds for their affinity towards both human MAO isoforms. It was proposed that the phthalimide moiety could be used as important scaffold for the synthesis of MAO-B inhibitors. Most of the synthesized compounds exhibited MAO-B inhibitory activity with IC_{50} values in the nanomolar range. In the series of reported compounds 5-(benzylsulfanyl) phthalimide **(41)** shown in **Fig. 2.12**, with an IC_{50} value of 4.5 nM was found to be most potent MAO-B inhibitor with a 427-fold selectivity for MAO-B compared to MAO-A. It was proposed that the lead compound obtained with selectivity towards MAO-B could developed as drug candidate for the treatment of parkinsonian disease (Van der Walt *et al.*, 2012).

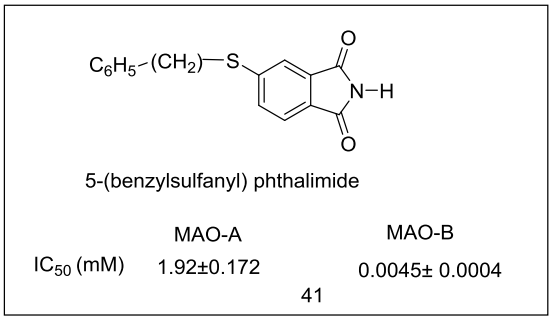

Fig. 2.12 Sulphanylpthalimide derivatives as MAO inhibitors

Geldenhuys and team have synthesized **thiazolidinedione** (TZD) analogues and ligand based virtual screening was performed so that the scaffold hopping from this compound would provide additional insight into the SAR of previously discovered compounds. The lead compound **(42)** in **Fig. 2.13** obtained in the series was found to be potent inhibitor of both MAO-A (IC_{50}= 268 nM) and MAO-B (IC_{50}= 99 nM) and literature search has highlighted this compound to be a derivative of the naturally occurring bioactive

flavonoid, sulfuretin which possesses protective activity against mitochondrial toxins in a Parkinson's disease model. The SAR, furthermore, revealed that the tertiary dimethylamine group in the *para* position of the phenyl ring and ortho hydroxyl group reduced the inhibitory activity of the compound from 99 nM **(42)** to 11.55 Nm **(43)** (Geldenhuys *et al.*, 2012).

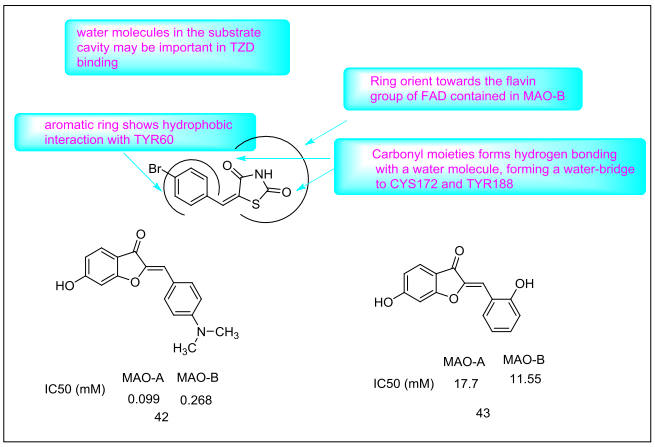

Fig. 2.13 Thiazolidinedione derivatives as MAO inhibitors

Okaecwe and team investigated the MAO inhibitory potential of series of **8-phenoxymethylcaffeine and 8-[(phenylsulfanyl)methyl]caffeine derivatives.** It was reported that that the 8-phenoxymethylcaffeine derivatives acted as potent reversible inhibitors of MAO-B, with IC_{50} values ranging from 0.148 to 5.78μM. However, the 8-[(phenylsulfanyl)methyl]caffeine derivatives were found to be weak inhibitors of MAO-B, with IC_{50} values ranging from 4.05 to 124μM.In addition both the series of compounds displayed low binding affinities for MAO-A. It was observed that when a heteroatom was introduced into the C-8 side chain of caffeine derived structures, substitution directly on C-8 of the caffeine ring led to the most potent MAO-B inhibitor **(44)** in **Fig. 2.14**. It was concluded that 8-phenoxymethylcaffeines might act as useful leads for the design of MAO-B selective inhibitors and such compounds might find applications in the therapy of neurodegenerative disorders such as PD (Okaecwe & Dorcas, 2012).

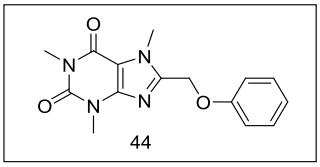

Fig. 2.14 Caffeine derivatives as MAO inhibitors

Chaurasiya and group treated **5-phenoxy** analogs with MAO and evaluated their potency towards the enzyme inhibition. The results showed that the analogs displayed better inhibitory activity towards both isoforms when compared with standard drug primaquine and the compound 5-(4-Trifluoromethylphenoxy)-4-methylprimaquine **(45) in Fig. 2.15** was found to be most active with selectivity towards MAO-B. Though concluded that these aminoquinolines can be used as a lead for designing and synthesizing new MAO inhibitors (Chaurasiya *et al.*, 2012).

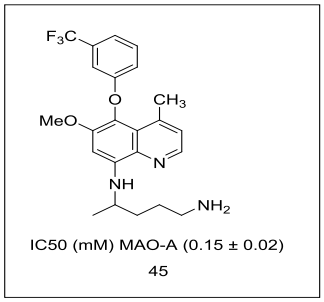

Fig. 2.15 Phenoxy analogues as MAO inhibitors

Strydom and group designed a series of C-6 substituted **phthalide analogues** ie. phthalide [2-benzofuran-1(3H)-one] derivatives and studied their inhibitory activity against MAO isoforms. All the phthalide derivatives showed high binding affinities to both human MAO isoforms however C-6 substituted phthalide exhibited MAO-B specific inhibition. A number of para-phenyl substituted derivatives of 6-benzyloxyphthalide were screened and the general order of potency (CF_3> I > Br > Cl > F > CH_3> H) was observed. The most potent MAO-B inhibitor obtained in the series was (**46)** in **Fig. 2.16**,

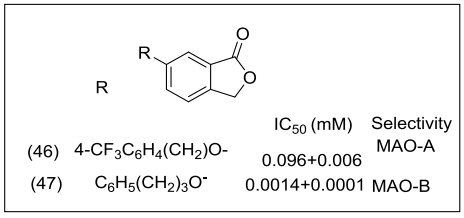

Fig. 2.16 Phthalide analogues as MAO inhibitors

the CF_3 substituted benzyloxyphthalide homologue, with an IC_{50} value of 1.4 nM while compound (**47)** was most potent MAO-A inhibitor. It was also concluded that the synthesized phthalides were reversible and competitive inhibitors at both MAO isoforms and were suitable lead compounds for the development of novel therapies for PD (Strydom *et al.*, 2013).

Meiring and colleagues synthesized a series of **3,4-dihydro-2(1H)-quinolinone** derivatives and explored them for their human MAO-A & B inhibitory activity. These compounds were structurally related to coumarin (1-benzopyran-2-one) derivatives which were potent MAO-B inhibitors. The proposed compounds showed highly potent and selective MAO-B inhibitory activity. The compound 7-(3-bromobenzyloxy)-3,4-dihydro-2(1H)-quinolinone **(48)** in **Fig.2.17** was found to be the most potent MAO-B inhibitor. SAR studies suggested that C-7 position of 3, 4-dihydro-2(1H)-quinolinone was significantly important for the MAO-B inhibitory activity than C-6 position and the benzyloxy group at C-7 position was more important for the inhibition than phenylethoxy and phenylpropoxy substitution. Thus concluded that the C-7subsituted 3,4-dihydro-2(1H)-quinolinone derivatives could be used as a promising lead for the treatment of Parkinson's disease (Meiring *et al.*, 2013).

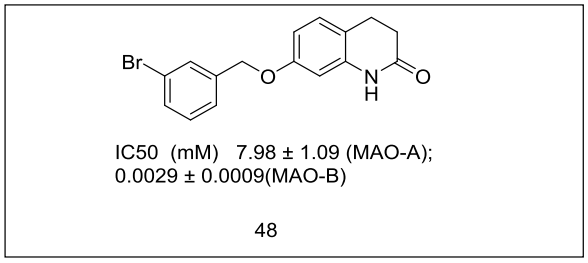

IC50 (mM) 7.98 ± 1.09 (MAO-A); 0.0029 ± 0.0009(MAO-B)

48

Fig. 2.17 Quinolinone derivatives as MAO inhibitors

Desideri and team reported a series of (2E,4E)-1-(2-hydroxyphenyl)-5-phenylpenta-2,4-dien-1-ones and (2Z,4E)-3-hydroxy-1-(2-hydroxyphenyl)-5-phenylpenta-2,4-dien-1-ones compounds and evaluated *in vitro* as inhibitors of the two hMAO isoforms, MAO-A and MAO-B. Most of the synthesized compounds were found to be selective towards MAO-B isoform with activity in low micro molar or nano molar range. The lead compounds (2E, 4E)-5-(4-Chlorophenyl)-1-(2-hydroxy-4-methoxy phenyl) penta-2,4-dien-1-one and (2E,4E)-5-(4-chlorophenyl)-1-(2,4-dihydroxyphenyl) penta-2,4-dien-1-one were found to

be most potent hMAO-B inhibitors exhibiting IC_{50} of 4.51 nM and 11.35 nM, respectively with high selectivity. The inhibitory potencies were examined by measuring their effects on the production of H_2O_2 from p-tyramine by using the Amplex Red MAO assay kit and microsomal MAO isoforms prepared from insect cells (BTI-TN-5B1-4) infected with recombinant baculovirus containing cDNA inserts for hMAO-A or hMAO-B. Structure activity relationship studies revealed that the replacement of the methoxyl group in the potent hMAO-B inhibitor (**49)** with the hydroxyl group in the same position resulted in compound (**50)** in **Fig. 2.18** capable to inhibit both hMAO isoforms**.** The compound**(50)** was reported as most potent with activity in the nanomolar range and excellent selectivity (IC_{50}=11.35 nM, SI=1354) (Desideri *et al.*, 2012).

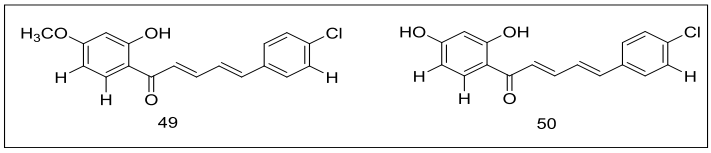

Fig. 2.18 Penta-2,4-dien-1-one derivatives as MAO inhibitors

Passos and team isolated 13 psychotria alkaloids from the ethanolic extract of *P. laciniata* and molecular docking studies was carried out to evaluate their interactions with MAO A and B enzymes. The monoterpene indole alkaloid angustine (**51)** was found to be the reversible and competitive inhibitor. In addition it was found that all the screened compound inhibited AChE, BChE and MAO-A enzyme and thus concluded that these secondary metabolites are the multifunctional compounds **(52)** in **Fig. 2.19** and can be used as a lead for the treatment for various neurodegeneration diseases. (Passos *et al.*, 2013)

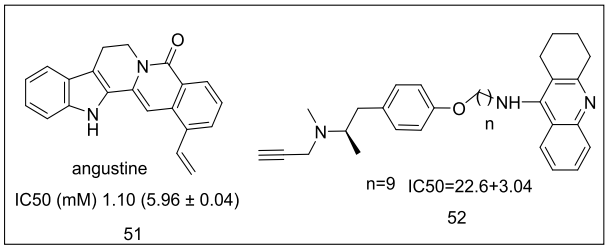

Fig. 2.19 Psychotria alkaloids as MAO inhibitors

Luhrand group synthesized two series of phenylethylamine analogues and performed docking studies to examine the assumption of increasing MAO inhibitory potency by

fixing the amine chain in six membered ring conformation. The benzyloxy analogues **(53)** and **(54)** in **Fig. 2.20** were the most potent and selective for both MAO-B and hMAO-B. They concluded that the justification of these compounds should contribute to the development of new selective and reversible MAO-B inhibitors with a potential for use in the therapy of neurodegenerative diseases **(Luhr *et al.*, 2010).**

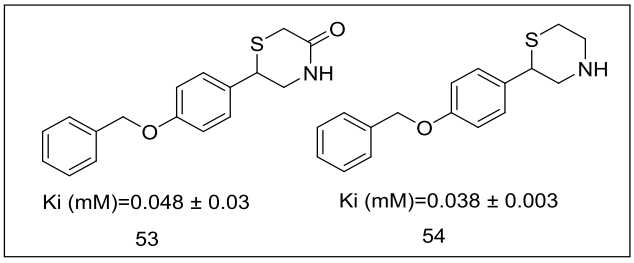

Fig. 2.20 Benzyloxy analogues as MAO inhibitors

Khattab and Co-workers synthesized a series of 2-benzyl-3-(2-arylidenehydrazinyl) quinoxalines, 4-benzyl-1-aryl-[1,2,4]triazolo[4,3-a]quinoxalines and phenyl(1-aryl-[1,2,4]triazolo[4,3-a]quinoxalin-4-yl)methanones derivatives and performed their *Invitro* testing for MAO-A &B inhibition. The results revealed that the compounds showed MAO-A activity greater than the standard MAO-A inhibitor. The molecular modelling studies revealed that the proposed compounds showed hydrophobic interaction with Phe208 and hydrogen bonds to Ser209, Pro72, Tyr69, Tyr444, Glu74 and Glu216 and the compound **(55) (Fig. 2.21)** was found out to be the most active analogue having three hydrogen bonds with good scoring and is selective against MAO-A isoform (Khattab *et al.*, 2010).

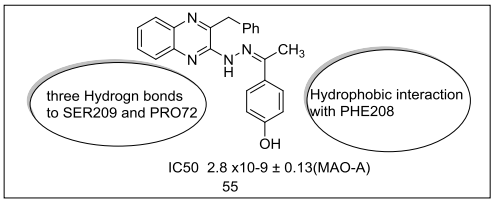

Fig. 2.21 Quinoxazoline derivative

Reiners and team synthesized a series of β-carboline derivatives. The proposed compounds were further evaluated for their MAO-A & B inhibition activity and compared with the standard drug harmine. the results suggested MAO-A inhibitory activity increases with the O-alkylated compounds which are having lipophilic groups like

cyclohexyl, phenyl and aliphatic chains but are less active against MAO-B. From all the proposed compounds, compound (**56)** having trifluorobutyloxy group showed maximum MAO-A inhibition on comparison with harmine. The computational studies revealed that the triflurobutyloxy group occupies the hydrophobic pocket of the enzyme which is vacant by harmine compound. Compound **(57)**, with the cyclohexylmethoxy chain shows inhibitory activity towards MAO-B shown in **Fig. 2.22** (Reniers *et al.*, 2011).

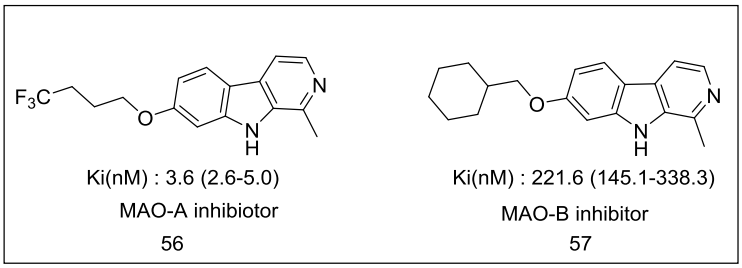

Fig. 2.22 β-carboline derivatives.

Valente et al reported a new series of 3-(1H-pyrrol-3-yl)-2-oxazolidinonesderivatives ass reversible, highly potent and selective MAO-A inhibitors. Compound (**58)** shown in **Fig. 2.23** was found out to be the most potent compound shows 20000 times more selectivity against MAO-A enzyme (Valente *et al.*, 2011).

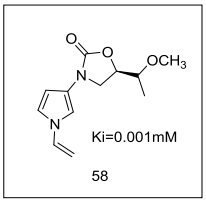

Fig. 2.23 Oxazolidinone derivatives as MAO inhibitors

Senturk and team synthesized a new series of 3-aryl-5-(4-fluorophenyl)-N-substituted-4,5-dihydro-1H-pyrazole-1-carbothioamide derivatives and evaluated their MAO inhibitory activity. Docking results suggested that the potent compound (**59)** shown in **Fig. 2.24**, bind efficiently with the MAO-A enzyme, and the presence of methoxy or chloro on the 3-phenyl ring increases the potency and selectivity towards MAO-A. thus can be considered as a promising candidate for antidepressants (Senturk *et al.*, 2012).

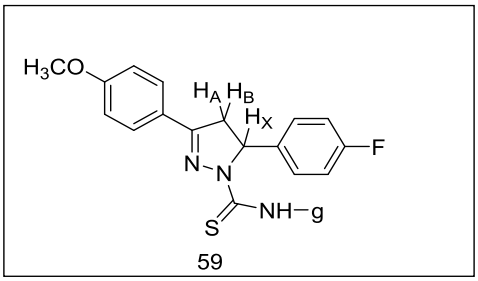

Fig. 2.24 Carbothioamide derivatives as MAO inhibitors

Prashanth and team synthesized a series of piperamide derivatives and evaluated their antidepressant and antioxidant activity. The antidepressant activity was assessed using tail suspension test and forced swim test. Compounds were explored for their MAO-A and MAO-B inhibitory activity. The results suggested that the compound (**60)** and (**61)** shown in **Fig. 2.25,** were active in both the tests with slightly high potency towards MAO-A than MAO-B and on comparison with the standard drug clorgyline the compounds showed significant inhibitory effect. The results revealed that all the proposed compound showed significant antioxidant property and compound (**61)** was found to be the most potent antioxidant.

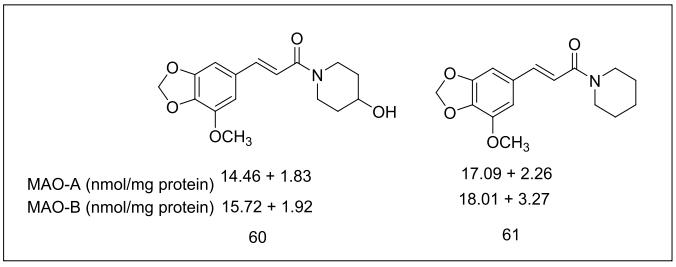

Fig. 2.25 Piperamide derivatives as MAO inhibitors

Thus concluded that the proposed compounds were explored for their antioxidant, antidepressant and antimicrobial property thus can be used as a lead for the further synthesis of selective antidepressant drug candidates (Prashanth *et al.*, 2012).

Mu and co-workers designed and synthesized a series of piperine derivatives and evaluated them in-vitro for MAO-A and MAO-B inhibitory activity and selectivity. They reported that the small amine moieties on piperidino proved to be more potent and selective inhibitor of MAO-B rather than MAO-A and the compound 5-(3,4-methylenedioxyphenyl)-2*E*,4*E*-pentadienoic acid *n*-propyl amide **(62)** showed the greatest MAO-B inhibitory activity (IC_{50} for MAO-B = 0.045 μM) and good selectivity (IC_{50} for MAO-A = 3.66 μM**)** (Mu *et al.*, 2012)

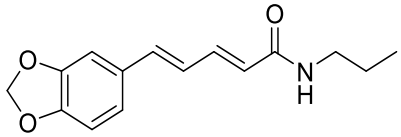

5-(3,4-methylenedioxyphenyl)-2E,4E-penta dienoic acid n-propyl amide

62

Lewellyn et.al. disclosed that aplysinopsin analogs can be used as selective MAO-A inhibitors for the treatment of AD. They synthesized fifty compounds and reported that the three compounds showed significant MAO inhibitory activity and selectivity. They reported that the compound (E)-5-[(6-bromo-1H-indol-3-yl) methylene]-2-imino-1,3-dimethylimidazolidin-4-one **(63)** shown in **Fig. 2.26**, possessed an IC_{50} of 5.6 nM at MAO-A and had a selectivity index of 80.24. The tryptophan derived aplysinopsins have been isolated from variety of marine organisms and the literature showed that they aplysinopsin analogs possess various biological activities such as neurotransmitter modulation. The SAR studies disclosed that the multiple N-methylations of the imidazolidinone moiety, one of which should be the methylation of N-2' in addition to either N-3'or N-4'and bromination at C-5 and C-6 plays a vital role for MAO-A potency and selectivity (Lewellyn *et al.*, 2012). Villarinho and group examined the MAO inhibitory activity and antidepressant activity of 2-(3,4-dimethoxy-phenyl)-4,5-dihydro-1H-imidazole (2-DMPI) in the Mice. From their evaluation they disclosed that the 2-DMPI exhibited inhibitory activity against the both MAO isoforms with high affinity or selectivity towards MAO-A. They suggest that the 2-DMPI **(64)** is a new, reversible and preferential MAO-A inhibitor that employs its antidepressant-like activity by decreasing

5-HT and DA turnover without disrupting motor performance, even at high doses. Therefore, it can be used as lead for the development of novel antidepressants (Villarinho *et al.*, 2012)

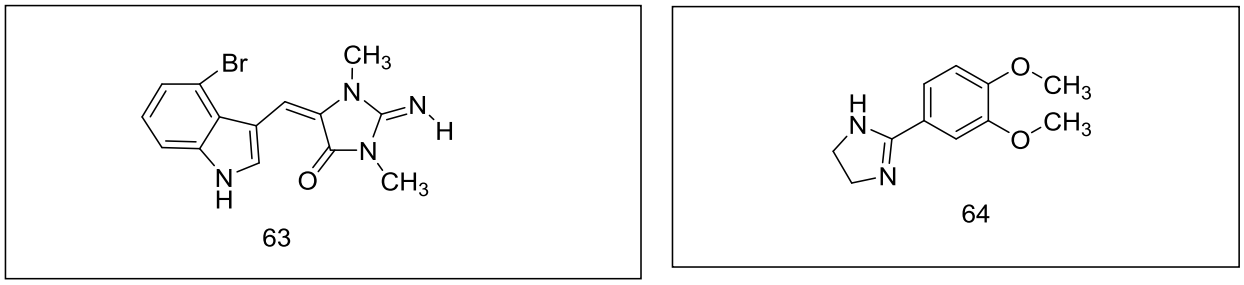

Fig.2.26 Imidazole derivative

Demirkiran and team proposed the benzophenone glycosides in **Fig. 2.27** as a MAO inhibitor selectively against MAO-A isoform. They purified the 80% ethanol extract of *Hypericumthasium* Griseb. from n-BuOH and isolated three new benzophenone compounds along with flavonoid glycoside. Further, they screened all the three as well as previously isolated glycoside i.e. quercetin and kaempferol against MAO-A inhibitory activity and compared their IC_{50} values with the standard MAO-A inhibitor clorgyline and concluded that the compounds showed promising inhibitory activity against MAO-A isoforms (Demırkıran, 2012).

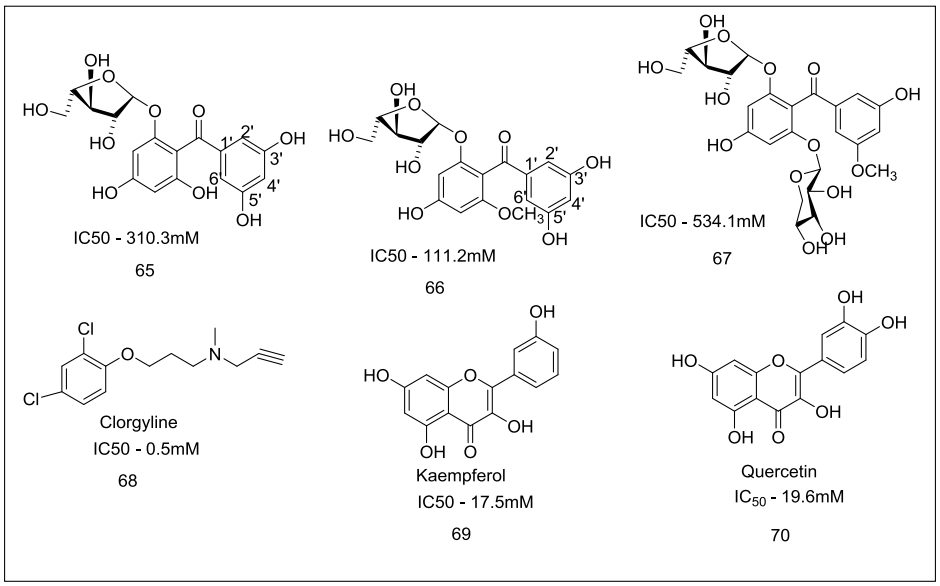

Fig. 2.27 Benzophenone derivatives

Bonaiuto and group proposed a series of new **polyamines derivatives** and evaluated them against MAO enzymes. The compound (71) given in the **Fig. 2.28** was found to be most potent and selective MAO-B inhibitor and irreversibly bind to MAO-A enzyme. In particular, two new types of MAO inhibitors, selective respect to VAP-1, emerged in this study: the spermine analogue, bearing a thiophene ring**,** which acts as mixed reversible inhibitor (Ki 23mM), selective for MAO-B; and compound **(71)**obtained by transforming the primary amine function of very good AOs substrates in an ITC moiety. Although, **(72)** exhibits high affinity for both MAO isoforms (KI about 5±1μM), it specifically acts as competitive inhibitor of MAO B and as irreversible inhibitor of MAO-A. As resulting by the docking studies, Lys305 of the MAO-A active site has been proposed as a new target for covalently binding the ITC reactive moiety of **(72)**, leading to MAO-A irreversible inhibition shown in **Fig. 2.28** (Bonaiuto *et al.*, 2013)

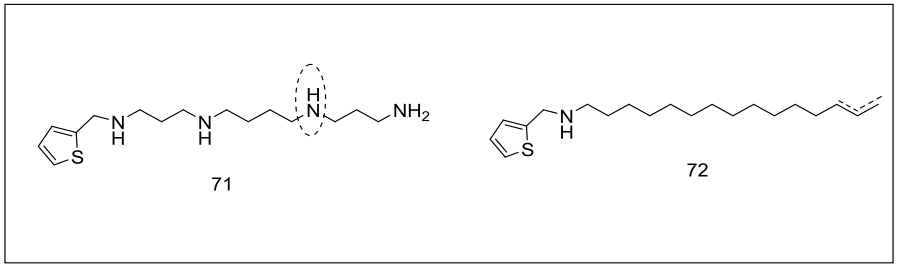

Fig. 2.28 Polyamine derivatives

Pisaniand team synthesized a series of 6'-substituted-(E)-2-(benzofuran-3(2H)-ylidene)-N-alkylacetamides and reported that the 6'-Sulfonyloxy derivatives have affinities towards MAO-A, whereas 6'-benzyloxy derivatives showed potency towards MAO-B isoform. SAR studies revealed the importance of rigidity in planer conformation of exocyclic double bond suggesting its role in binding. The *E* conformation was found out to possess high binding affinity of the exocyclic double bond compared to *Z* form. The electronic and steric environment of the compound plays a decisive role and influences the activity of compounds. They concluded that synthesized novel MAO inhibitors may be further explored for their promising therapeutic intervention for Depression, PD or other neurodegenerative diseases(Pisani *et al.*, 2013).They described the (hetero)aryl sulfonate esters showing good affinity and selectivity towards MAO-A (selectivity index >> 500), as compared to esuprone as the reference coumarin compound, and

much greater than moclobemide, which is a prototype reversible MAO-A inhibitor and one of the most widely used antidepressive agents shown in **Fig. 2.34.**

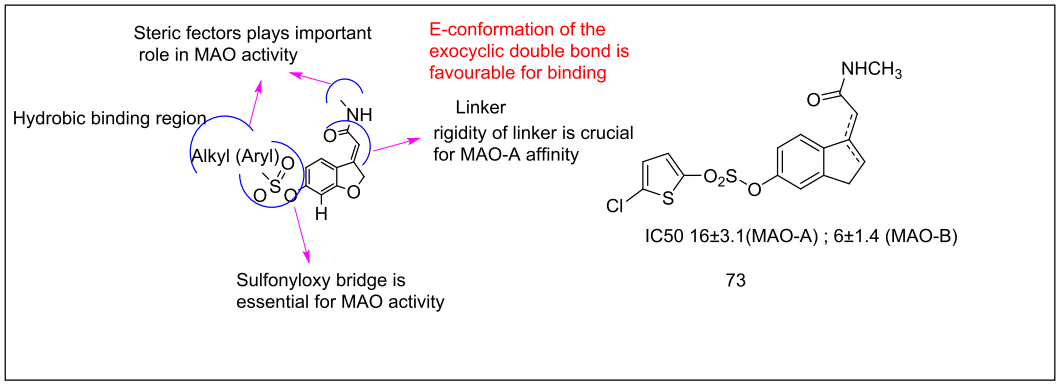

Fig. 2.29 Sulphonate esters as MAO inhibitors

Srivastav and group designed a new series of **quinazoline derivatives** in **Fig. 2.30**. It was reported that quinazoline derivatives exhibits MAO inhibition. Thus, based on this revelation, 6,7-dimethoxy-N^2-(substituted benzyl)-N^2-propylquinazoline-2,4-diamine derivatives have been designed and synthesized and further characterized for their antidepressant as well as anxiolytic activity. The proposed compounds showed excellent antidepressant activity when compared with Imipramine (standard drug). SAR studies revealed that the substitution on phenyl ring linked with tertiary amine group attached to the 2nd position of the quinazoline ring is essential for the activity. The substitution of electron withdrawing group like –Cl, F and NO_2 on phenyl ring at *ortho, meta* and *para*position decreases the activity whereas the presence of hydroxyl group (OH) at *ortho* position increases its antidepressant activity and decreases the potency at *meta* and *para* position. Moreover, the presence of electron releasing groups like -CH_3,-OCH_3 -C_2H_5 and -OC_2H_5 at para position showed excellent antidepressant activity (Srivastav *et al.*, 2013).

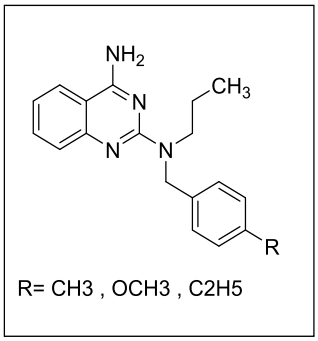

Fig. 2.30 Quinazoline Derivatives

Desideri and team reported a series of 1,5-Diphenylpenta-2,4-dien-1-ones and evaluated their MAO inhibition activity. The studies suggested that the compounds showed inhibitory activity, potency and high selectivity towards MAO-B and the most potent and active compounds showed inhibitory activity in the nanomolar range (Desideri *et al.*, 2013).

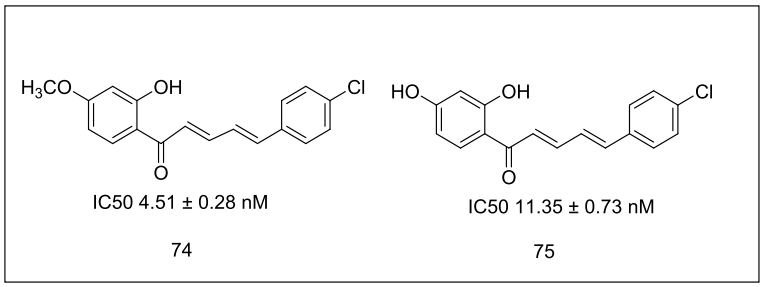

Fig. 2.31 dienone derivatives

CHAPTER- 3

RATIONALE AND OBJECTIVES

The x-ray crystal structure of MAO-A & MAO-B are well explored now. It has been reported that the active site of MAO-A has pocket which interact with slightly polar molecules while active site of MAO-B contain lipophilic pocket which preferably interact with bulky and lipophilic ligands. Therefore, the target molecules are designed by taking into consideration the crystal structures of both the enzymes i.e. MAO-A and MAO-B. On the basis of various literature reports, it was concluded that piperazine nucleus is an integral part in most of the psychoactive compounds and hence we have focused our work on piperazine containing scaffolds. Piperazine is an organic compound that consists of a six-membered ring containing two nitrogen atoms at opposite positions in the ring. Piperazine exists as small alkaline deliquescent crystals with a saline taste (Ahmeda *et al.*, 2012). The piperazine are a broad class of chemical compounds, many with important pharmacological properties, which contain a core piperazine functional group. Piperazine is considered as the most promising heteroaromatic nucleus in the field of medicinal chemistry. Piperazine derivatives were already proved as important key intermediates for the synthesis of medicinally important derivatives with a pharmacological profile such as antianginal, antidepressant, antipsychotics, antihistamines, anticancer, antidiabetic, antiparkinson's properties. Since the size of piperazine nucleus is small and are lipophilic in nature that contains 2 nitrogen atom which are hydrogen bond acceptor and can interact at the receptor site. In addition the small molecules can easily pass through blood brain barrier (BBB) thus can be used in various neurodegenerative diseases.

Piperazine ring containing few Important marketed drug and their associated biological activities(Meher *et al.*, 2013)

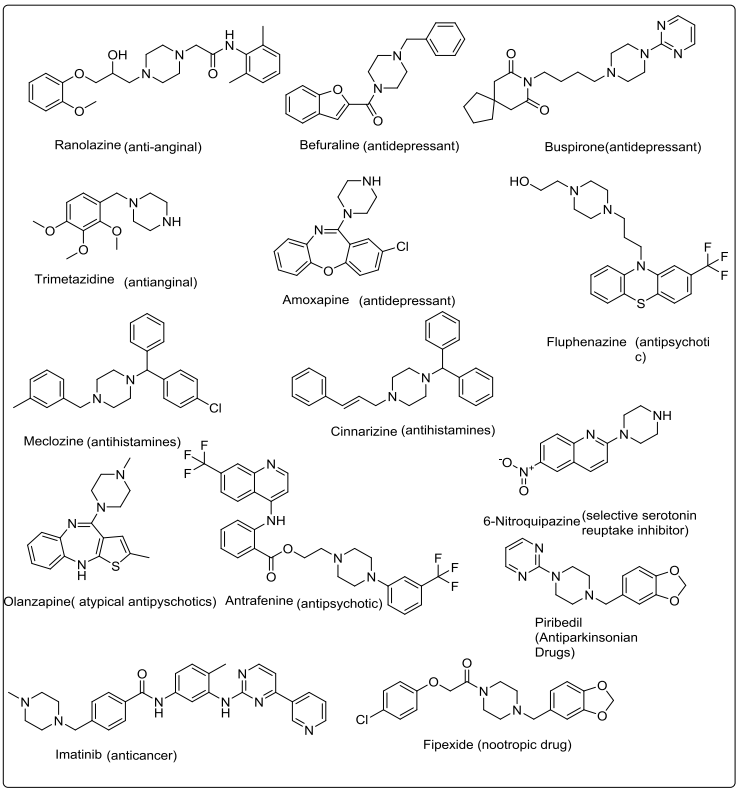

Fig. 3.1 Biological importance of Piperazine ring (Meher *et al.*, 2013)

We came across some recent reports on piperazine derivatives as MAO inhibitors. For example, Pessoa-Mahana *et al*. reported a series of 4-Arylpiperazine derivatives of Moclobemide, as potential antidepressants showing MAO-A inhibitory effect and affinity towards 5-HT1$_A$ (Pessoa-Mahana *et al.*, 2004).

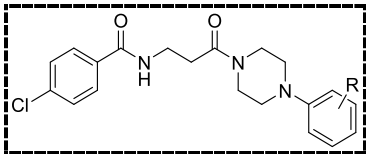

Fig. 3.2 4-Arylpiperazine derivatives

Similarly para-substituted 4-phenylpiperidines and 4-phenylpiperazine has been synthesized in **Fig. 3.3** and evaluated as monoamine oxidase inhibitors (Pettersson *et al.*, 2012). As reported MAO-A has a predominant effect on dopamine catabolism, leading to production of the metabolite DOPAC (3, 4-dihydrophenylacetic acid) and MAO-A inhibitors (e.g. clorgyline) therefore reduce striatal DOPAC levels.

Fig. 3.34-phenylpiperidines and 4-phenylpiperazine derivatives

SAR studies reveals that the para-substituted phenethylamines, benzylamines, and amphetamines had shown correlation between MAO affinity and different physiological properties of the para-substituent. *Para*-substituent with low dipole moment increases affinity to MAO-A, while substituent with high dipole moment have weak affinity. MAO-B affinity is modulated by bulk of the para-substituent and large hydrophobic substituent's produce compounds with high MAO-B affinity (Pettersson *et al.*, 2012)

The same research group recently reported mono-substituted 4-phenylpiperidines and 4-phenylpiperazines which gave strong correlation between the levels of striatal DOPAC and the affinities to DA D2 and MAO-A.SAR studies reveals that substitution at the *ortho*-position increases the DOPAC levels. In *meta*-position electron withdrawing groups produces more increase in DOPAC than electron donating groups. A number of different

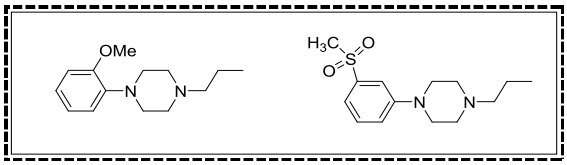

Fig. 3.4 Monosubstituted 4-phenylpiperidines and 4-phenylpiperazines

alkylsulfones were tested in the *meta*-position and in this group the size of the alkyl determine the effect on DOPAC. The response decline with increasing bulk. Substitution in the *para*-position produces completely different effects compared to Ortho and Meta. Instead of increases in the DOPAC-response, these compounds could only produce decreased levels. Electronic properties also proved important in this position with electron-donating groups yielding decreased DOPAC-levels while electron-withdrawing groups rendered inactive compounds (Pettersson *et al.*, 2013)**.**

Inspired by this work on various phenylpiperazine derivatives, we proposed the design, synthesis and screening of some phenylpiperazine derivatives as potential MAO inhibitors with improved pharmacological profile.

Objectives:

1. *In silico* studies of the designed molecules via molecular modelling on MAO-A and MAO-B enzyme
2. Exploration of MAO-A binding site through piperazine based ligands with polar substituents.
3. Synthesis of bulky and lipophilic piperazine derivatives to explore binding site in MAO-B.
4. Biological evaluation of synthesized compounds for MAO inhibition**.**

Chapter- 4

Molecular Docking Studies

Methods

4.1 Molecular Docking using AutoDock 4.2 &AutoVina

AutoDock Vina is a new generation of docking software from the Molecular Graphics Lab. It achieves significant improvements in the average accuracy of the binding mode predictions, while also being up to two orders of magnitude faster than AutoDock 4.AutoDockVina does not require choosing atom types and pre-calculating grid maps for them. Instead, it calculates the grids internally, for the atom types that are needed, and it does this virtually instantly. Because, the scoring functions used by AutoDock 4.2 and AutoDock Vina are different and inexact, on any given problem, either program may provide a better result. AutoDock Vina needs file in .pdbqt format both for receptor and ligand which is prepared in AutoDock 4.2.

4.1.1 Protein preparation

The PDB for the crystal structure of MAO-A co-crystallized with selective inhibitor 7-Methoxy-1-methyl-9*H*-beta carboline [Harmine, PDB entry code 2Z5X, 2.20 A˚resolution] (Son *et al.*, 2008) and MAO-B co-crystallized with Farnesol [PDB entry code 2BK3, 1.80 Å resolution](Hubalek *et al.*, 2005) were retrieved from PDB. During the protein preparation only polar hydrogens and kollman charges were added. The atoms in the protein were assigned for AutoDock 4.2 type. Now the PDBQT file of the protein was saved in which its different pdb records from “ATOM” select till **“**END” were added.

4.1.2 Ligand preparation

The 3D structure of the ligand was created using ChemBio Draw 3D, and saved in “.mol2” (SYBYL2) format. The ligand energy is minimized through MMFF94 parameter displayed in ChemBio Draw 3D. The ligand was selected from the ligand menu of autodock and from the torsion tree, its roots were first detected and then selected. Now it will show number of rotatable bonds in the ligand. The resultant ligand file is saved in standard autodock“.pdbqt” file format.

4.1.3 Grid generation

From the GRID menu of autodock, the macromolecule (targeting protein/enzyme) was selected and the enzyme/protein is initialized in the autodock for the grid generation. Here in this step additional charges and bond orders are assigned. The PDBQT file generated in this step overwrites the previously created PDBQT file. The Grid was generated by taking the bound ligand as the center of grid. The grid maps representing the proteins will be calculated using auto grid and grid size was set to x=40.582, y=26.931, z=-14.54 for 2Z5X and x=16.012, y= 127.65, z=23.57 for 2BK3 with grid spacing of 0.375 Å.

4.1.4 Docking

Docking of protein to ligands were carried out using LGA (Lamarckian Genetic Algorithm) with standard docking protocol on the basis a population size of 150 randomly placed individuals; a maximum number of 2.5 $x10^7$energy evaluations, a mutation rate of 0.02, a crossover rate of 0.80 and an elitism value of 1. Ten independent docking runs will be carried out for each ligand and results were clustered according to the 2.0 Å root mean square deviation (RMSD) criteria.

4.2 Molecular docking using Schrodinger

Schrodinger maestro is a powerful software tool for molecular docking. This software comes with graphical user interface for windows and through this software I have performed static docking, where the maximum glide score is considered compared with standard to check whether the synthesized molecule shows valid interaction or not. In Schrodinger maestro software where the protein preparation wizard is there where complete protein preparation is done. Ligand is prepared by selecting the ligand in required receptor and then there is automatically grid and co-ordinates selection around the particular area. Docking is performed using XP (Extra precision) method to calculate the exact interaction compared to standard. The glide score comes for each ligand and hence compared with standard molecule.

4.3 Molecular docking using MOE

MOE stands for *Molecular Operating Environment* which is a molecular modelling suite. Docking is one of the tool that is used to evaluate the suitability of the fitting of the designed or synthetics. In the meantime we did docking, implicating similar MAO-A and MAO-B PDB used earlier in Schrodinger and AutoVina. Similarly we remove extra water of crystallization and further protonate the system for making it likely to the body physiological conditions. Ligands were prepared and minimized *via* MM2 force field in chembio 3D ultra. Later on the ligands were saved in MOE database file. Finally docking was done by applying London DG force field.

Table4.1: IUPAC names and structures of the docked compounds

S. No.	Structure	IUPAC Name
VS-1	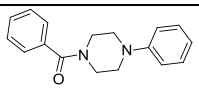	phenyl(4-phenylpiperazin-1-yl)methanone
VS-2	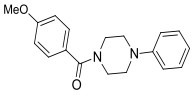	(4-methoxyphenyl)(4-phenylpiperazin-1-yl)methanone
VS-3	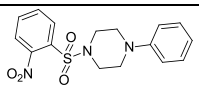	1-((2-nitrophenyl)sulfonyl)-4-phenylpiperazine
VS-4	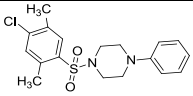	1-((4-chloro-2,5-dimethylphenyl)sulfonyl)-4-phenylpiperazine
VS-5	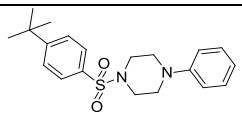	1-((4-(tert-butyl)phenyl)sulfonyl)-4-phenylpiperazine
VS-6	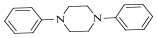	1,4-diphenylpiperazine
VS-7	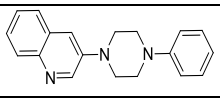	3-(4-phenylpiperazin-1-yl)quinolone

VS-8	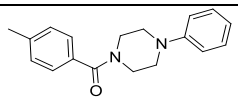	(4-methylpiperazin-1-yl)(p-tolyl)methanone
VS-9	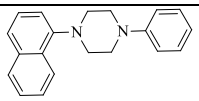	1-(naphthalen-1-yl)-4-phenylpiperazine
VS-10	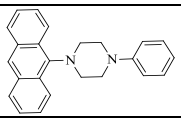	1-(anthracen-9-yl)-4-phenylpiperazine
VS-11	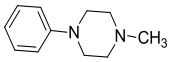	1-methyl-4-phenylpiperazine
VS-12	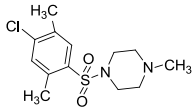	1-((4-chloro-2,5-dimethylphenyl) sulfonyl)-4-methylpiperazine
VS-13	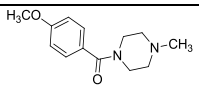	(4-methylpiperazin-1-yl)(p-tolyl) methanone
VS-14	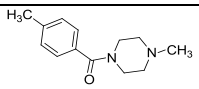	(4-methylpiperazin-1-yl)(p-tolyl) methanone
VS-15	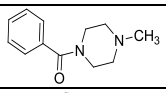	(4-methylpiperazin-1-yl)(phenyl) methanone
VS-16	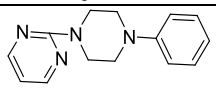	2-(4-phenylpiperazin-1-yl)pyrimidine

In order to obtain preliminary expectations about the pharmacodynamics and pharmacokinetics characteristics of our candidates, docking analyses were performed by targeting human MAO-A and MAO-B crystal structure. Docking studies can also give us a virtual insight into compound's orientation within the active site of our target. Based on our results of docking studies, it is obvious that all the compounds exhibit an extended conformation that will occupy both the entrance cavity and the substrate cavity within the active site of MAO-B crystal. Similarly for MAO-A all the proposed compound shows better binding affinity and interaction with the active site amino acids. Such orientation will force Ile199 residue to gain an open configuration leading to the fusion of both entrance cavity and substrate cavity. The active site residues for MAO-A includes Tyr69, Asn181, Phe208, Val210, Gln215, Cys323, Ile325, Ile336, Leu337, Phe352,

Tyr407, Tyr444 and FAD. The results of docking studies showed that the compounds showed pi-pi interactions with the various active site amino acids.

Initially we have docked the substrate Tyramine with both the crystal structure of MAO-A (2Z5X) and MAO-B (2BK3).

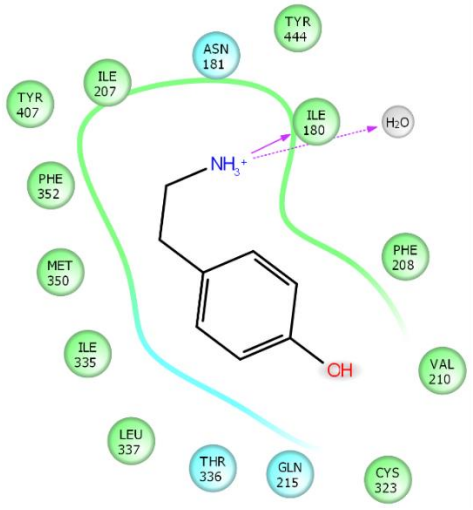

(A)

Tyramine interaction with the MAO-A enzyme using PDB ID 2Z5X Molecule showing H-bond interactions with ILE180 with $NH_2$and H_2O molecule. Active site residues includes ILE207, ASN181, 1LE180 in Fig. 4.1 (A).

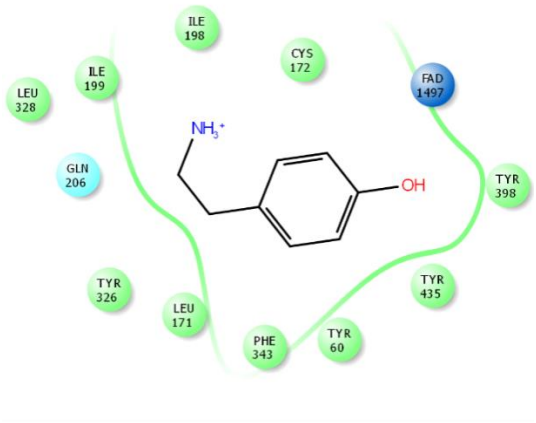

(B)

Structure represents the docking interaction of tyramine with the MAO-B enzyme using PDB ID 2BK3. In Fig.4.1 (B) the molecule is interacting with the FAD cofactor. The active site residues includes ILE199, PHE343, LEU171.

Fig. 4.1 Tyramine interactions with MAO-A (2Z5X) (A) and MAO-B (2BK3) (B)

Table 4.2: Docking energy of the compounds with MAO-A enzyme using, AutoDock, AutoVina & MOE software's

Compounds	Protein	Schrodinger docking score Binding Energy (kcal/mol)	MOE docking score binding energy (kcal/mol)	AutoVina score binding energy (kcal/mol)	AutoDock Binding energy (kcal/mol)	Inhibitory Constants(Ki) (Calcd. By AutoDock)
VS-1	MAO-A	-4.74	-11.2383	-6.5	-5.89.	60.21 µM
VS-2	MAO-A	-5.01	-11.4746	-6.7	-5.96	58.06 µM
VS-3	MAO-A	-4.65	-11.5990	-6.2	-6.02	32.3 µM
VS-4	MAO-A	-5.34	-11.6047	-5.3	-6.87	49.67 µM
VS-5	MAO-A	-4.80	-10.5946	-4.6	-4.05	49.85 µM
VS-6	MAO-A	-3.99	-9.4305	-7.1	-2.17	1.66 µM
VS-7	MAO-A	-5.73	-11.0859	-6.9	-6.36	3.67 µM
VS-8	MAO-A	-5.59	-11.5572	-7.7	-3.11	2.11 µM
VS-9	MAO-A	-5.27	-10.2048	-6.5	-8.57	230.32 µM
VS-10	MAO-A	-5.26	-10.7324	-4.9	-5.04	1.06nM
VS-11	MAO-A	-2.73	-8.6537	-7.1	-3.95	1.27 µM
VS-12	MAO-A	-2.00	-12.5877	-6.2	-6.27	35.65 µM
VS-13	MAO-A	-3.65	-11.6146	-7.2	-4.87	48.89 µM
VS-14	MAO-A	-3.50	-10.3489	-7.7	-8.67	127.34nM
VS-15	MAO-A	-3.51	-10.0590	-7.7	-7.34	89.65nM
VS-16	MAO-A	-4.44	-9.9231	-7.4	-10.67	76.34nM

Table 4.3: Docking energy of the compounds with MAO-B enzyme using, AutoDock, AutoVina & MOE Software's

Compounds	Protein	Schrodinger docking score Binding Energy (kcal/mol)	MOE docking score binding energy (kcal/mol)	AutoVina score binding energy (kcal/mol)	AutoDock Binding energy (kcal/mol)	Inhibitory Constants(Ki) (Calcd. By AutoDock)
VS-1	MAO-B	-6.02	-8.8	-9.7	-8.50	85.34nM
VS-2	MAO-B	-6.91	-10.33	-9.0	-9.53	103.4nM
VS-3	MAO-B	-6.83	-10.01	-7.5	-10.1	39.52nM
VS-4	MAO-B	-7.13	-8.36	-5.2	-10.95	9.37nM
VS-5	MAO-B	-5.84	-9.53	-7.7	-11.35	4.83nM
VS-6	MAO-B	-4.90	-8.13	-9.5	-8.87	316.93nM
VS-7	MAO-B	-7.46	-8.56	-11.2	-10.53	19.06nM
VS-8	MAO-B	-7.00	-9.57	-9.6	-9.68	80.63nM
VS-9	MAO-B	-6.79	-8.67	-10.3	-10.8	12.16nM
VS-10	MAO-B	-7.99	-7.15	-9.0	-12.25	1.06nM
VS-11	MAO-B	-4.16	-10.66	-6.7	-6.46	18.45µM
VS-12	MAO-B	-5.79	-9.91	-6.9	-9.23	9.83nM
VS-13	MAO-B	-5.66	-10.25	-7.0	-5.35	120.7nM
VS-14	MAO-B	-6.03	-9.89	-7.4	-7.05	7.35nM
VS-15	MAO-B	-5.20-	-8.95	-7.4	-7.06	6.74 µM
VS-16	MAO-B	-6.34	-9.57	-8.5	-5.36	118.3 µM

Some of the best poses of the compounds which are synthesized for MAO-A and MAO-B are shown below:

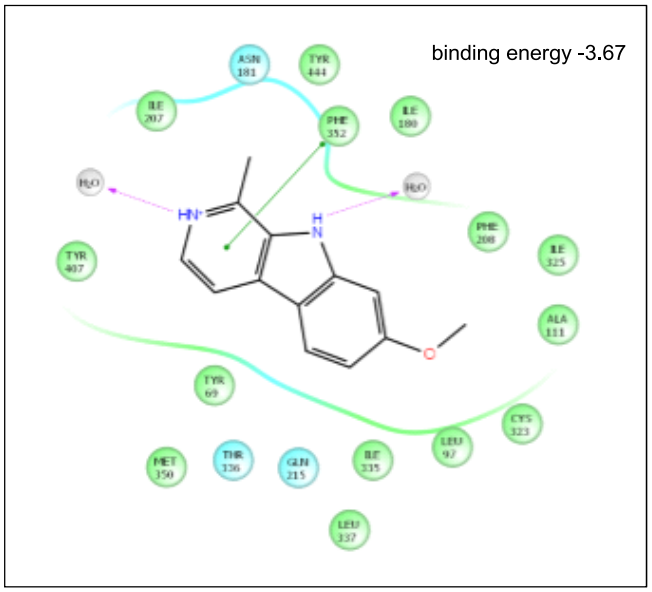

Fig. 4.2 Interactions of standard drug Harmine docked with protein (PDB ID 2Z5X) using Schrodinger software. The compound shows pi-pi interactions with PHE352. Two hydrogen bonding interactions are shown. Most of the active site is hydrophobic and some is hydrophilic. Hydrophilic site contains 3 amino acids i.e. ASN181, THR336 and GLN215. From the fig. it is clear that the compound fits well into the active site**.**

All the compounds were docked with the enzyme MAO-A and MAO-B and their binding energies were calculated. The compounds shows good binding energies with the protein. It has been determined that the compound 4 (Ki= -5.34)and compound 7 (Ki= -5.73) showed high binding energies with MAO-A. Compounds 4 and 7 were superimposed with the standard drug harmine to determine the affinity of the compounds towards the active site in comparison to harmine. The superimposed poses of compounds are shown below:

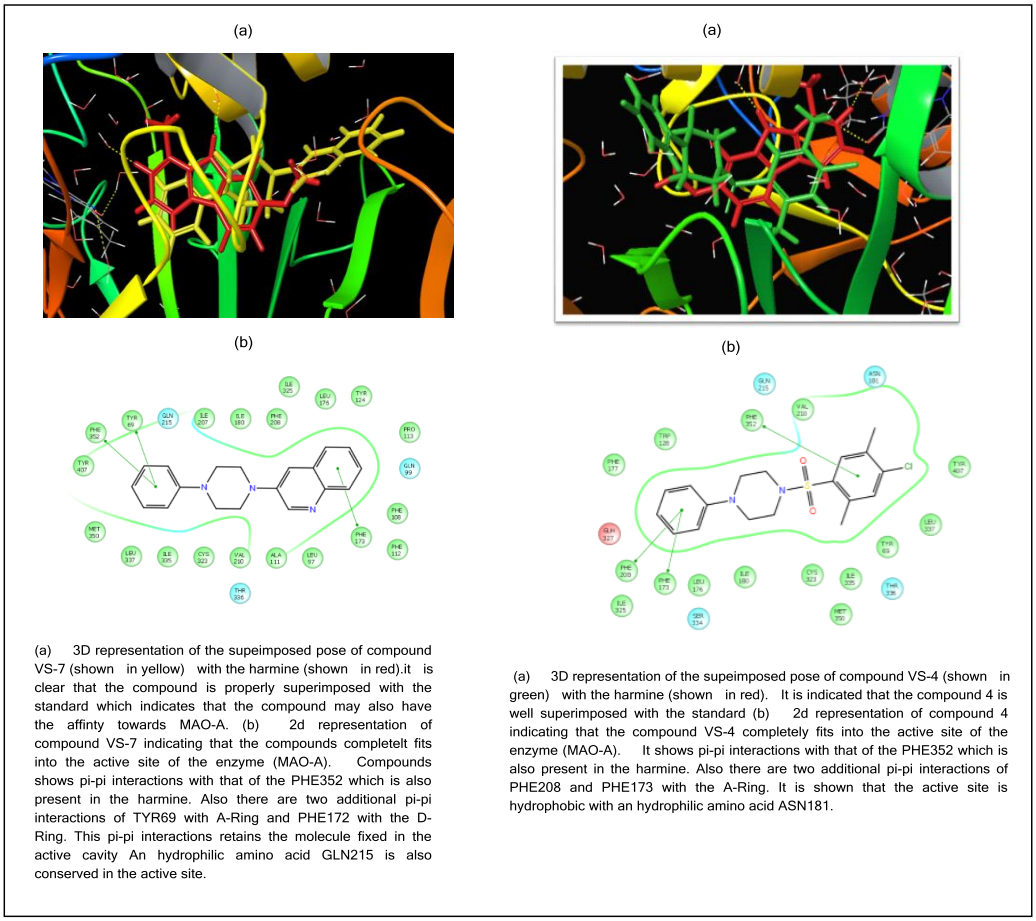

(a) 3D representation of the supeimposed pose of compound VS-7 (shown in yellow) with the harmine (shown in red).it is clear that the compound is properly superimposed with the standard which indicates that the compound may also have the affinty towards MAO-A. (b) 2d representation of compound VS-7 indicating that the compounds completelt fits into the active site of the enzyme (MAO-A). Compounds shows pi-pi interactions with that of the PHE352 which is also present in the harmine. Also there are two additional pi-pi interactions of TYR69 with A-Ring and PHE172 with the D-Ring. This pi-pi interactions retains the molecule fixed in the active cavity An hydrophilic amino acid GLN215 is also conserved in the active site.

(a) 3D representation of the supeimposed pose of compound VS-4 (shown in green) with the harmine (shown in red). It is indicated that the compound 4 is well superimposed with the standard (b) 2d representation of compound 4 indicating that the compound VS-4 completely fits into the active site of the enzyme (MAO-A). It shows pi-pi interactions with that of the PHE352 which is also present in the harmine. Also there are two additional pi-pi interactions of PHE208 and PHE173 with the A-Ring. It is shown that the active site is hydrophobic with an hydrophilic amino acid ASN181.

Fig. 4.3 Docking poses of compounds **VS-7** and **VS-4**interacts with the MAO-A (2Z5X)

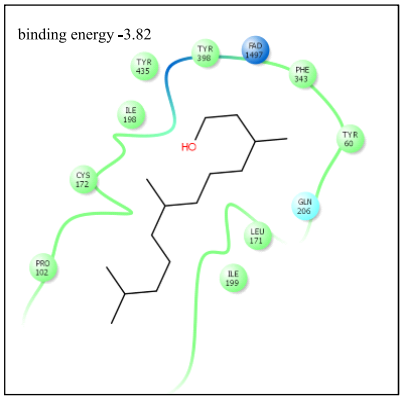

Fig. 4.4 Standard drug Farnesol docked with protein (PDB ID 2BK3) using Schrodinger software. The active site is hydrophobic and the compound was completely fits into the active site with high affinity. The active site amino acids includesTYR398, FAD1497, PHE343, TYR60, GLN206, LEU171, CYS172 and PRO102**.**

The compounds showed good binding energies with the MAO-B. Both the compounds were superimposed with the standard drug farnesol to determine the affinity of the compounds towards the active site in comparison to farnesol. It was found that the compound **VS-3** (-6.83) and **VS-8** (-7.0) showed good interactions with MAO-B.

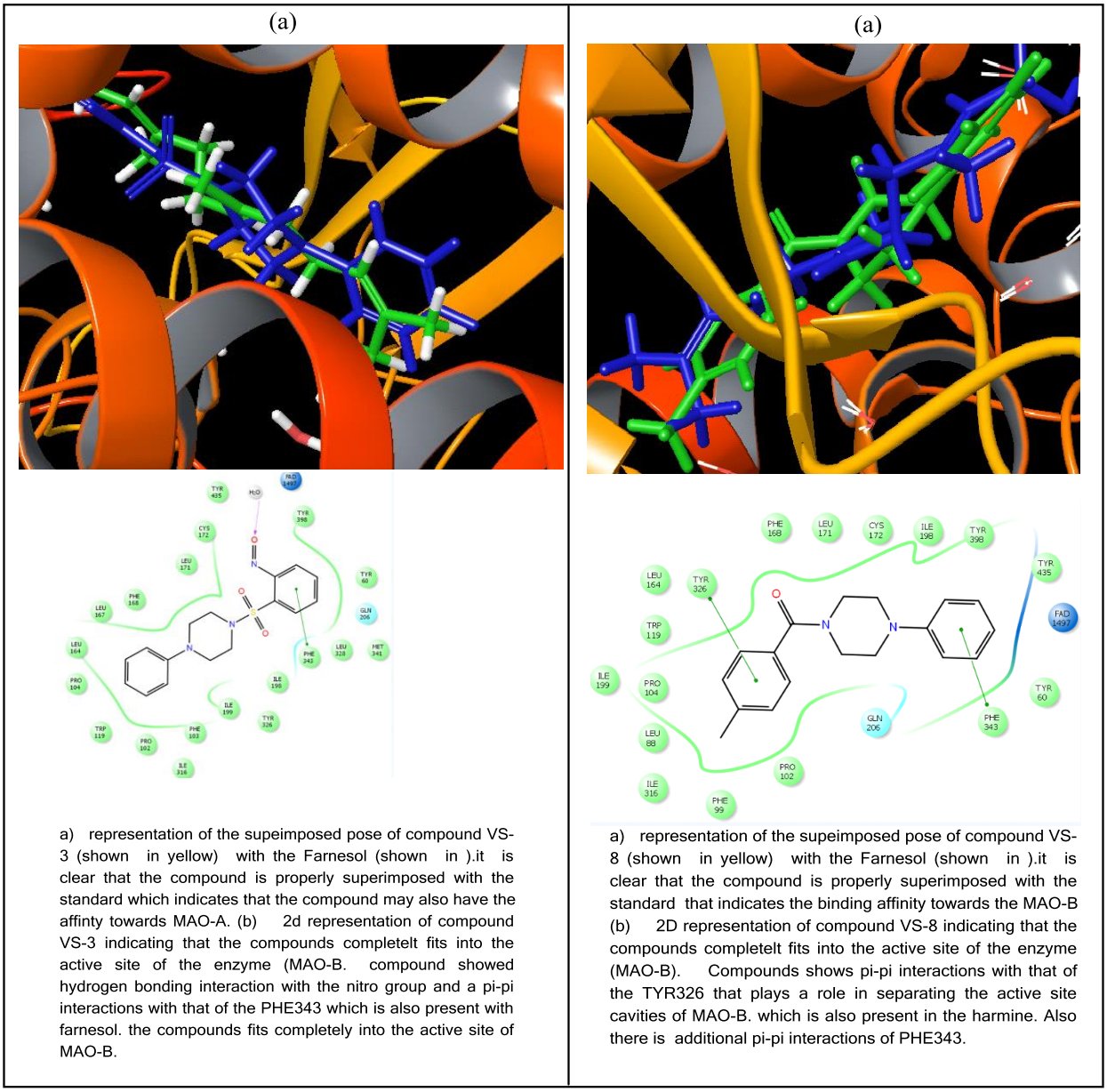

a) representation of the supeimposed pose of compound VS-3 (shown in yellow) with the Farnesol (shown in).it is clear that the compound is properly superimposed with the standard which indicates that the compound may also have the affinty towards MAO-A. (b) 2d representation of compound VS-3 indicating that the compounds completelt fits into the active site of the enzyme (MAO-B. compound showed hydrogen bonding interaction with the nitro group and a pi-pi interactions with that of the PHE343 which is also present with farnesol. the compounds fits completely into the active site of MAO-B.

a) representation of the supeimposed pose of compound VS-8 (shown in yellow) with the Farnesol (shown in).it is clear that the compound is properly superimposed with the standard that indicates the binding affinity towards the MAO-B (b) 2D representation of compound VS-8 indicating that the compounds completelt fits into the active site of the enzyme (MAO-B). Compounds shows pi-pi interactions with that of the TYR326 that plays a role in separating the active site cavities of MAO-B. which is also present in the harmine. Also there is additional pi-pi interactions of PHE343.

Fig. 4.5 Docking poses of compounds **VS-3** and **VS-8** interacts with the MAO-B **(2BK3)**

The compounds shows π - π interactions and hydrogen bonding with the various active site amino acids and showed good binding affinity towards MAO-A and MAO-B with good docking score. On the basis of docking results we further synthesize 10 compounds **(VS-1 to VS-10)** that shows good binding affinity and good interactions with the MAO-A & B.

CHAPTER-5

SYNTHESISOF COMPOUNDS

5.1 Materials and methods

5.1.1 General

1. The reagents were purchased from Sigma-Aldrich, Loba-Chemie Pvt. Ltd., S.D. Fine Chemicals, Avra synthesis and used without further purification.

2. Thin layer chromatography was done on glass silica plates with silica gel G as the adsorbent. Ethyl acetate: Petroleum ether (1:1), (2:3) and Methanol: Chloroform (0.5% methanol in chloroform with 2-3 drops of ammonium hydroxide) mixtures were used as solvent system for the chromatographic purification of compounds. Spots were visualized under UV light and iodine chamber.
3. Infrared spectra of compounds were recorded on Bruker IR spectrophotometer.
4. The ^{1}H and ^{13}C NMR of the compounds were recorded on Bruker Advance II instrument at 400 MHz frequency, in $CDCl_3$, DMSO and TMS (δ=0) as internal standard at IIT Ropar, and Panjab University, Chandigarh.
5. Mass spectra were recorded on GC-MS (ESI), Central Instruments laboratory (CIL), Central University of Punjab, Bathinda.
6. Reactions were carried out under Reflux conditions at 90^{o}C and on simple stirring at room temperature.

5.2 Synthesis

5.2.1 Synthesis of piperazine based analogues as MAO inhibitors

It was proposed to synthesize two series of compounds wherein first series involve reaction of benzoyl halides or phenylsulfonyl with phenylpiperazine while the second series involve C-N coupling of aryl bromides with phenylpiperazines.

5.2.2 Synthesis of first series of compounds

For the synthesis of first series of compounds initially benzoyl chloride was reacted with phenylpiperazine in DCM under ice cold conditions in the presence of potassium carbonate as base. The reaction mixture was stirred at room temperature and after completion of reaction as confirmed by TLC, the reaction mixture was worked up and

the product was analyzed through GCMS. Similarly a series of compounds were synthesized as reported in Table 5.1 by using substituted benzoyl chlorides and phenylsulfonyl chlorides. General procedure for the synthesis of compounds is reported as given below.

5.2.3 General Procedure for compounds (VS-1 to VS-5 and VS-8)

In 100ml round bottom flask (RBF) a dichloromethane (7ml) , aryl/alkyl amine (0.5eq.) and potassium carbonate (2eq.) was added kept it on stirring for 5 min at 0^{o}C. Then substituted benzoyl or sulfonyl chloride (1.5eq.) was added slowly in proportions and the reaction was kept on stirring for 4-8 hr at room temperature. The reaction was confirmed through the TLC. After completion of the reaction, DCM was evaporated on rotavapor, the reaction mixture was extracted with water and ethylacetate, then washing with brine and passed the product through anhydrous sodium sulphate. Then the product was dried on rotavapor and was confirmed by checking TLC at 50% ethylacetate in petroleum ether. The purification of the product was done by column chromatography.

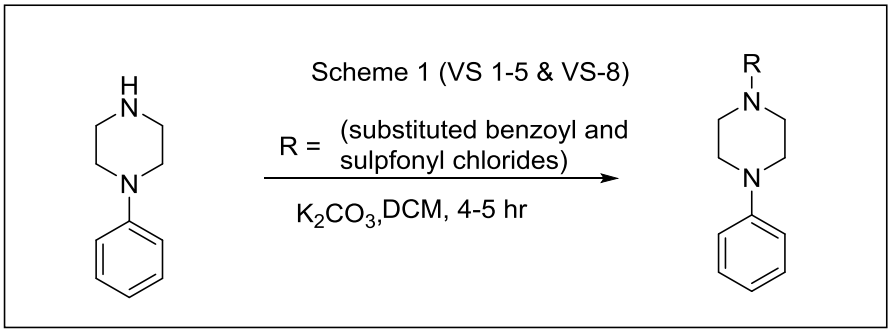

Fig. 5.1 General reaction scheme for compounds VS-1 to VS-5& VS-8

5.2.4 Synthesis of second series of compounds

For the process optimization of C-N bond formation, the reaction was carried out in presence of phenylpiperazine, bromobenzene, sodium hydride (NaH), and DMF (dry) at 0^{o}C, the reaction was unsuccessful as confirmed by TLC.

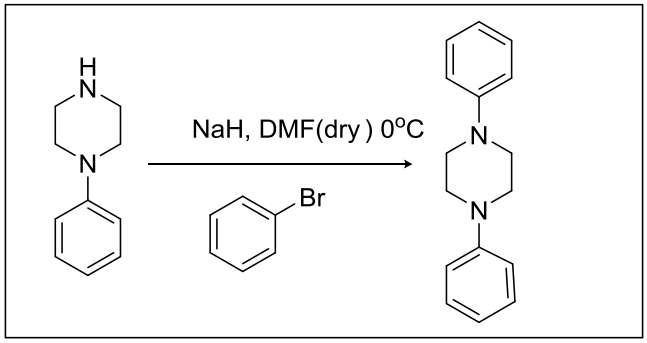

Fig. 5.2 Process optimization for C-N bond formation reaction

Then the 2nd scheme is applied for C-N bond formation where the reaction was carried out in microwave in presence of ionic liquid.

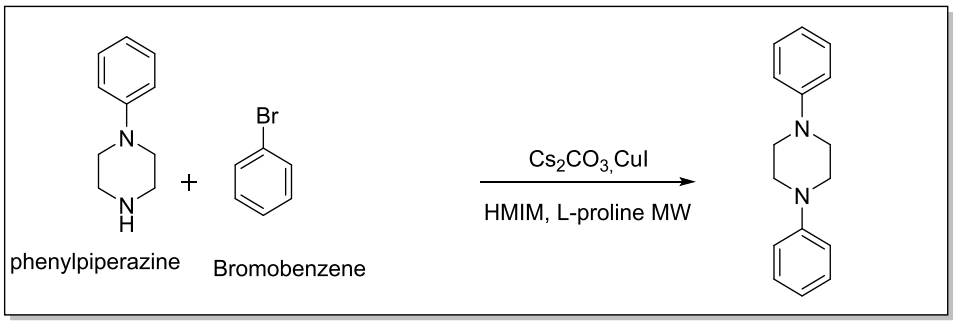

Fig. 5.3 C-N bond formation reaction in presence of ionic liquid under microwave

The reaction was completed and product peak was observed by GCMS however the yield was very low.

Thereafter a copper catalyzed protocol (Zhang *et al.*, 2005) was explored for the C-N bond formation reaction in which the CuI was used as a catalyst and amino acid proline act as a promoter and DMSO as a solvent. The chelation of Cu(I) with an amino acid makes Cu(I) species more reactive toward the oxidative addition, or/and stabilize the oxidative addition, thereby promoting the coupling reaction. In the absence of L-proline the product yield was not so good but in the presence of L-proline sufficient yield was obtained which indicates that the L-proline is a reliable promotor for aryl/alkyl bromides with aryl/alkyl amine. The reaction was successful and different arylhalides were coupled with phenylpiperazine for the formation of target molecules.

5.2.5 General Procedure for Compounds (VS-6, VS-7, VS 9 & VS-10)

A mixture of alkyl amine (phenylpiperazine),aryl halide (1.1equiv.), $CsCO_3$(2equiv.), CuI (0.1 equiv.), and the appropriate amino acid (L-proline 0.2 equiv.) in DMSO was refluxed and heated at 90^{o}C for 24 hr. Around 10ml of ammonium chloride, was added in the reaction mixture and kept it on stirring for half hour. The cooled mixture was partitioned between water and ethylacetate. The organic layer was separated, and the aqueous layer was extracted with ethyl acetate. The combined organic layers were washed with brine, dried over Na_2SO_4, and concentrated on rotavapor. The product was purified by Column chromatography.

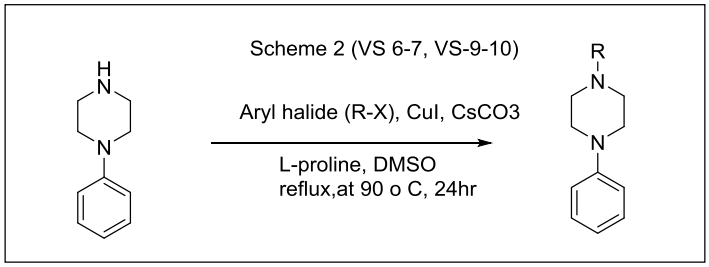

Fig. 5.4 General reaction scheme for compounds VS-6, VS-7,VS-9 & VS-10

Table 5.1: Spectral analysis data of the synthesized compounds VS-1 to VS-10

Product name	Structure	Spectral analysis
VS-1 $C_{17}H_{18}N_2O$	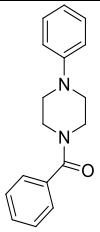	**IR (KBr cm^{-1})**: 3329 (NH stretch), 2212 (CN stretch), 1683 (C=O stretch), 1830.10 (C=C stretch).**^{1}H NMR** (400MHz, $CDCl_3$, TMS = 0)δ: 3.25 (4H, t, *J*= 4 Hz), 3.65 (4H, t, *J*= 8 Hz), 6.95(2H, d, *J*= 8 Hz), 7.25 (1H, t, *J*= 8 Hz), 7.30 (2H, d, *J*= 8 Hz), 7.43(1H, t, *J*= 8 Hz), 7.60(2H, d, *J*= 4 Hz), 8.08 (2H, d, *J*= 8 Hz).**^{13}C NMR** (100 MHz, $CDCl_3$, TMS = 0) δ: 130.0, 129.4, 128.7, 127.2, 117.0, 49.12, 47.52 **Mass spectrometry:*m/z:*** 266

VS-2 $C_{18}H_{20}N_2O_2$	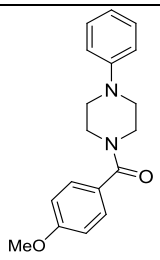	**IR (KBr cm^{-1})**: 1683 (C=O stretch), 1239(CN stretch), 2961(CH stretch), 1310(CO stretch), 1298.15 (CC stretch) 1830.10 (C=C stretch),**^{1}H NMR** (400MHz, $CDCl_3$, TMS = 0) 3.13 (3H, s,)3.78 (4H, t, *J*= 8 Hz), 3.82 (4H, t, *J*= 8 Hz),6.69 (2H, d, *J*= 4 Hz), 7.23 (1H, t, *J*= 8 Hz), 7.36(2H, d, *J*= 8 Hz),**^{13}C NMR** (100 MHz, $CDCl_3$, TMS = 0) δ: 171.09, 170.55, 164.66, 164.06, 162.39, 160.99, 132.94, 132.42, 129.35, 121.69, 116.88, 114.21, 113.86, 113.82, 55.6, 49.98, 47.5. **Mass spectrometry:*m/z:*** 296
VS-3 $C_{16}H_{17}N_3O_4S$	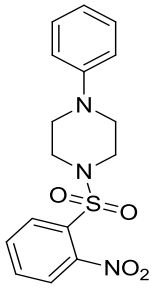	**IR (KBr cm^{-1}):** 1237(CN stretch), 2988(CH stretch), 1690(C=O stretch), 1298.15 (CC stretch) 1050.87 (S=O stretch), 1529 (NO_2 Symmetric stretch)**^{1}H NMR** (400MHz, $CDCl_3$, TMS = 0)3.26(4H, t, *J*= 4Hz), 3.49 (4H, t, *J*= 8Hz), 6.94 - 7.00 (3H, m), 7.26 -7.30 (2H, m), 7.63 – 7.64 (1H, m), 7.70 - 7.73 (2H, m), 8 (1H, d, *J*= 8 Hz).**^{13}C NMR** (100 MHz, $CDCl_3$, TMS = 0) δ: 148.21, 134.06, 131.73, 131.10, 129.53, 124.33, 117.42, 49.97, 45.87 **Mass spectrometry: *m/z:*** 347

VS-4 $C_{18}H_{21}ClN_3O_4S$	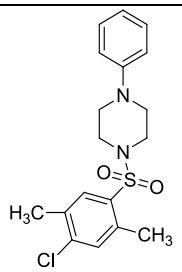	**IR (KBr cm^{-1})**: 1231.34(CN stretch), 2932.14(CH stretch), 1166.13 (CC stretch) 1830.10 (C=C stretch), 942.41(S=O stretch)**^{1}H NMR** (400MHz, $CDCl_3$, TMS = 0) 2.33 (3H, s), 2.51 (3H, s), 3.15 (4H, bd), 3.24 (4H, bd), 6.84 (3H, m), 7.18-7.20 (2H, m), 7.24 (1H, s), 7.72(1H, s).**^{13}C NMR** (100 MHz, $CDCl_3$, TMS = 0) δ: 150.80, 139.39, 137.05, 134.39, 133.58, 133.23, 132.73, 129.41, 121.03, 117.08, 49.51, 45.39, 20.34, 19.72. **Mass spectrometry:*m/z:*** 364
VS-5 $C_{20}H_{26}N_2O_2S$	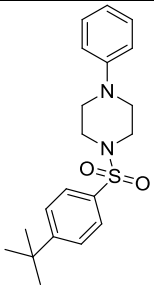	**IR (KBr cm^{-1}):** 1242(CN stretch), 3069(CH stretch), 946.58(S=O stretch), 1166.39 (CC stretch), 1919.17(C=C stretch)**^{1}H NMR** (400MHz, $CDCl_3$, and TMS = 0) 1.33 (9H, s), 3.22 (4H, t, *J*= 8 Hz), 3.24 (4H, t, *J*= 8 Hz), 6.87 (3H, m), 7.24 (2H, m), 7.53 (2H, d, *J*= 8 Hz), 7.69 (2H, d, *J*= 8 Hz). **^{13}C NMR** (100 MHz, $CDCl_3$, and TMS **=** 0) δ: 156.93, 150.79, 132.19, 129.40, 127.92, 126.23, 121.02, 117.04, 49.34, 46.21, 35.34, and 31.22**. Mass spectrometry:*m/z:*** 358
VS-6 $C_{16}H_{18}N_2$	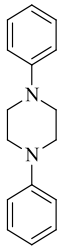	**^{1}H NMR** (400MHz, $CDCl_3$, and TMS = 0) 3.37(8H, s), 6.91 (2H, m), 7.01 (4H, m), 7.26 (4H, m) **^{13}C NMR** (100 MHz, $CDCl_3$, and TMS = 0) δ: 129.38, 116.63, 49.58, and 31.11 **Mass spectrometry:*m/z:*** 238.

VS-7 $C_{19}H_{19}N_3$	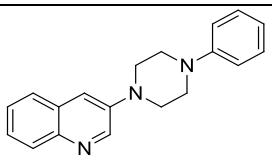	**^{1}H NMR** (400MHz, $CDCl_3$, and TMS = 0) 2.61 - 2.77 (4H, m), 3.36 – 3.38 (4H, m), 3.47(4H, t, *J*= 8 Hz), 7.26 (3H, m), 7.35 (1H, d, *J*= 4 Hz), 7.46 (4H, m), 7.48 (1H, d, *J*= 4 Hz), 7.98(1H, d, *J*= 8 Hz), 8.79 (1H, bd) **^{13}C NMR** (100 MHz, $CDCl_3$, and TMS = 0) δ:145 11, 143.01, 128.99, 127.14, 126.76, 126.70, 117.76, 54.83, 49.06,. **Mass spectrometry:*m/z:*** 289.
VS-8 $C_{18}H_{20}N_2O$	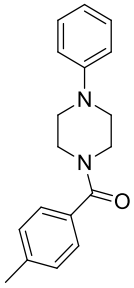	**IR (KBr cm^{-1}):** 3329 (NH stretch), 2212 (CN stretch), 1683 (C=O stretch), 1034.68 (CC stretch). **^{1}H NMR** (400MHz, $CDCl_3$, TMS = 0) 2.31 (3H, s), 3.08 – 3.15 (4H, bd), 3.56 – 3.85 (4H, bd), 6.82 – 6.87 (3H, m), 7.15 (2H, d, *J*= 8 Hz), 7.18 – 7.23 (2H, m), 7.27 (2H, d, *J*= 8 Hz)**^{13}C NMR** (100 MHz, $CDCl_3$, TMS = 0) δ: 170.74, 151.08, 140.18, 132.69, 129.39, 129.26, 127.37, 120.77, 116.88, 50.05, 47.84, 42.28, 21.55. **Mass spectrometry:*m/z:*** 280.
VS-9 $C_{20}H_{20}N_2$	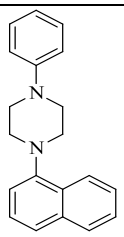	**IR (KBr cm^{-1})**: 1116.36(CN stretch), 2944(CH stretch), 1030.98 (CC stretch) 1830.10 (C=C stretch)**^{1}H NMR** (400MHz, $CDCl_3$, TMS = 0) 3.34(4H, s), 3.52 (4H, s), 6.97 (1H, bd), 7.16 (1H, d, *J*= 4 Hz), 7.26 (2H, m), 7.35 (2H, m), 7.43 - 7.46 (1H, m), 7.49 (2H, m), 7.59 (1H, d, 8 Hz), 7.84 (1H, d, 8 Hz), 8.23 (1H, d, *J*= 8 Hz) **^{13}C NMR**(100 MHz, $CDCl_3$, and TMS = 0) δ: 134.87, 129.51, 128.63, 126.06, 126.01, 125.68, 124.04, 123.46, 115.01, 114.98, 52.90, 50.0. **Mass spectrometry:*m/z:*** 288.

VS-10		**Mass spectrometry:*m/z:*** 338. NMR spectra was not clear. It may be possible that the product was degraded during transportation for NMR. TLC showed single spot

Table 5.2: Chemical Analysis data of the synthesized compounds

Code	Molecular weight	Color	Yield (%)
VS-1(25)	266.34	Apricot	62
VS-2(26)	296.36	Apricot	56
VS-3(27)	347.39	Off white	82
VS-4(28)	364.89	light orange	76
VS-5(29)	358.50	Off white	85
VS-6(19)	238.33	Brown	42
VS-7(20)	289.37	Dark brown	68
VS-8(37)	280.36	Off white	87
VS-9(30)	288.39	Chocolate	43
VS-10(31)	338.44	Yellow	41

CHAPTER- 6

BIOLOGICAL STUDIES

6.1 Chemicals and Reagents

1. RPMI 1640 and DMEM, Penicillin/ Streptomycin antibiotic solution, phosphate buffer saline (PBS) and fetal bovine serum (FBS) media were used for culture of the neuronal cell lines and were purchased from HiMedia.
2. DMSO, extrapure AR was purchased from SRL/ HiMedia.
3. Amplex red monoamine oxidase kit was purchased from Molecular probes (Invitrogen) Life technologies, India.
4. MTT dye used for MTT assay was purchased from HiMedia

6.2 Instruments

Table 6.1 List of Instruments used in Biological Studies.

Instruments Used	**Company**	**Purpose**
CO_2 Incubator	Galaxy, New Brunswick	Incubation
Centrifuge 5430 R	Eppendorf, Germany	Centrifugation
Laminar air flow	Klen Airflow	For aseptic condition
Microplate Reader	Biotek	Absorption studies and Fluorescence studies
Inverted microscope	Magnus, Olympus	Visualization of the cells

6.3 Cell lines used for biological studies

Table 6.2: Cell Lines under Study

Properties	**SH-SY5Y**	**IMR-32**
Organism	*Homo sapiens*, human	*Homo sapiens*, human
Adherent or Non-adherent	Adherent	Adherent

Disease	Neuroblastoma	Neuroblastoma
Storage conditions	Liquid nitrogen vapor phase	Liquid nitrogen vapor phase
Culture conditions	**Atmosphere:** air, 95%; carbon dioxide (CO_2), 5% **Temperature:** 37°C	**Atmosphere:** air, 95%; carbon dioxide (CO_2), 5% **Temperature:** 37°C

6.4 Routine Assay performed in Cell Culture Laboratory

A. Culturing of the cell lines

Human neuroblastoma cells were grown in the appropriate medium (DMEM). Trypsin is added to detach the cells (trypsinization). Subsequently, trypsin was inactivated by the addition of media containing serum (1mL). Centrifugation was done on 1200 rpm at 4˚C for 5-10 min for harvesting the cells. Further, supernatant was disposed and resuspension of the cell pellet was done using 2 mL of the complete media. The cell number was counted using haemocytometer or automated cell counter (Invitrogen).

B. Maintenance and sub-culturing of cell lines

The maintenance of cultured cell lines (SH-SY5Y & IMR-32) was done in 25 cm^2 or 75 cm^2 flasks containing DMEM medium supplemented with 10% FBS, 1X Penicillin and Streptomycin antibiotic solution and afterward incubated at 37˚C in a humidified atmosphere containing 5% CO_2 and 95% humidity.

The cells were sub cultured in 25 cm^2 flasks and maintained until they attained 70-80% confluency. The reagents necessary for the procedure were placed in water bath maintained at 37˚C for 10-15 min earlier to the sub-culturing. During sub-culturing, trypsin was added. After 5 min, 1 mL of media containing serum was added for ceasing the action of trypsin. Cells were then transferred to 15 mL centrifuge tubes and

centrifuged for 10 min at 1200 rpm. The supernatant was cast aside and the pellet was again resuspended in complete media. The cell lines were transferred to fresh media every three days.

6.5 MAO inhibitory assay

The phenylpiperazine derivatives (1-10) that were synthesized in the previous chapter, were investigated as inhibitors of MAO-A & B. Compounds acting as inhibitors may be considered as potential lead compounds for the development of drugs for the treatment of Neurological disorders. These studies should establish if the goal of this study was achieved, namely the design of new potent, reversible and competitive inhibitors of the MAOs. As outlined in the Introduction, the objectives of this chapter were as follows: The phenylpiperazine analogues **(VS-1 to VS-10)** that were synthesized in the previous chapter, will be evaluated as inhibitors of MAO-A and MAO–B. The inhibition potencies will be expressed as the IC_{50} values for the inhibition of the MAO`s. For this purpose, the recombinant human enzyme (isolated through mitochondrial lysate) was employed. A fluorometric assay was used to measure the enzyme activities. The MAO activity measurements were based on measuring the amount of H_2O_2 that is produced in the oxidation process. The H_2O_2 reacts with amplex Red in the presence of peroxidase form “resorufin”. The quantity of resorufinin the reactions is proportional to the amount of H_2O_2 produced by the enzyme and was subsequently be determined by measuring the fluorescence of the supernatant at an excitation wavelength of 560 nm and an emission wavelength of 590 nm (Zhou & Panchuk-Voloshina, 1997) and as per the manufacturer’s protocol (Life technologies).

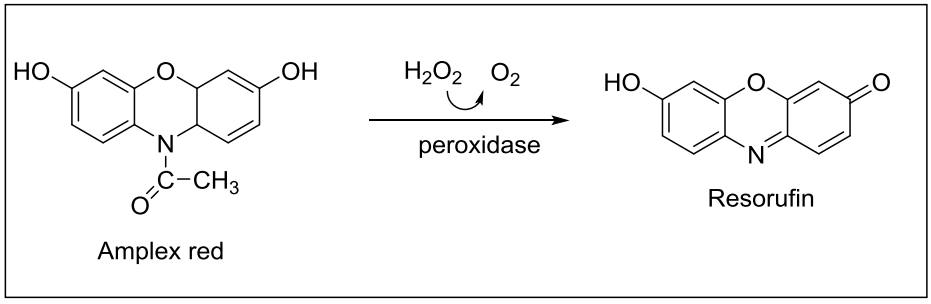

Fig.6.1 Reaction scheme for the formation of resorufin, the fluorescent product from amplex Red.

Step1.*Isolation of mitochondria*

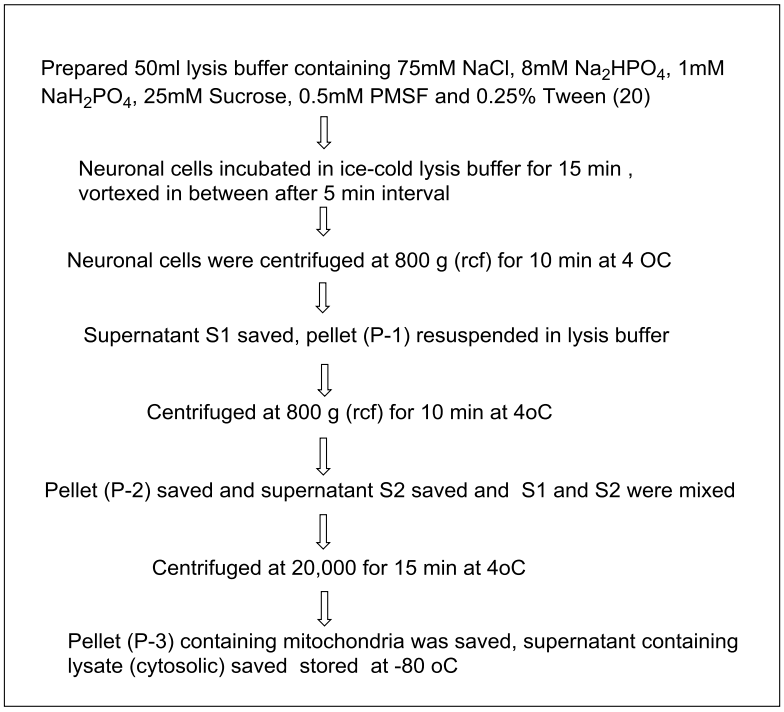

Fig. 6.2 Schematic representation of mitochondrial isolation protocol.

Step2. *Preparation of mitochondrial lysate*

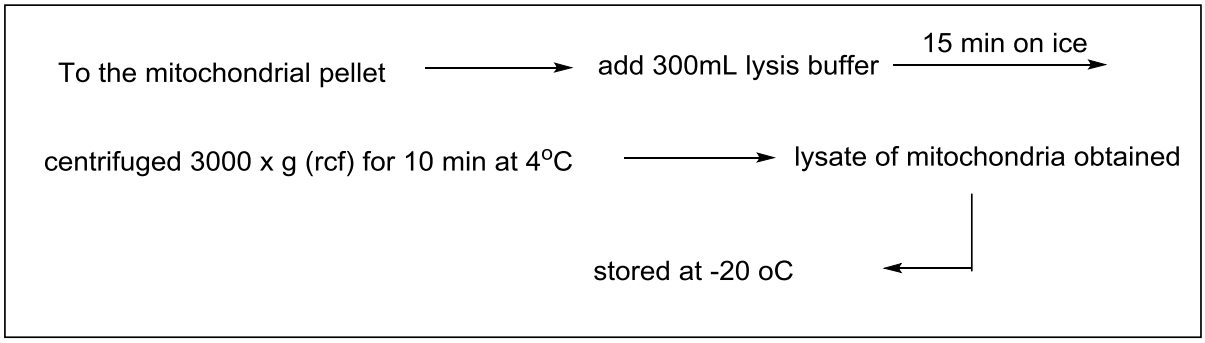

Fig. 6.3 Schematic representation of mitochondrial lysate preparation protocol.

Step 3. *Determination of protein concentration using Bradford assay*

The **Bradford protein assay** is a spectroscopic analytical procedure used to measure the concentration of protein in a solution. The protein concentration in mitochondrial lysate isolated from SH-SY5Y cells was estimated using Bradford method (Zor &

Selinger, 1996). This method involves binding of Coomassie Brilliant Blue with protein causing shift in absorption maximum at 595nm. The color reagent was prepared by dissolving 0.050g of CBB G-50 in 25% ethanol and 42.5% orthophosphoric acid and volume was made up to 100ml with distilled H_2O.The standard curve was prepared using various concentration of 1mg/ml BSA stock. The 20µl of coloring reagent was added to each tube and absorbance was measured after 10 minutes at 595 nm on spectrophotometer in multiplate reader (Biotek).

Step 4. Determination of MAO-A and MAO-B activities

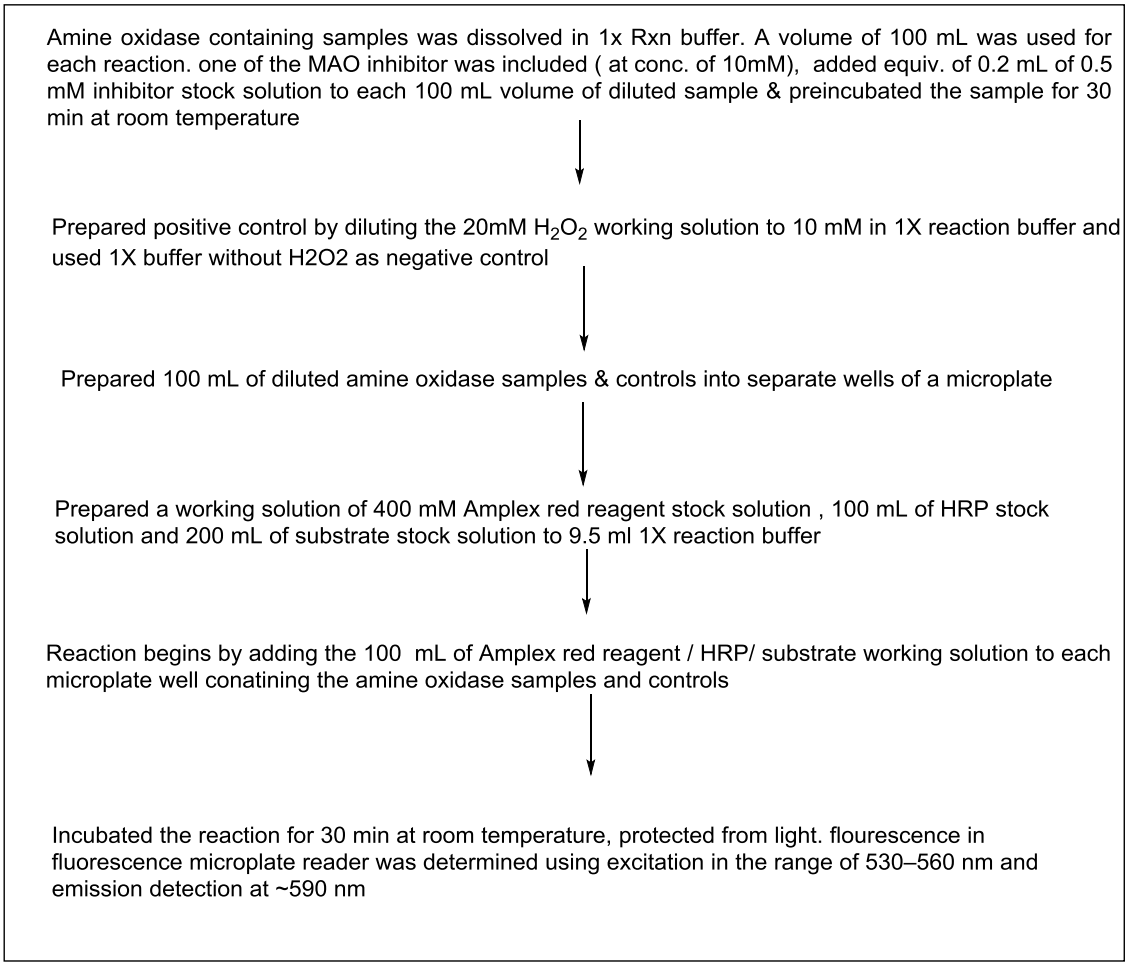

Fig. 6.4 Protocol for MAO inhibitory assay

Recent reports were shown that cytotoxicity is the critical issues for the success of the new therapeutic agent. Therefore now a days it is becoming indispensable to evaluate the cytotoxicity profile of the new chemical entity in the preliminary clinical studies.

Hence we performed MTT assay for the validation of our newly synthetics for the cytotoxicity.

6.6 MTT (3-(4, 5-dimethylthiazol-2-yl)-2, 5-diphenyl tetrazolium bromide) Assay:

MTT assay is a colorimetric assay(Mirzayans *et al.*, 2007)which is a cell proliferation or cell viability assay. MTT, a yellow tetrazole, is 3-(4, 5-dimethylthiazole-2-yl)-2, 5-diphenyl tetrazolium salt of bromine which is reduced to purple formazan in living cells. Mitochondrial reductase (succinate dehydrogenase) has the ability to reduce the MTT to a purple colored formazan product. This conversion is achieved only in the metabolically active cells and not otherwise. The underlying principle of MTT assay involves the tetrazole dye entering the cells. If the cells are metabolically active then they are reduced by succinate dehydrogenase to the formazan product as shown below. This formazan is not easily solubilized; thus either dimethylsulfoxide, an acidified ethanol solution or a solution of 51 detergent SDS in dilute HCl is added. The absorbance of the colored product is read spectrophotometrically at wavelength between 500-600nm.

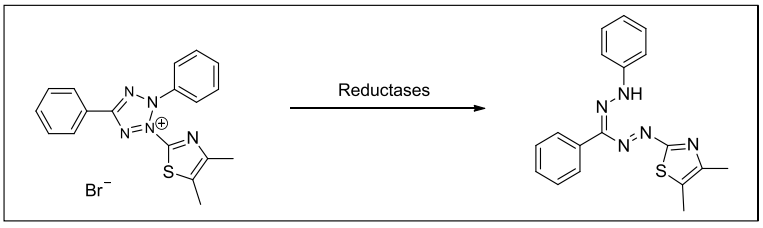

Fig. 6.5 Reduction of MTT by reductases

Material: MTT (3-[4,5-dimethylthiazol-2-yl]-2,5-diphenyl tetrazolium bromide), PBS, DMSO

Procedure: The number of cells from the SH-SY5Y and IMR-32 cell lines were counted on the automated cell counter. About 8,000-10,000 cells were seeded in each well of the 96 well plate. The plate was incubated at 37˚C with 5% CO_2 for 24 hr. At the end of the 24 hr, treatment was given to the cells in triplicate concentrations of 5 µM, 25 µM and 50 µM. The cells were further incubated for 48 hr. The media was removed from each well and MTT solution (5 mg/10mL) was added. This was incubated in the dark for 4 h. At the end of 4 hr, the MTT solution was disposed from each well and the

intracellular precipitate was dissolved in DMSO solution and the absorbance of the violet colour formed as consequence of DMSO addition is read spectrometrically at 570 nm.

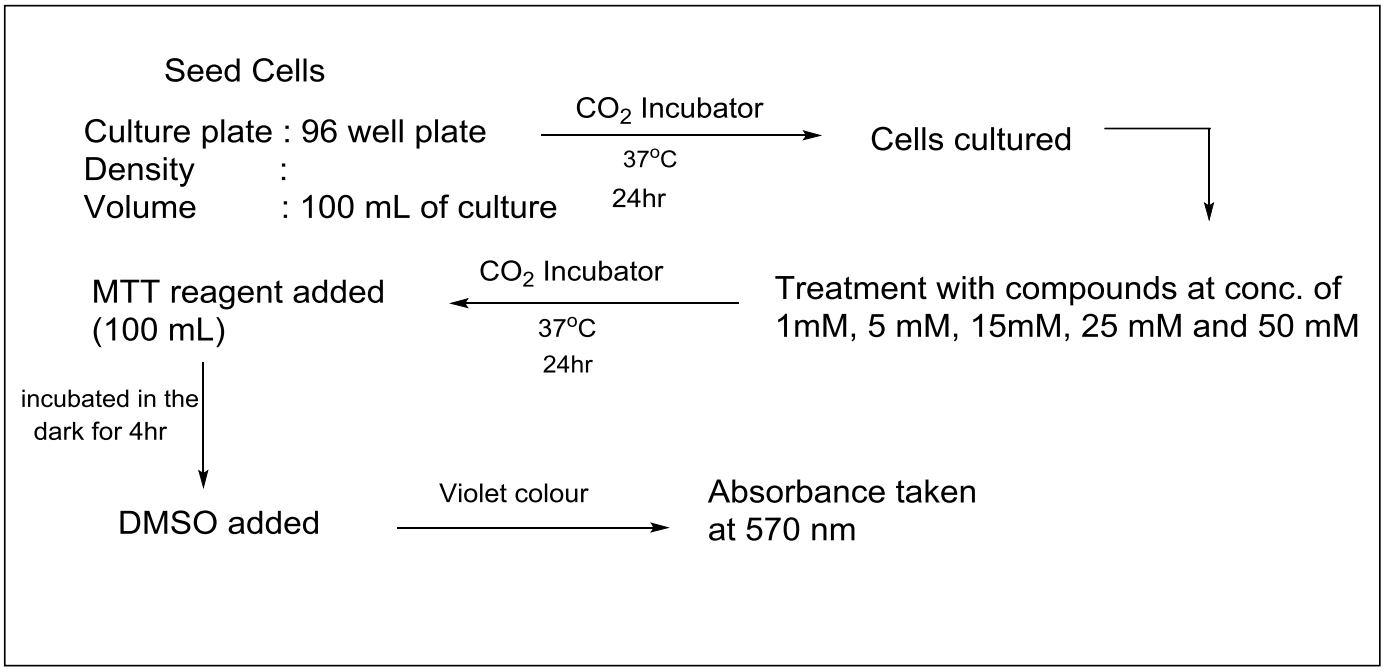

Fig.6.6 Schematic Representation of MTT Assay Protocol

CHAPTER- 7

RESULTS AND DISCUSSION

7.1 Molecular docking studies

From review of literature it is clear that the cavity of MAO-A enzyme is hydrophobic and slightly impinged with hydrophilic amino acid which suggest that the molecules designed for the MAO-A activity should be lipophilic in nature having slight polarity. Docking studies of compounds VS1 to VS-16 were performed on four different software's including Schrodinger, AutoDock, MOE and AutoDock Vina. All the compounds were docked with both MAO-A and MAO-B enzyme using PDB ID 2Z5X for MAO-A; and 2BK3 for MAO-B. From the docking studies of compounds with MAO-A, the binding energy score suggested that the molecule with polar substitution show better binding inside the active cavity. From interaction patterns of proposed compounds it reveals that the compounds are surrounded by the active site amino acid residues hence completely fits into the active site. Compounds having heterocyclic nucleus along with phenylpiperazine moiety **(VS-7)** shows good binding energy. As the fused heterocyclic nucleus is replaced with single aromatic ring having carbonyl group with sulphoxide **(VS-4)** results in a slight increase in binding energy. Thus, it is clear that the compound with electron donating group showed higher binding affinity as compared to electron withdrawing groups. Electron donating group increases the electron cloud inside the ring which favors the π-π interactions with different amino acids of the active site cavity and fix the position of the molecule into the active site. So the compound with polar substitution such as **VS-4** shows better binding affinity than the compounds with non-polar substitution or less polar compounds. On the other hand, the active site of MAO-B contain lipophilic pocket which preferably interacts with the bulky and lipophilic ligands. Compounds**VS-3** and **VS-8** were found to be the best fitted compounds into the active site and showed good interactions with the active site amino acids of the MAO-B.There is an additional interaction with binding sites which suggested that the compound utilizes the conserved water molecule as in case of **VS-3 (Fig 4.4)** and other hydrophilic amino acids for additional binding and better pharmacological action. The docking study of the compounds suggested that the molecule having bulky groups such as anthracene moiety shows better binding affinity in comparison to others ligands. The molecule with electron withdrawing group shows almost equal effect as that of electron

donating group as there is only slight variation in their binding energy. Infact the molecule having no substitution or branching **(VS-6)** also shows good binding affinity with the receptor. As in case of MAO-B the polar substitutions decreases the binding affinity towards receptor, so the molecules which have nonpolar substitution are better molecule for MAO-B. The MAO-B cavity is mostly surrounded by hydrophobic amino acids, some hydrophilic amino acids are also present but they confine mainly at the periphery of cavity and they are not involve in the any interactions with ligands. So the proposed compounds such as anthracene substituted, and others shows better binding affinity than the compounds with polar substitution.

7.2 Synthesis

Research over the years has led to the development and introduction of several synthetic routes for the efficient synthesis of C-N bond formation. For the synthesis of the target compound, proposed **Scheme 1** (Zhang *et al.*, 2005) & **scheme 2** was followed.

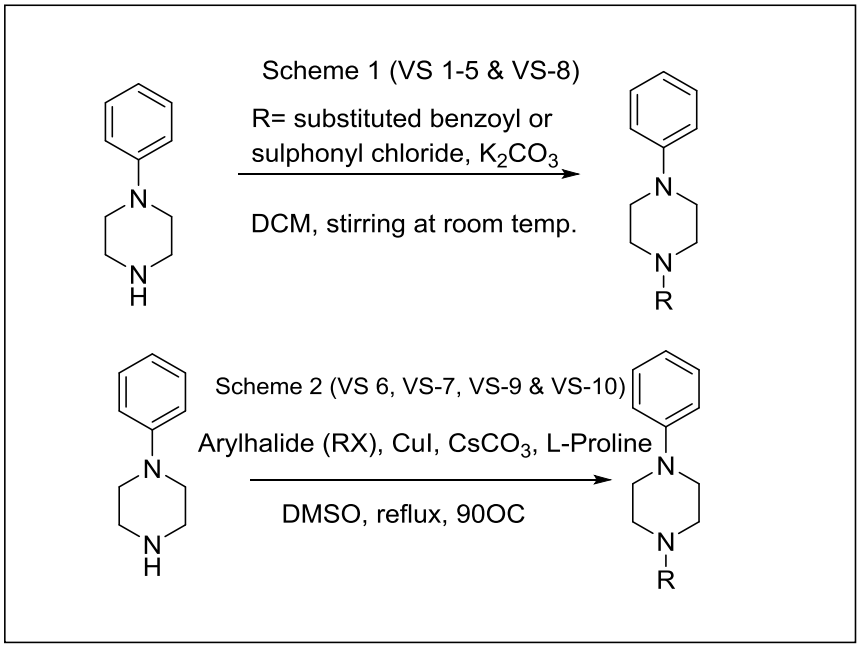

Fig. 7.1 Reaction schemes for synthesizing compounds **(VS-1 to VS-10)**

During the synthetic process, it was observed that the time taken for the completion of the reaction varied from compound to compound. The reaction time

was less in case of compounds prepared through **scheme 1** and yields were high as compared to the **scheme 2** compounds, where the product loss occurs due to the presence of DMSO. For the synthesis of compounds **VS-1 to VS-5 and VS-8,**the mixture of phenylpiperazine and substituted benzoyl or sulphonyl chloride was stirred in DCM as a solvent and K_2CO_3 at room temperature for 4 to 5hr and the progress of the reaction was monitored by TLC. In all the synthesized compounds, benzoyl chloride, 4-Methoxy benzoyl chloride, 2-Nitrobenzene sulfonyl chloride, 4-Chloro-2, 5-dimethylbenzene sulphonyl chloride, 4-*tert*-butylbenzene sulfonyl chloride, 4- Methyl benzoyl chloride used for the synthesis of **VS-2, VS-3, VS-4**,**VS-5 ad VS-8** respectively whereas for the synthesis of compounds **VS-6, VS-7, VS-9 and VS-10** the mixture of phenylpiperazine and aryl halide was refluxed in DMSO as solvent and CuI and L-proline were used as catalysts. The reaction was refluxed at 90^0C for 24 hr **(Scheme 2).** The progress of the reaction was monitored by TLC. Aryl halides for the compounds synthesized from scheme 2 includes Bromobenzene, 3-Bromoquinoline, and 1-Bromonapthalene. In all the cases, the completion of the reaction was ascertained primarily by TLC. The compounds were characterized by their FT-IR, Mass spectrometry and NMR Spectra.

IR spectra showed the peaks for aromatic amines in the range of 1242-1239 cm^{-1} which were lower than the normal value of 1335-1250 cm^{-1}.This lower than the expected value believed to be due to conjugation. The carbonyl groups in the range of 1690-1683 cm^{-1}, which were near to the normal value of 1710 cm^{-1}. Spectrum also represented other peaks at 1050-946 cm^{-1}(S=O) in case of sulfonyl, 1310 cm^{-1}(C-O stretch) in case of methoxy, 1653-1585 cm^{-1}(C=C aromatic), 1529 cm^{-1} (N-O asymmetric stretch).

The ^{1}H spectrum of representative compounds showed that the α -hydrogen to substituted nitrogen of phenyl piperazine is more deshielded than the normal range of 2.2-2.9 ppm and it comes in the range of 3.32-3.40 ppm. This is due to attachment of electron deficient substituents in various synthesized compounds which decreases the electron density around α – hydrogen and results in deshielding of NMR values. Another indication of product formation is the absence of direct coupling ^1J between nitrogen and attached hydrogen, having coupling constant in the range of 50 Hz. Product

formation is further confirmed by ^{13}C spectra in which, normally the unsubstituted aromatic carbon comes around 122 but N-C (aromatic carbon) peaks comes around 150 indicates that there is deshielding due to the presence of nitrogen, thus indicating the C-N bond formation. This is due to attachment of nitrogen of phenylpiperazine, directly to aromatic carbon. The deshielding effect is more pronounced in carbon spectra than proton spectra because of two atom effect than one i.e. H-C-X.

7.3 Biological evaluation of synthesized compounds

(a)Total MAO activity

A fluorescence based total MAO (A & B) activity was determined with Tyramine as substrate was performed. The known MAO-A and MAO-B inhibitors namely Clorgyline and Pargyline respectively showed significant inhibition in MAO-A activity by 36% and MAO-B activity by 52% respectively as compared to the vehicle control (total MAO-A + B) activity.

Table 7.1 Total MAO activity determined in the mitochondrial extracts of SH-SY5Y cells against known inhibitors and synthesized compounds designed as potential MAO inhibitors.

S.No.	Sample		Total MAO Activity(%)	% Inhibition
1	Control		100±0	---
2	Clorgyline (MAO-A Inhibitor)		64±2	36
3	Pargyline (MAO-B Inhibitor)		48±3	52
4	VS-1	1µM	58±10	42
		5µM	54±7	46
		10µM	49±3	51
		50µM	46±3	54
5	VS-2	1 µM	44±3	56
		5µM	45±4	55
		10µM	45±3	55
		50µM	51±4	49
6	VS-3	1µM	49±3	51
		5µM	54±3	46
		10µM	55±4	45
		50µM	90±5	10
7	VS-4	1µM	46±3	54

		5µM	48±3	52
		10µM	53±4	47
		50µM	57±3	43
8	VS-5	1µM	55±4	45
		5µM	53±5	47
		10µM	57±5	43
		50µM	52±4	48
9	VS-6	1µM	51±4	49
		5µM	52±5	48
		10µM	53±5	47
		50µM	60±4	40
10	VS-7	1µM	57±4	43
		5µM	58±6	42
		10µM	57±4	43
		50µM	61±5	39
11	VS-8	1µM	54±4	46
		5µM	54±4	46
		10µM	55±4	45
		50µM	58±4	42
12	VS-9	1µM	54±4	46
		5µM	52±3	48
		10µM	52±3	48
		50µM	52±3	48
13	VS-10	1µM	51±2	49
		5µM	51±3	49
		10µM	53±3	47
		50µM	59±4	41

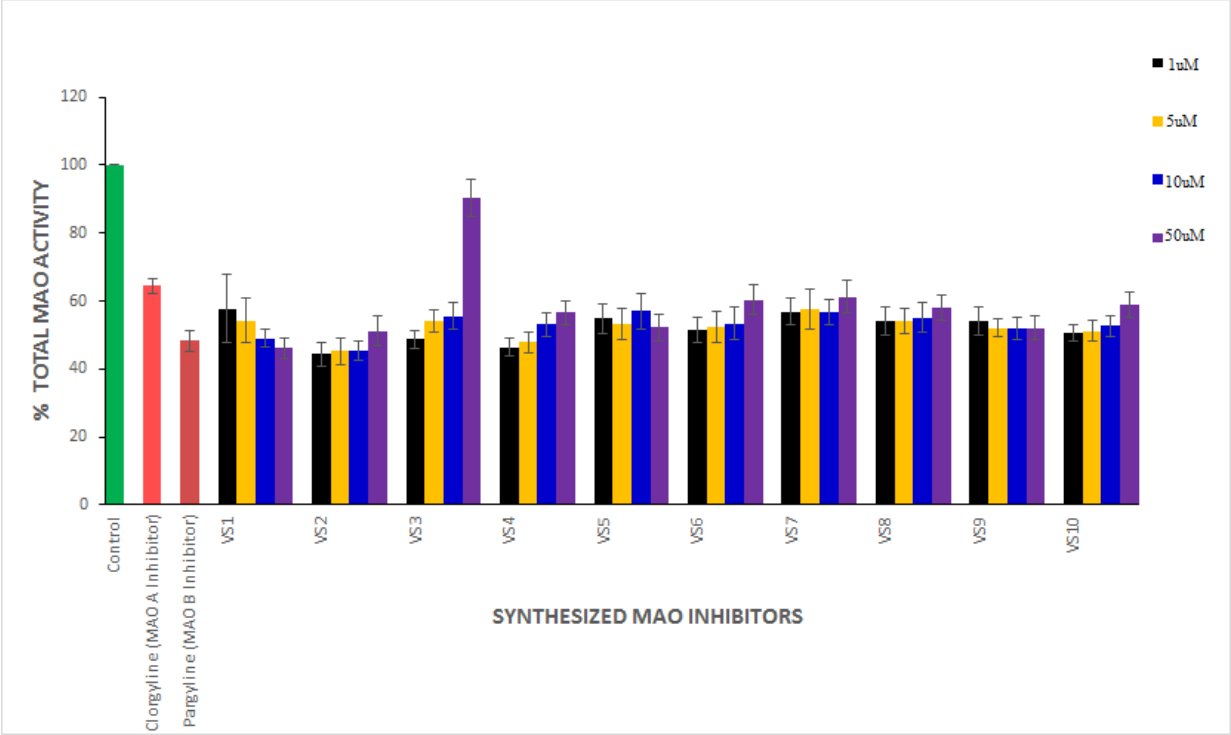

Fig. 7.2 Total MAO (A & B) activity in mitochondria lysates made from SH-SY5Y cells in the presence or absence of known and synthesized compounds designed as potential inhibitors for MAO.

The synthesized compound **VS-1**containing simple substituted benzoyl ring showed 42 % to 54 % inhibition in total MAO activity as compared to the control. **VS-5** containing a *tert*-butyl group and having substituted sulfonyl group, due to the presence of *tert*-butyl group lipophilicity of the compound increases and thus it displayed a moderate dose dependent inhibition in total MAO activity. Whereas, **VS-2, VS-3, VS-4, VS-6** and **VS-10** compounds also displayed slight inhibitory response. The **VS-3** compound displayed an interaction with the water molecule **(MD simulation studies**) and showed binding affinity towards MAO-B. Due to its hydrophilic nature **VS-3** was found out to be less inhibitory. Additionally, **VS-3** contains nitro group which makes the compound polar indicating that the presence of nitro group decreases the total MAO activity measured. Other compounds like **VS-7, VS-8** and **VS-9** displayed constant inhibitory response at all concentrations as compared to the control. These results indicate that the synthesized compounds possesses moderate inhibitory effect on total MAO (A & B)

activity. Further studies are required to evaluate specificity of these compounds by using MAO-B substrate benzylamine to establish specific nature of their inhibition.

With an aim to test the cytotoxicity of the synthesized compounds **(VS-1 to VS-10)**, MTT assay was carried out with human neuroblastomaSH-SY5Y and IMR-32 cell lines. Approximately 8,000-10,000 cells were seeded per well of 96 well plate, overnight grown and treated as indicated in the experimental design. Cells were grown with synthesized compounds at various concentrations (1µM, 5µM, 15µM, 25µM and 50µM) for 24 hr and 48 hr in humidified CO_2 incubator, maintained at 37 ^oC with 5% CO_2 under serum free condition.

After the treatment and incubation, cell viability assay was performed. Test compounds containing media was removed and 100µL of MTT (0.5 mg/ml) dissolved in 1x PBS. The 94 well plate was incubated for another 3 hr, which indicated purple colour crystals formation, which were subsequently dissolved in acidified DMSO. Dissolved purple colour crystals were read out at 570 nM in microplate reader (Biotek).

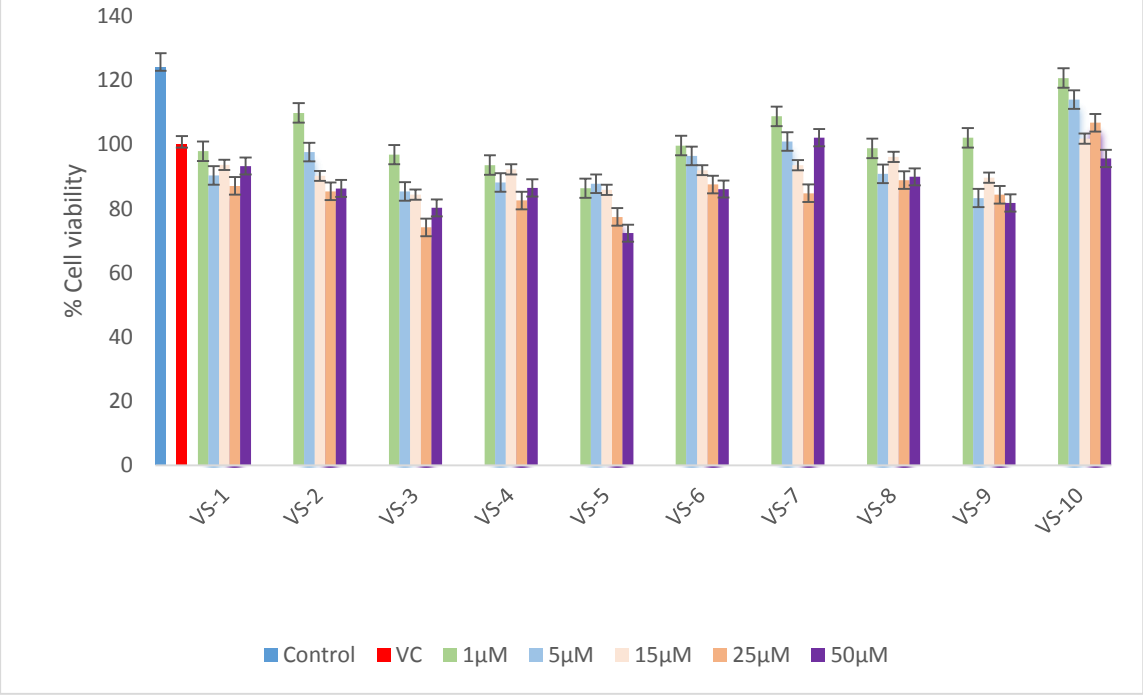

Fig. 7.3 Cell viability of SH-SY5Y cells in response to the treatment of synthesized compounds at various concentrations (1µM, 5µM, 15 µM, 25 µM, and 50 µM) for a time duration of 24 hr.

Table 7.2 Cell viability (%) of SH-SY5Y cells at different concentrations of synthesized compounds after 24 hr.

S.No.	Sample		Cell viability (%)
1.	Control		124±4
2.	Vehicle Control		100±2
3.	VS-1	1µM	98±5
		5µM	90±7
		15µM	94±0
		25 µM	87±5
		50µM	93±4
4.	VS-2	1µM	110±10
		5µM	98±16
		15µM	90±6
		25 µM	85±5
		50µM	86±4
5.	VS-3	1µM	97±5
		5µM	85±8
		15µM	84±2
		25 µM	74±10
		50µM	80±3
6.	VS-4	1µM	93±7
		5µM	88±2
		15µM	92±4
		25 µM	82±4
		50µM	86±8
7.	VS-5	1µM	86±6
		5µM	88±5
		15µM	86±4
		25 µM	77±5
		50µM	72±4
8.	VS-6	1µM	100±22
		5µM	96±7
		15µM	92±8
		25 µM	87±2
		50µM	86±2
9.	VS-7	1µM	109±20
		5µM	101±11
		10µM	93±3
		25 µM	85±5
		50µM	102±13
10.	VS-8	1µM	99±7
		5µM	91±5
		15µM	96±5

		25 µM	89±2
		50µM	90±2
11.	VS-9	1µM	102±6
		5µM	83±2
		10µM	90±8
		25 µM	84±6
		50µM	82±8
12.	VS-10	1µM	121±9
		5µM	114±2
		10µM	102±17
		25 µM	107±19
		50µM	96±1

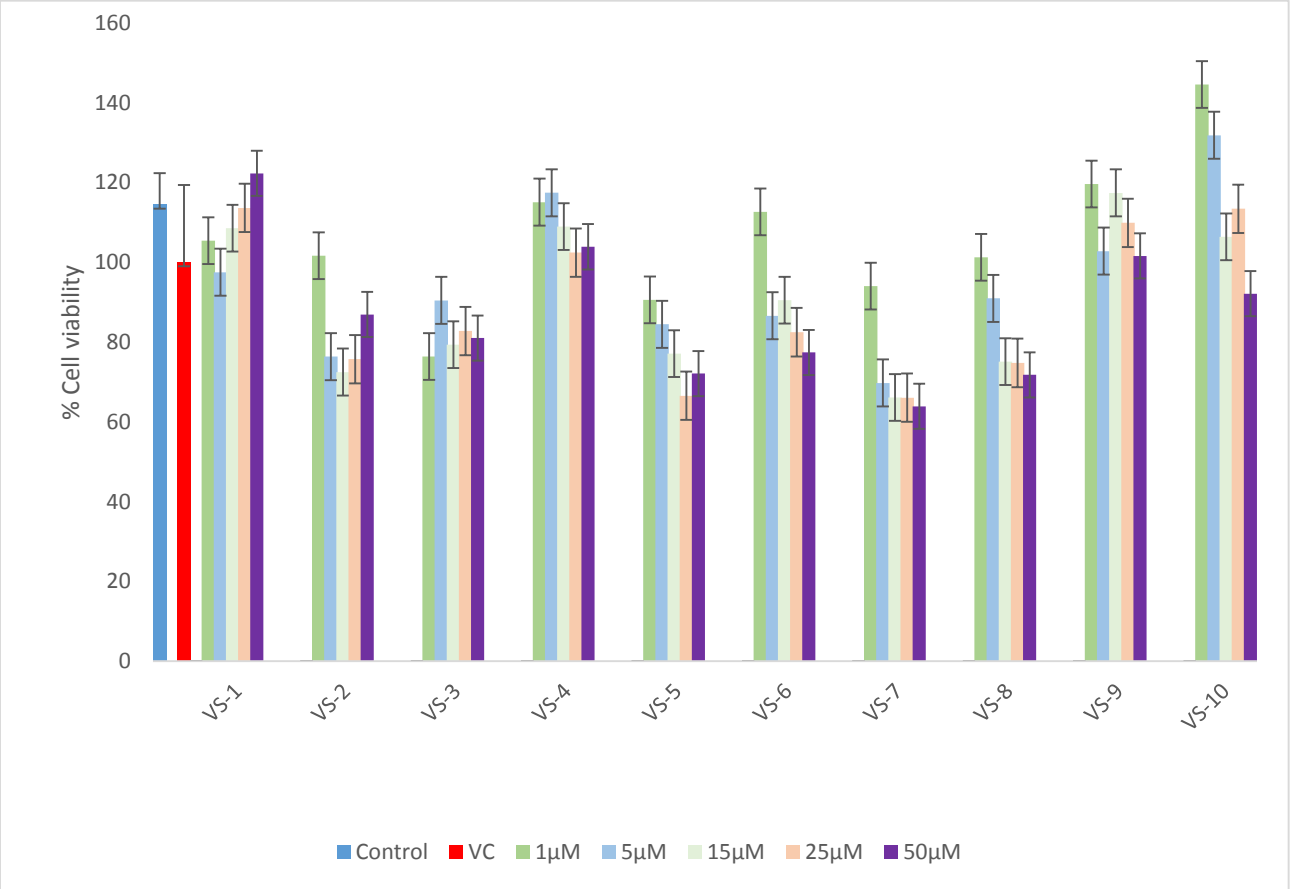

Fig. 7.4 Cell viability of SH-SY5Y cells in response to the treatment of synthesized compounds at various concentrations(1µM, 5µM, 15 µM, 25 µM, and 50 µM) for a time duration of 48 hr.

Table 7.3 Cell viability (%) of SH-SY5Y cells at different concentrations of synthesized compounds after 48 hr of treatment.

S.No.	Sample		Cell viability (%)
1.	Control		114±19
2.	Vehicle Control		100±7
3.	VS-1	1µM	105±30
		5µM	97±14
		15µM	108±14
		25 µM	114±11
		50µM	122±6
4.	VS-2	1µM	102±4
		5µM	76±6
		15µM	72±13
		25 µM	76±3
		50µM	87±6
5.	VS-3	1µM	76±14
		5µM	90±3
		15µM	79±10
		25 µM	83±11
		50µM	81±12
6.	VS-4	1µM	115±17
		5µM	117±15
		15µM	109±7
		25 µM	102±13
		50µM	104±18
7.	VS-5	1µM	91±7
		5µM	84±6
		15µM	77±3
		25 µM	66±8
		50µM	72±4
8.	VS-6	1µM	113±2
		5µM	87±3
		15µM	90±11
		25 µM	82±4
		50µM	77±10
9.	VS-7	1µM	94±10
		5µM	70±15
		10µM	66±10
		25 µM	66±6
		50µM	64±6
10.	VS-8	1µM	101±9
		5µM	91±18
		15µM	75±15
		25 µM	75±2

		50µM	72±2
11.	VS-9	1µM	120±5
		5µM	103±7
		10µM	117±24
		25 µM	110±8
		50µM	102±11
12.	VS-10	1µM	144±8
		5µM	132±5
		10µM	106±12
		25 µM	113±10
		50µM	92±11

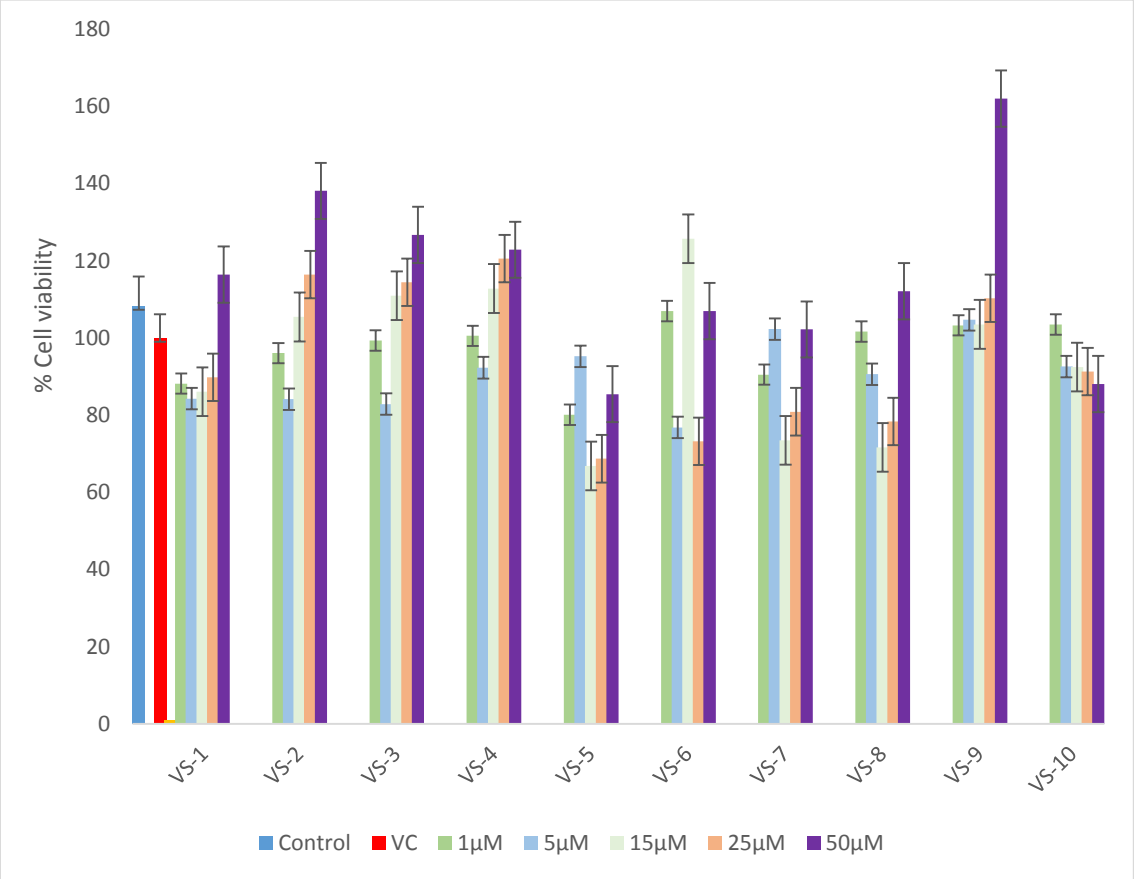

Fig. 7.5 Cell viability of IMR-32 in response to the treatment of synthesized compounds at various concentrations (1µM, 5µM, 15 µM, 25 µM, and 50 µM) for a time duration of 24 hr.

Table 7.4 Cell viability (%) of IMR-32 at different concentrations of various synthesized compounds after 24 hr of treatment.

S.No.	Sample		Cell viability (%)
1.	Control		108±7
2.	Vehicle Control		100±6
3.	VS-1	1µM	88±3
		5µM	84±14
		15µM	86±9
		25 µM	90±8
		50µM	116±3
4.	VS-2	1µM	96±1
		5µM	84±16
		15µM	105±9
		25 µM	116±6
		50µM	138±12
5.	VS-3	1µM	99±6
		5µM	83±14
		15µM	111±7
		25 µM	114±7
		50µM	127±5
6.	VS-4	1µM	100±15
		5µM	92±8
		15µM	113±9
		25 µM	120±0
		50µM	123±10
7.	VS-5	1µM	80±16
		5µM	95±3
		15µM	67±8
		25 µM	69±3
		50µM	85±4
8.	VS-6	1µM	107±12
		5µM	77±14
		15µM	126±3
		25 µM	73±4
		50µM	107±3
9.	VS-7	1µM	90±3
		5µM	102±11
		10µM	73±3
		25 µM	81±5
		50µM	102±11
10.	VS-8	1µM	102±13
		5µM	90±7
		15µM	72±8
		25 µM	78±6

		50µM	112±6
11.	VS-9	1µM	103±8
		5µM	105±8
		10µM	103±5
		25 µM	110±5
		50µM	162±9
12.	VS-10	1µM	103±6
		5µM	92±3
		10µM	92±5
		25 µM	91±3
		50µM	88±7

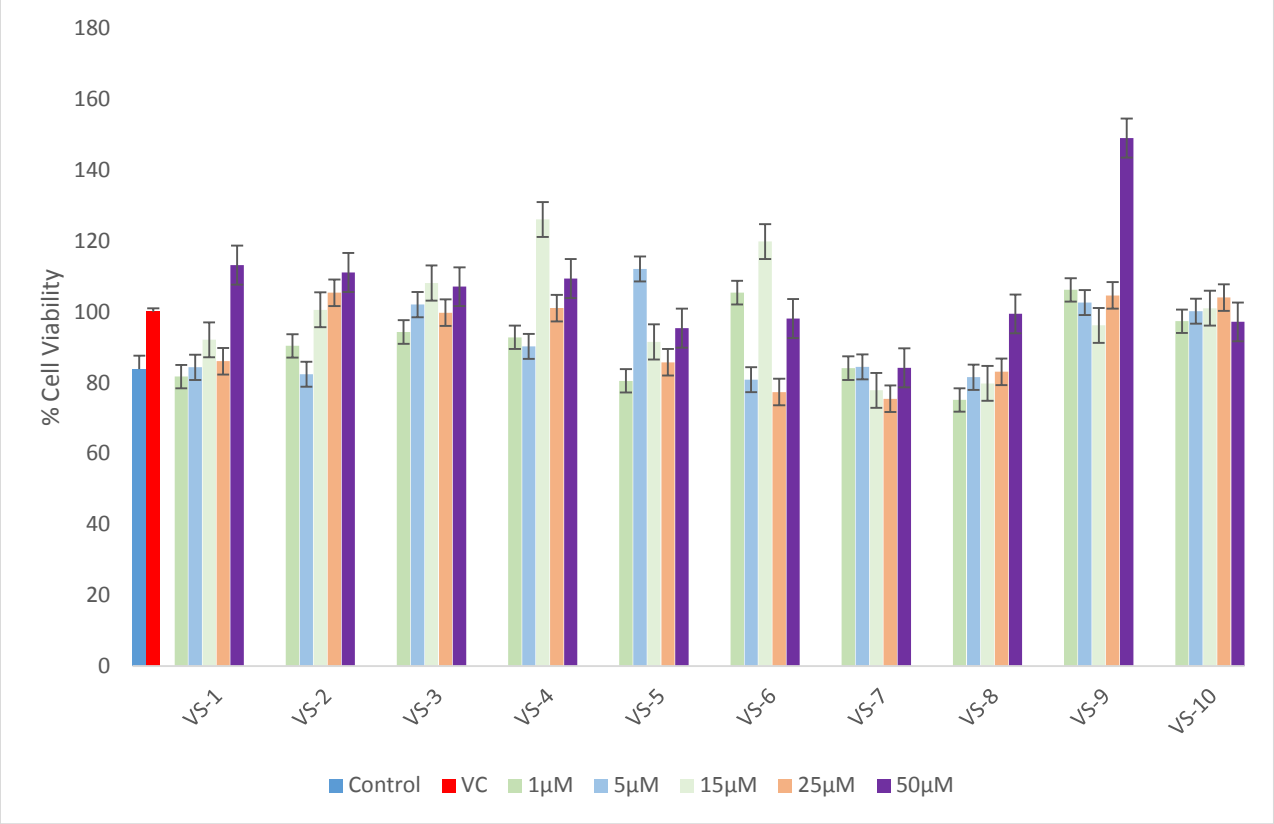

Fig.7.6 Cell viability of IMR-32 cells in response to the treatment of synthesized compounds at concentrations (1µM, 5µM, 15 µM, 25 µM, and 50 µM) for a time duration of 48 hr.

Table 7.5 Cell viability (%) of IMR-32 cells at different concentrations of various synthesized compounds after 48 hr of treatment.

S.No.	Sample		Cell viability (%)
1.	Control		83.76±3
2.	Vehicle Control		100±16
3.	VS-1	1µM	82±7
		5µM	84±1
		15µM	92±5
		25 µM	86±5
		50µM	113±5
4.	VS-2	1µM	90±6
		5µM	82±1
		15µM	100±9
		25 µM	105±8
		50µM	111±5
5.	VS-3	1µM	94±10
		5µM	102±0
		15µM	108±11
		25 µM	100±11
		50µM	107±4
6.	VS-4	1µM	93±6
		5µM	90±11
		15µM	126±11
		25 µM	101±4
		50µM	109±8
7.	VS-5	1µM	80±8
		5µM	112±6
		15µM	91±16
		25 µM	86±9
		50µM	95±2
8.	VS-6	1µM	105±4
		5µM	81±4
		15µM	120±0
		25 µM	77±7
		50µM	98±1
9.	VS-7	1µM	84±4
		5µM	84±8
		10µM	78±13
		25 µM	75±9
		50µM	84±5
10.	VS-8	1µM	75±10
		5µM	81±1
		15µM	80±10

		25 µM	83±4
		50µM	99±6
11.	VS-9	1µM	106±3
		5µM	102±12
		10µM	96±9
		25 µM	104±4
		50µM	149±12
12.	VS-10	1µM	97±4
		5µM	100±15
		10µM	101±5
		25 µM	104±7
		50µM	97±5

CHAPTER- 8

SUMMARY AND CONCLUSIONS

MAO inhibitors were the first drugs indicated for the treatment of depression. Though, they were used extensively from the 1950's and followed for the next two decades but their use declined because of the reported side effects in addition to their significant food and drug interactions i.e. Cheese effect. A large number of compounds are known which owe their MAO inhibitory potential to the heterocyclic ring present in the core structure. Taking evidence from such compounds, we also made an effort to synthesize 10 compounds having phenylpiperazine ring as the core structure. The progression and the subsequent completion of the reaction for each of 10 phenylpiperazine derivatives were confirmed by TLC. The purity of all the compounds were ascertained by column chromatography and characterized by IR spectroscopy, Mass spectrometry and NMR (^{1}H-NMR and ^{13}C-NMR) spectroscopy. The docking studies were also performed on both the isoforms of MAO enzyme using PDB ID (2Z5X) for MAO-A and (2BK3) for MAO-B. The docking studies revealed that the compounds fits well to the active site of enzyme with good binding energy and showing good interactions (including pi-pi interactions and H-bond interactions). The compound **VS-4** and **VS-7** was found to be more selective for MAO-A, whereas compounds **VS-3** and **VS-8** showed good binding affinity towards MAO-B. From the results it is clear that the compounds with electron donating group showed higher binding affinity towards MAO-A as compared to electron withdrawing groups. Electron donating group increases the electron cloud inside the ring which favors the π-π interactions with different amino acids of the active site cavity and fix the position of the molecule into the active site whereas, the molecule having bulky groups such as anthracene moiety shows better binding affinity towards MAO-B.

An attempt was made to evaluate the compounds for their MAO inhibitory activity. The MAO inhibition studies reveal that the known MAO-A and MAO-B inhibitors, Clorgyline and Pargyline respectively showed inhibition in MAO-A activity by 36 % and in MAO-B activity by 52 % respectively as compared to the control (total MAO) activity. The benzoyl and sulphonyl containing compounds having electron donating groups showed significant and promising MAO inhibitory nature. Thus concluded that the compounds having less polar substituents and low dipole moment possesses MAO inhibitory

potential as compared to the compounds having polar groups like nitro, which displayed less inhibitory effect. Further studies are required to evaluate specificity of these compounds by using MAO-B substrate benzylamine to establish specific nature of their inhibition. The cytotoxic nature of the synthesized compounds were assessed using two human neuroblastoma SH-SY5Y and IMR-32 cell lines. The synthesized compounds did not show cytotoxic response in both SH-SY5Y and IMR-32 indicating that these compounds are safe to be used.

CHAPTER-9

REFERENCES

Abdelhafez, O. M., Amin, K. M., Ali, H. I., Abdalla, M. M., & Batran, R. Z. (2012). Synthesis of New 7-Oxycoumarin Derivatives As Potent and Selective Monoamine Oxidase A Inhibitors. *Journal of Medicinal Chemistry* ***55***(23): 10424-10436.

Abdelhafez, O. M., Amin, K. M., Ali, H. I., Abdalla, M. M., & Batran, R. Z. (2013). Monoamine oxidase A and B inhibiting effect and molecular modeling of some synthesized coumarin derivatives. *Neurochemistry Internationa,* ***62***(2): 198-209.

Ahmeda, A., Molvia, K., Nazima, S., Baigb, I., & Memon Rahila, T. M. (2012). *Journal of Chemical and Pharmaceutical Research* ***4***(1): 872-880.

Al-Baghdadi, O., Prater, N. I., Van der Schyf, C. J., & Geldenhuys, W. J. (2012). Inhibition of monoamine oxidase by derivatives of piperine, an alkaloid from the pepper plant *Piper nigrum*, for possible use in Parkinson's Disease. *Bioorganic & Medicinal Chemistry Letter* ***22***(23): 7183-7188.

Alcaro, S., Gaspar, A., Ortuso, F., Milhazes, N., Orallo, F., Uriarte, E., Yanez, M., & Borges, F. (2010). Chromone-2- and -3-carboxylic acids inhibit differently monoamine oxidases A and B. *Bioorganic & Medicinal Chemistry Letter* ***20***(9): 2709-2712.

Blackwell, B., & Mabbitt, L. (1965). Tyramine in cheese related to hypertensive crises after monoamine-oxidase inhibition. *The Lancet* ***285***(7392): 938-940.

Blaschko, H., Richter, D., & Schlossmann, H. (1937). The oxidation of adrenaline and other amines. *Biochemical Journa,* ***31***(12): 2187.

Bolea, I., Juarez-Jimenez, J., de los Rıos, C., Chioua, M., Pouplana, R., Luque, F. J., Unzeta, M., Marco-Contelles, J., & Samadi, A. (2011). Synthesis, biological evaluation, and molecular modeling of donepezil and N-[(5-(benzyloxy)-1-methyl-1 H-indol-2-yl) methyl]-N-methylprop-2-yn-1-amine hybrids as new multipotent cholinesterase/monoamine oxidase inhibitors for the treatment of Alzheimer's disease. *Journal of Medicinal Chemistry* ***54***(24): 8251-8270.

Bonaiuto, E., Milelli, A., Cozza, G., Tumiatti, V., Marchetti, C., Agostinelli, E., Fimognari, C., Hrelia, P., Minarini, A., & Di Paolo, M. L. (2013). Novel polyamine analogues: From substrates towards potential inhibitors of monoamine oxidases. *European Journal of Medicinal Chemistry* ***70***: 88-101.

Carradori, S., D'Ascenzio, M., De Monte, C., Secci, D., & Yanez, M. (2013). Synthesis and Selective Human Monoamine Oxidase B Inhibition of Heterocyclic Hybrids Based on Hydrazine and Thiazole Scaffolds. *Archiv der Pharmazie* ***346***(1): 17-22.

Chaurasiya, N. D., Ganesan, S., Nanayakkara, N., Dias, L. R., Walker, L. A., & Tekwani, B. L. (2012). Inhibition of human monoamine oxidase A and B by 5-phenoxy 8-aminoquinoline analogs. *Bioorganic & Medicinal Chemistry Letter* ***22***(4): 1701-1704.

Christen, Y. (2000). Oxidative stress and Alzheimer disease. *The American Journal of Clinical Nutrition* ***71***(2): 621-629.

Cummings, J. L., Ross, W., Absher, J., Gornbein, J., & Hadjiaghai, L. (1995). Depressive symptoms in Alzheimer disease: assessment and determinants. *Alzheimer Disease & Associated Disorders* ***9***(2): 87-93.

D'Ascenzio, M., Carradori, S., Secci, D., Mannina, L., Sobolev, A. P., De Monte, C., Cirilli, R., Yanez, M., Alcaro, S., & Ortuso, F. (2014). Identification of the

stereochemical requirements in the 4-aryl-2-cycloalkylidenhydrazinylthiazole scaffold for the design of selective human monoamine oxidase B inhibitors. *Bioorganic & Medicinal Chemistry* ***22***(10): 2887-2895.

Da Prada, M., Zurcher, G., Wuthrich, I., & Haefely, W. (1987). On tyramine, food, beverages and the reversible MAO inhibitor moclobemide. *Journal of Neural Transmission. Supplementum* ***26***: 31-56.

De Colibus, L., Li, M., Binda, C., Lustig, A., Edmondson, D. E., & Mattevi, A. (2005). Three-dimensional structure of human monoamine oxidase A (MAO A): relation to the structures of rat MAO A and human MAO B. *Proceedings of the National Academy of Sciences of the United States of America* ***102***(36): 12684-12689.

Delogu, G., Picciau, C., Ferino, G., Quezada, E., Podda, G., Uriarte, E., & Vina, D. (2011). Synthesis, human monoamine oxidase inhibitory activity and molecular docking studies of 3-heteroarylcoumarin derivatives. *European journal of medicinal chemistry,* ***46***(4), 1147-1152.

Demırkıran, O. (2012). Three new benzophenone glycosides with MAO-A inhibitory activity from *Hypericum thasium* Griseb. *Phytochemistry Letters* ***5***(4): 700-704.

Desideri, N., Bolasco, A., Fioravanti, R., Proietti Monaco, L., Orallo, F., Yanez, M., Ortuso, F., & Alcaro, S. (2011). Homoisoflavonoids: natural scaffolds with potent and selective monoamine oxidase-B inhibition properties. *Journal of Medicinal Chemistry* ***54***(7): 2155-2164.

Desideri, N., Fioravanti, R., Proietti, L. M., Biava, M., Yanez, M., Ortuso, F., & Alcaro, S. (2012). 1, 5-Diphenylpenta-2, 4-dien-1-ones as potent and selective monoamine oxidase-B inhibitors. *European Journal of Medicinal Chemistry* ***59***: 91-100.

Distinto, S., Yanez, M., Alcaro, S., Cardia, M. C., Gaspari, M., Sanna, M. L., Meleddu, R., Ortuso, F., Kirchmair, J., & Markt, P. (2012). Synthesis and biological assessment of novel 2-thiazolylhydrazones and computational analysis of their recognition by monoamine oxidase B. *European Journal of Medicinal Chemistry* ***48***: 284-295.

Edmondson, D. E., Bhattacharyya, A. K., & Walker, M. C. (1993). Spectral and kinetic studies of imine product formation in the oxidation of p-(N, N-dimethylamino) benzylamine analogs by monoamine oxidase B. *Biochemistry* ***32***(19): 5196-5202.

Edmondson, D. E., Binda, C., & Mattevi, A. (2004). The FAD binding sites of human monoamine oxidases A and B. *Neurotoxicology* ***25***(1): 63-72.

Fioravanti, R., Bolasco, A., Manna, F., Rossi, F., Orallo, F., Yanez, M., Vitali, A., Ortuso, F., & Alcaro, S. (2010). Synthesis and molecular modelling studies of prenylated pyrazolines as MAO-B inhibitors. *Bioorganic & Medicinal Chemistry Letters* ***20***(22): 6479-6482.

Fowler, J., MacGregor, R., Wolf, A., Arnett, C., Dewey, S., Schlyer, D., Christman, D., Logan, J., Smith, M., & Sachs, H. (1987). Mapping human brain monoamine oxidase A and B with 11C-labeled suicide inactivators and PET. *Science* ***235***(4787): 481-485.

Ganrot, P., Rosengren, E., & Gottfries, C. (1962). Effect of iproniazid on monoamines and monoamine oxidase in human brain. *Cellular and Molecular Life Sciences* ***18***(6): 260-261.

Garcia-Alloza, M., Gil-Bea, F., Diez-Ariza, M., Chen, C.-H., Francis, P. T., Lasheras, B., & Ramirez, M. (2005). Cholinergic–serotonergic imbalance contributes to

cognitive and behavioral symptoms in Alzheimer's disease. *Neuropsychologia* ***43***(3): 442-449.

Geldenhuys, W. J., Funk, M. O., Van der Schyf, C. J., & Carroll, R. T. (2012). A scaffold hopping approach to identify novel monoamine oxidase B inhibitors. *Bioorganic & Medicinal Chemistry Letters* ***22***(3): 1380-1383.

Hubalek, F., Binda, C., Khalil, A., Li, M., Mattevi, A., Castagnoli, N., & Edmondson, D. E. (2005). Demonstration of isoleucine 199 as a structural determinant for the selective inhibition of human monoamine oxidase B by specific reversible inhibitors. *Journal of Biological Chemistry* ***280***(16): 15761-15766.

Karuppasamy, M., Mahapatra, M., Yabanoglu, S., Ucar, G., Sinha, B. N., Basu, A., Mishra, N., Sharon, A., Kulandaivelu, U., & Jayaprakash, V. (2010). Development of selective and reversible pyrazoline based MAO-A inhibitors: Synthesis, biological evaluation and docking studies. *Bioorganic & Medicinal Chemistry* ***18***(5): 1875-1881.

Khattab, S. N., Hassan, S. Y., Bekhit, A. A., El Massry, A. M., Langer, V., & Amer, A. (2010). Synthesis of new series of quinoxaline based MAO-inhibitors and docking studies. *European Journal of Medicinal Chemistry* ***45***(10): 4479-4489.

Kier, A., Han, J., & Jacobson, L. (2005). Chronic treatment with the monoamine oxidase inhibitor phenelzine increases hypothalamic-pituitary-adrenocortical activity in male C57BL/6 mice: relevance to atypical depression. *Endocrinology* ***146***(3): 1338-1347.

Kirksey, T. J., Kwan, S.-W., & Abell, C. W. (1998). Arginine-42 and threonine-45 are required for FAD incorporation and catalytic activity in human monoamine oxidase B. *Biochemistry* ***37***(35): 12360-12366.

Kragten, E., Lalande, I., Zimmermann, K., Roggo, S., Schindler, P., Müller, D., van Oostrum, J., Waldmeier, P., & Fürst, P. (1998). Glyceraldehyde-3-phosphate Dehydrogenase, the Putative Target of the Antiapoptotic Compounds CGP 3466 andR-(−)-Deprenyl. *Journal of Biological Chemistry* ***273***(10): 5821-5828.

Lange, D. J., Murphy, P. L., Diamond, B., Appel, V., Lai, E. C., Younger, D. S., & Appel, S. H. (1998). Selegiline is ineffective in a collaborative double-blind, placebo-controlled trial for treatment of amyotrophic lateral sclerosis. *Archives of Neurology* ***55***(1): 93-96.

Legoabe, L., Kruger, J., Petzer, A., Bergh, J. J., & Petzer, J. P. (2011). Monoamine oxidase inhibition by selected anilide derivatives. *European Journal of Medicinal Chemistry* ***46***(10): 5162-5174.

Legoabe, L., Petzer, A., & Petzer, J. P. (2012a). Inhibition of monoamine oxidase by selected C6-substituted chromone derivatives. *European Journal of Medicinal Chemistry,* ***49***, 343-353.

Legoabe, L., Petzer, A., & Petzer, J. P. (2012b). Selected C7-substituted chromone derivatives as monoamine oxidase inhibitors. *Bioorganic Chemistry* ***45***: 1-11.

Legoabe, L., Petzer, A., & Petzer, J. P. (2014). α-Tetralone derivatives as inhibitors of monoamine oxidase. *Bioorganic & Medicinal Chemistry Letters* ***24***(12): 2758-2763.

Leonetti, F., Capaldi, C., Pisani, L., Nicolotti, O., Muncipinto, G., Stefanachi, A., Cellamare, S., Caccia, C., & Carotti, A. (2007). Solid-phase synthesis and insights into structure-activity relationships of safinamide analogues as potent

and selective inhibitors of type B monoamine oxidase. *Journal of Medicinal Chemistry* ***50***(20): 4909-4916.

Lewellyn, K., Bialonska, D., Chaurasiya, N. D., Tekwani, B. L., & Zjawiony, J. K. (2012). Synthesis and evaluation of aplysinopsin analogs as inhibitors of human monoamine oxidase A and B. *Bioorganic & Medicinal Chemistry Letters* ***22***(15): 4926-4929.

Lu, C., Zhou, Q., Yan, J., Du, Z., Huang, L., & Li, X. (2013). A novel series of tacrine-selegiline hybrids with cholinesterase and monoamine oxidase inhibition activities for the treatment of Alzheimer's disease. *European Journal of Medicinal Chemistry* ***62***: 745-753.

Luhr, S., Vilches-Herrera, M., Fierro, A., Ramsay, R. R., Edmondson, D. E., Reyes-Parada, M., Cassels, B. K., & Iturriaga-Vasquez, P. (2010). 2-Arylthiomorpholine derivatives as potent and selective monoamine oxidase B inhibitors. *Bioorganic & Medicinal Chemistry* ***18***(4): 1388-1395.

Manley-King, C. I., Bergh, J. J., & Petzer, J. P. (2011). Inhibition of monoamine oxidase by selected C5-and C6-substituted isatin analogues. *Bioorganic & Medicinal Chemistry* ***19***(1): 261-274.

Markesbery, W. R. (1997). Oxidative stress hypothesis in Alzheimer's disease. *Free Radical Biology and Medicine* ***23***(1): 134-147.

Matos, M. J., Vina, D., Janeiro, P., Borges, F., Santana, L., & Uriarte, E. (2010). New halogenated 3-phenylcoumarins as potent and selective MAO-B inhibitors. *Bioorganic & Medicinal Chemistry Letters* ***20***(17): 5157-5160.

Meher, C., Rao, A., & Omar, M. (2013). Piperazine-pyrazine and their multiple biological activities. *Asian Journal of Pharmaceutical Sciences and Research,* ***3***: 43-60.

Meiring, L., Petzer, J. P., & Petzer, A. (2013). Inhibition of monoamine oxidase by 3, 4-dihydro-2 (1*H*)-quinolinone derivatives. *Bioorganic & Medicinal Chemistry Letters* ***23***(20): 5498-5502.

Milczek, E. M., Binda, C., Rovida, S., Mattevi, A., & Edmondson, D. E. (2011). The 'gating'residues lle199 and Tyr326 in human monoamine oxidase B function in substrate and inhibitor recognition. *Federation of European Biochemical Societies* ***278***(24): 4860-4869.

Mu, L.-H., Wang, B., Ren, H.-Y., Liu, P., Guo, D.-H., Wang, F.-M., Bai, L., & Guo, Y.-S. (2012). Synthesis and inhibitory effect of piperine derivates on monoamine oxidase. *Bioorganic & Medicinal Chemistry letters* ***22***(9): 3343-3348.

Nicotra, A., Pierucci, F., Parvez, H., & Senatori, O. (2004). Monoamine oxidase expression during development and aging. *Neurotoxicology* ***25***(1): 155-165.

Novaroli, L., Daina, A., Favre, E., Bravo, J., Carotti, A., Leonetti, F., Catto, M., Carrupt, P.-A., & Reist, M. (2006). Impact of species-dependent differences on screening, design, and development of MAO B inhibitors. *Journal of Medicinal Chemistry* ***49***(21): 6264-6272.

O'Carroll, A.-M., Fowler, C. J., Phillips, J. P., Tobbia, I., & Tipton, K. F. (1983). The deamination of dopamine by human brain monoamine oxidase. *Naunyn-Schmiedeberg's Archives of Pharmacology* ***322***(3): 198-202.

Okaecwe, T., & Dorcas, A. (2012). *Inhibition of monoamine oxidase by selected 8-[(phenylsulfanyl) methyl] caffeine derivatives. Bioorganic & Medicinal Chemistry* ***20****(14): 4336-4347.*

Passos, C. S., Simoes-Pires, C. A., Nurisso, A., Soldi, T. C., Kato, L., de Oliveira, C., de Faria, E. O., Marcourt, L., Gottfried, C., & Carrupt, P.-A. (2013). Indole alkaloids of *Psychotria* as multifunctional cholinesterases and monoamine oxidases inhibitors. *Phytochemistry* ***86***: 8-20.

Pessoa-Mahana, H., Gajardo, G. R., Araya-Maturana, R., Cárcamo, J. K., & Pessoa-Mahana, C. D. (2004). Synthesis of 4-Arylpiperazine Derivatives of Moclobemide: Potential Antidepressants with a Dual Mode of Action. *Synthetic Communications* ***34***(14): 2513-2521.

Pettersson, F., Svensson, P., Waters, S., Waters, N., & Sonesson, C. (2012). Synthesis and evaluation of a set of para-substituted 4-phenylpiperidines and 4-phenylpiperazines as monoamine oxidase (MAO) inhibitors. *Journal of Medicinal Chemistry* ***55***(7): 3242-3249.

Pettersson, F., Svensson, P., Waters, S., Waters, N., & Sonesson, C. (2013). Synthesis, pharmacological evaluation and QSAR modeling of mono-substituted 4-phenylpiperidines and 4-phenylpiperazines. *European Journal of Medicinal Chemistry* ***62***: 241-255.

Pisani, L., Barletta, M., Soto-Otero, R., Nicolotti, O., Mendez-Alvarez, E., Catto, M., Introcaso, A., Stefanachi, A., Cellamare, S., & Altomare, C. (2013). Discovery, Biological Evaluation, and Structure–Activity and− Selectivity Relationships of 6′-Substituted (E)-2-(Benzofuran-3 (2 H)-ylidene)-N-methylacetamides, a Novel Class of Potent and Selective Monoamine Oxidase Inhibitors. *Journal of Medicinal Chemistry* ***56***(6): 2651-2664.

Prashanth, M., Revanasiddappa, H. D., Lokanatha Rai, K., & Veeresh, B. (2012). Synthesis, characterization, antidepressant and antioxidant activity of novel piperamides bearing piperidine and piperazine analogues. *Bioorganic & Medicinal Chemistry Letters* ***22***(23): 7065-7070.

Prins, L. H., Petzer, J. P., & Malan, S. F. (2010). Inhibition of monoamine oxidase by indole and benzofuran derivatives. *European journal of Medicinal Chemistry* ***45***(10): 4458-4466.

Qin, F., Shite, J., Mao, W., & Liang, C.-s. (2003). Selegiline attenuates cardiac oxidative stress and apoptosis in heart failure: association with improvement of cardiac function. *European Journal of Pharmacology* ***461***(2): 149-158.

Ramsay, R. (2012). Inhibitor design for monoamine oxidases. *Current Pharmaceutical Design* ***19***(14): 2529-2539.

Rao, T. S., & Yeragani, V. K. (2009). Hypertensive crisis and cheese. *Indian Journal of Psychiatry,* ***51***(1), 65.

Reniers, J., Robert, S., Frederick, R., Masereel, B., Vincent, S., & Wouters, J. (2011). Synthesis and evaluation of β-carboline derivatives as potential monoamine oxidase inhibitors. *Bioorganic & Medicinal Chemistry* ***19***(1): 134-144.

Sahoo, A., Yabanoglu, S., Sinha, B. N., Ucar, G., Basu, A., & Jayaprakash, V. (2010). Towards development of selective and reversible pyrazoline based MAO-inhibitors: Synthesis, biological evaluation and docking studies. *Bioorganic & Medicinal Chemistry Letters* ***20***(1): 132-136.

Salach, J. I., & Weyler, W. (1987). Preparation of the flavin-containing aromatic amine oxidases of human placenta and beef liver. *Methods in Enzymology* ***142***: 627.

Samadi, A., Chioua, M., Bolea, I., de los Rios, C., Iriepa, I., Moraleda, I., Bastida, A., Esteban, G., Unzeta, M., & Galvez, E. (2011). Synthesis, biological assessment and molecular modeling of new multipotent MAO and cholinesterase inhibitors as potential drugs for the treatment of Alzheimer's disease. *European Journal of Medicinal Chemistry* ***46***(9): 4665-4668.

Samadi, A., de los Rios, C., Bolea, I., Chioua, M., Iriepa, I., Moraleda, I., Bartolini, M., Andrisano, V., Galvez, E., & Valderas, C. (2012). Multipotent MAO and cholinesterase inhibitors for the treatment of Alzheimer's disease: Synthesis, pharmacological analysis and molecular modeling of heterocyclic substituted alkyl and cycloalkyl propargyl amine. *European Journal of Medicinal Chemistry* ***52***: 251-262.

Secci, D., Bolasco, A., Carradori, S., D'Ascenzio, M., Nescatelli, R., & Yanez, M. (2012). Recent advances in the development of selective human MAO-B inhibitors:(Hetero) arylidene-(4-substituted-thiazol-2-yl) hydrazines. *European Journal of Medicinal Chemistry* ***58***: 405-417.

Senturk, K., Tan, O. U., Ciftci, S. Y., Ucar, G., & Palaska, E. (2012). Synthesis and Evaluation of Human Monoamine Oxidase Inhibitory Activities of Some 3, 5-Diaryl-N-substituted-4, 5-dihydro-1H-pyrazole-1-carbothioamide Derivatives. *Archiv der Pharmazie* ***345***(9): 695-702.

Serra, S., Ferino, G., Matos, M. J., Vazquez-Rodriguez, S., Delogu, G., Vina, D., Cadoni, E., Santana, L., & Uriarte, E. (2012). Hydroxycoumarins as selective MAO-B inhibitors. *Bioorganic & Medicinal Chemistry Letters* ***22***(1): 258-261.

Shubbar, A. (2013). Novel neuroprotective compounds for use in Parkinson's disease. Kent State University.

Silverman, R. B., Hoffman, S. J., & Catus III, W. B. (1980). A mechanism for mitochondrial monoamine oxidase catalyzed amine oxidation. *Journal of the American Chemical Society* ***102***(23): 7126-7128.

Simon, L., Szilagyi, G., Bori, Z., Orbay, P., & Nagy, Z. (2001). (−)-d-Deprenyl attenuates apoptosis in experimental brain ischaemia. *European Journal of Pharmacology* ***430***(2): 235-241.

Son, S.-Y., Ma, J., Kondou, Y., Yoshimura, M., Yamashita, E., & Tsukihara, T. (2008). Structure of human monoamine oxidase A at 2.2-Å resolution: the control of opening the entry for substrates/inhibitors. *Proceedings of the National Academy of Sciences* ***105***(15): 5739-5744.

Song, B., Xiao, T., Qi, X., Li, L.-N., Qin, K., Nian, S., Hu, G.-X., Yu, Y., Liang, G., & Ye, F. (2012). Design and synthesis of 8-substituted benzamido-phenylxanthine derivatives as MAO-B inhibitors. *Bioorganic & medicinal Chemistry Letters* ***22***(4): 1739-1742.

Srivastav, M. K., Shamshuddin, M., & Shantakumar, S. (2013). Design, Synthesis and Characterization of Novel 6, 7-dimethoxy-N^2-(substituted benzyl)-N^2-propylquinazoline-2, 4-diamine Derivatives as Anxiolytic and Antidepressant Agents. *American Journal of Chemistry* ***3***(1): 14-22.

Stahl, S. M., & Felker, A. (2008). Monoamine oxidase inhibitors: a modern guide to an unrequited class of antidepressants. *CNS Spectr* ***13***(10): 855-870.

Sterling, J., Herzig, Y., Goren, T., Finkelstein, N., Lerner, D., Goldenberg, W., Miskolczi, I., Molnar, S., Rantal, F., & Tamas, T. (2002). Novel dual inhibitors of AChE and

MAO derived from hydroxy aminoindan and phenethylamine as potential treatment for Alzheimer's disease. *Journal of Medicinal Chemistry* ***45***(24): 5260-5279.

Strydom, B., Bergh, J. J., & Petzer, J. P. (2013). Inhibition of monoamine oxidase by phthalide analogues. *Bioorganic & Medicinal Chemistry Letters* ***23***(5): 1269-1273.

Thokozile, O., Swanepoel, A. J., Petzer, A., Bergh, J. J., & Petzer, J. P. (2012). *Bioorganic & Medicinal Chemistry*.

Tripathi, K. D. (2003). *Essentials of medical pharmacology*: Jaypee Bros.

Valente, S., Tomassi, S., Tempera, G., Saccoccio, S., Agostinelli, E., & Mai, A. (2011). Novel Reversible Monoamine Oxidase A Inhibitors: Highly Potent and Selective 3-(1 H-Pyrrol-3-yl)-2-oxazolidinones. *Journal of Medicinal Chemistry* ***54***(23): 8228-8232.

Van der Walt, M. M., Terre'Blanche, G., Petzer, A., & Petzer, J. P. (2012). Novel sulfanylphthalimide analogues as highly potent inhibitors of monoamine oxidase B. *Bioorganic & Medicinal Chemistry Letters* ***22***(21): 6632-6635.

Villarinho, J. G., Fachinetto, R., Pinheiro, F. d. V., Sant'Anna, G. d. S., Machado, P., Dombrowski, P. A., Cunha, C. d., Cabrini, D. d. A., Martins, M. A. P., & Bonacorso, H. G. (2012). Antidepressant-like effect of the novel MAO inhibitor 2-(3, 4-dimethoxy-phenyl)-4, 5-dihydro-1*H*-imidazole (2-DMPI) in mice. *Progress in Neuro-Psychopharmacology and Biological Psychiatry* ***39***(1): 31-39.

Waibel, S., Reuter, A., Malessa, S., Blaugrund, E., & Ludolph, A. C. (2004). Rasagiline alone and in combination with riluzole prolongs survival in an ALS mouse model. *Journal of Neurology* ***251***(9): 1080-1084.

Weyler, W., Hsu, Y.-P. P., & Breakafield, X. O. (1990). Biochemistry and genetics of monoamine oxidase. *Pharmacology & therapeutics* ***47***(3): 391-417.

Youdim, M. B., Edmondson, D., & Tipton, K. F. (2006). The therapeutic potential of monoamine oxidase inhibitors. *Nature Reviews Neuroscience* ***7***(4): 295-309.

Zhang, H.-Y. (2005). One-compound-multiple-targets strategy to combat Alzheimer's disease. *Federation of European Biochemical Societies* ***579*** (24): 5260-5264.

Zhang , H., Cai, Q., & Ma, D. (2005). Amino acid promoted CuI-catalyzed CN bond formation between aryl halides and amines or N-containing heterocycles. *The Journal of Organic Chemistry* ***70***(13): 5164-5173.

Zhou, M., & Panchuk-Voloshina, N. (1997). A one-step fluorometric method for the continuous measurement of monoamine oxidase activity. *Analytical Biochemistry* ***253***(2): 169-174.

Zor, T., & Selinger, Z. (1996). Linearization of the Bradford protein assay increases its sensitivity: theoretical and experimental studies. *Analytical Biochemistry* ***236***(2): 302-308.

APPENDIX

Spectral Data of synthesized compounds

phenyl(4-phenylpiperazin-1-yl)methanone VS-1

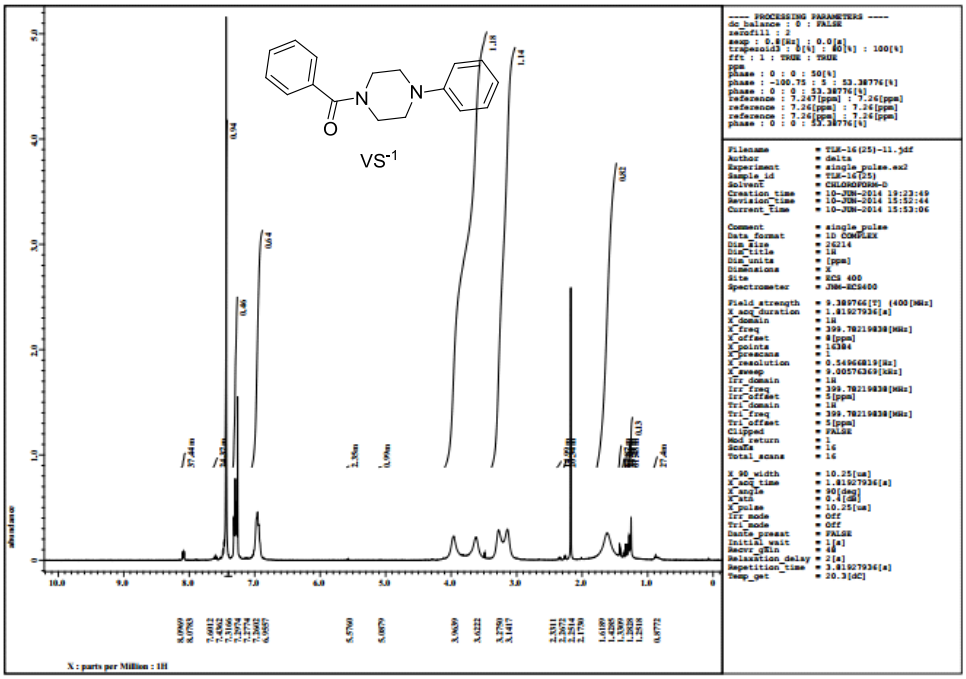

^{1}H-NMR of compound VS-1

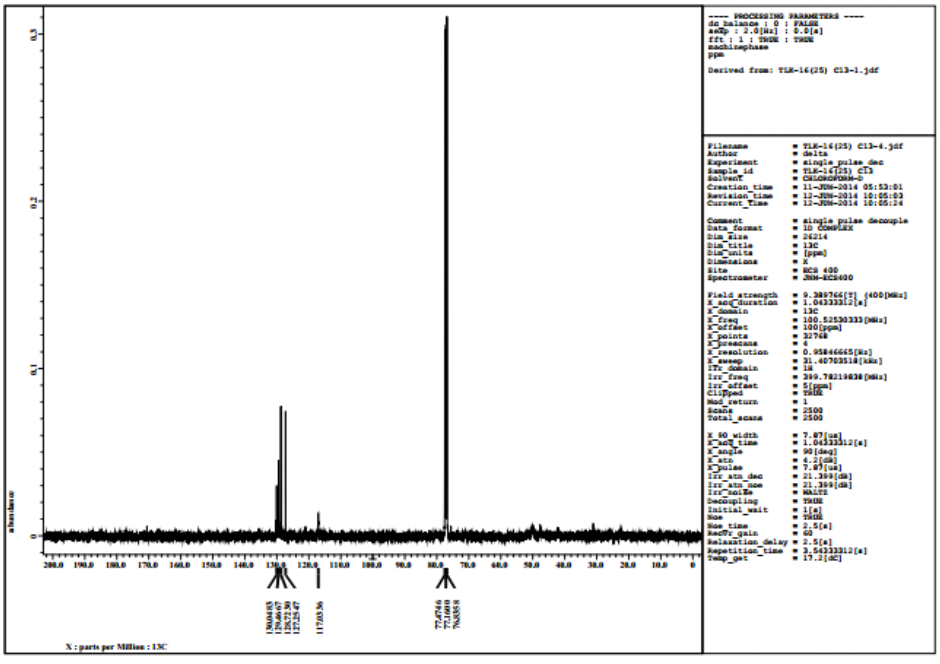

^{13}C-NMR of compound VS-1

((4-methoxyphenyl)(4-phenylpiperazin-1-yl)methanone) VS-2

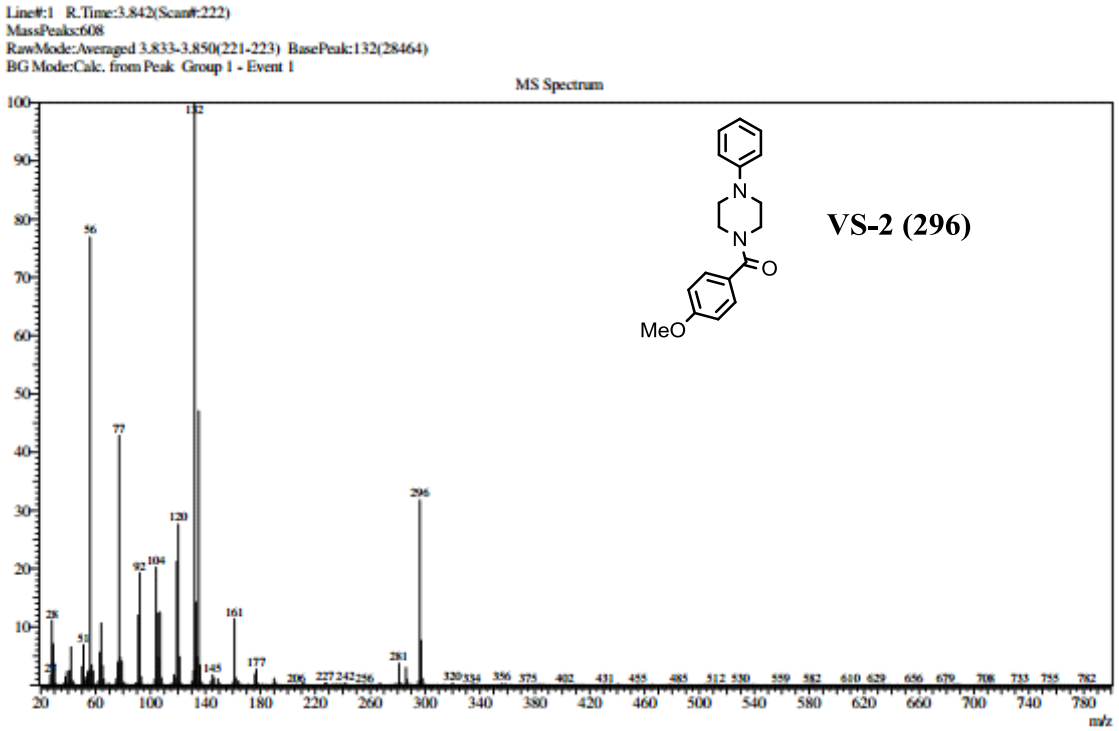

Mass spectrum of compound VS-2

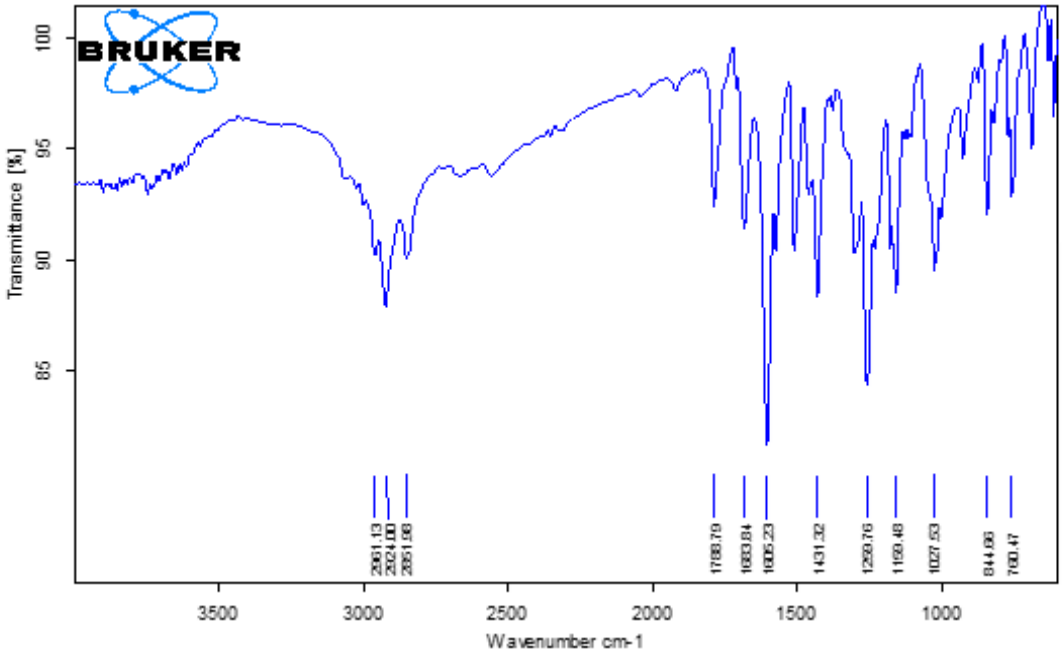

IR spectra of compound VS-2

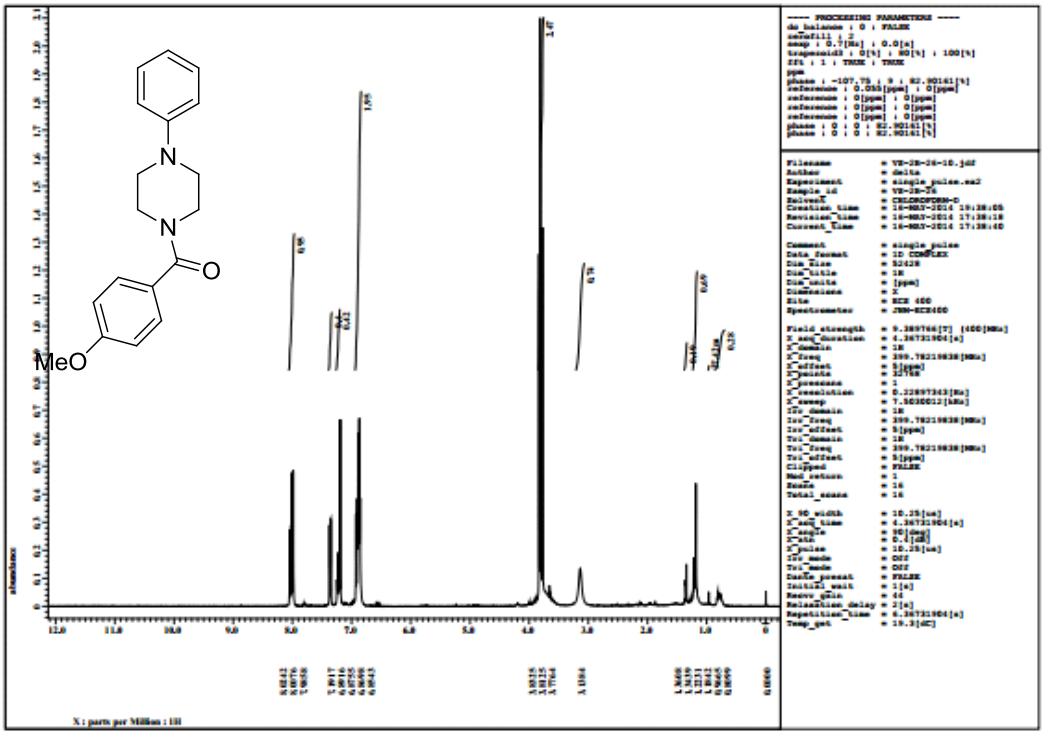

^{1}H-NMR of compound VS-2

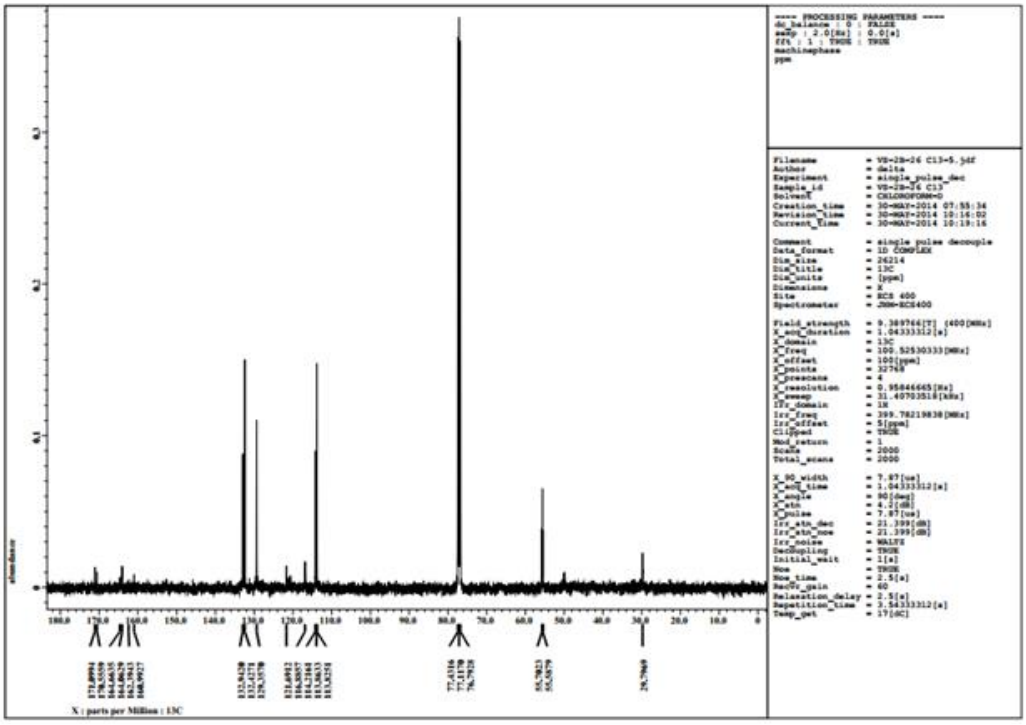

^{13}C-NMR of compound VS-2

(1-((2-nitrophenyl)sulfonyl)-4-phenylpiperazine) VS-3

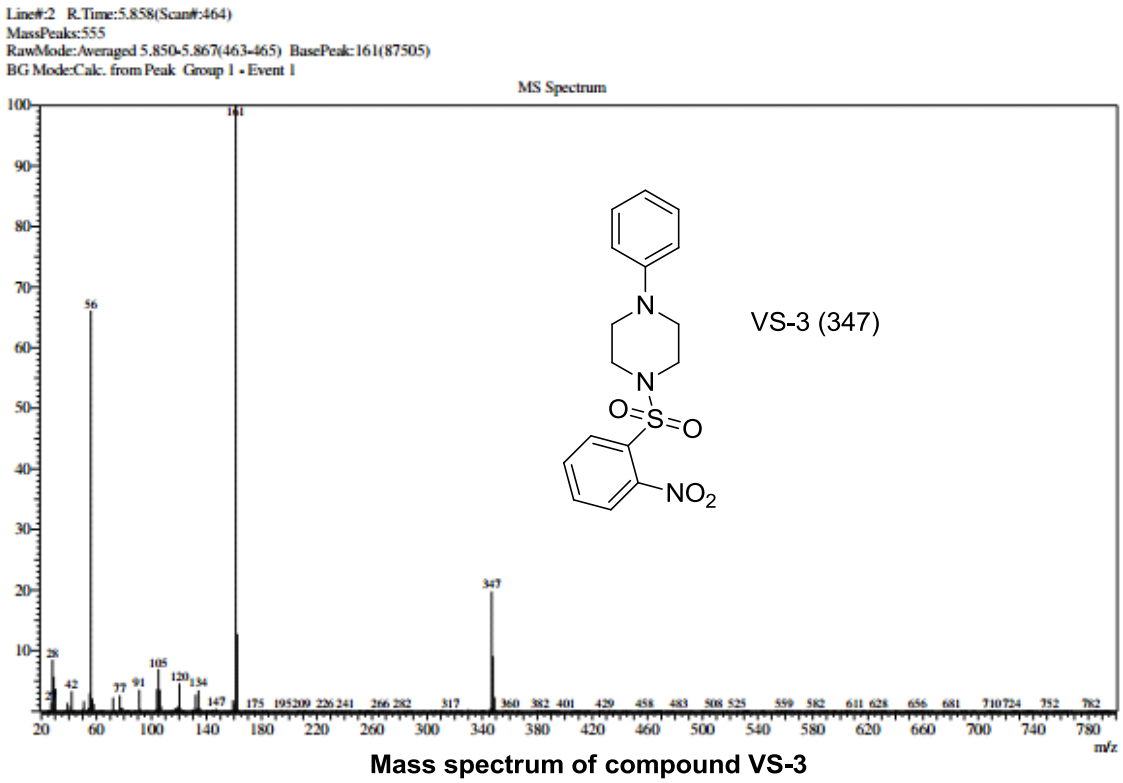

Mass spectrum of compound VS-3

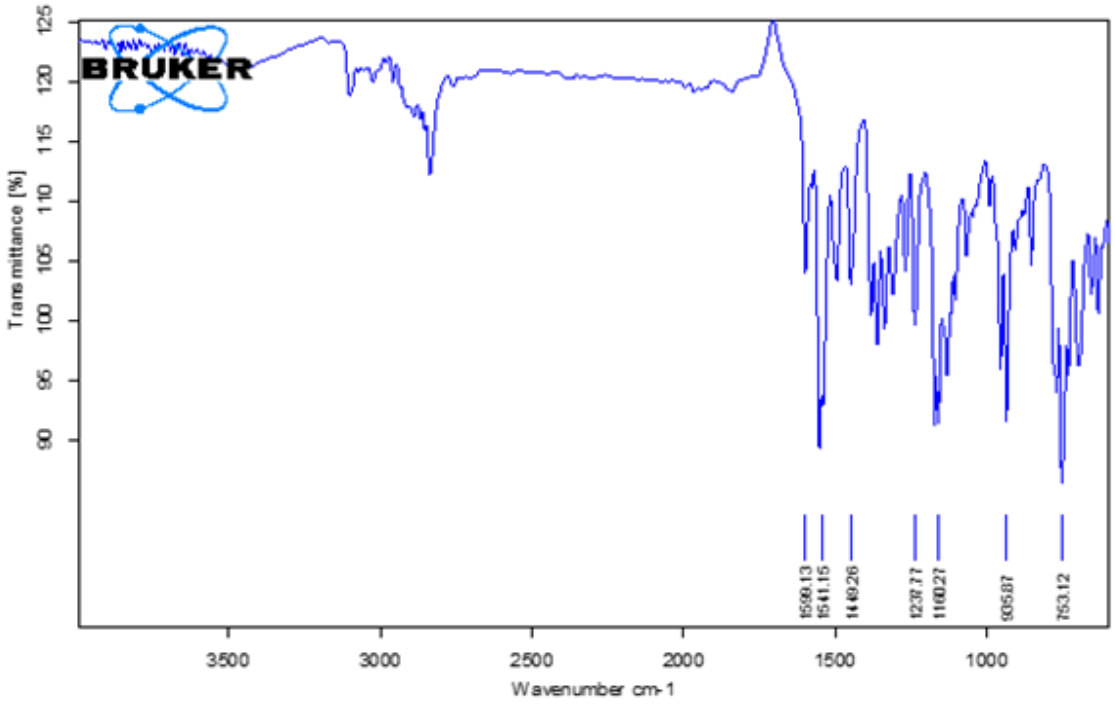

IR spectra of compound VS-3

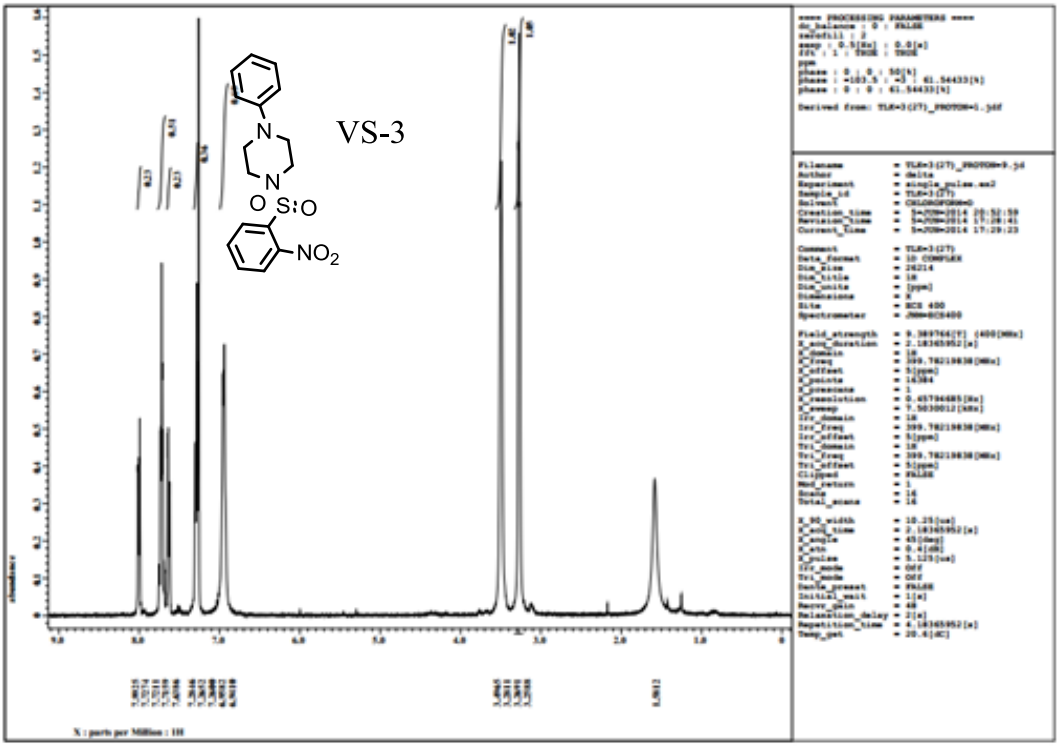

^{1}H-NMR of compound VS-3

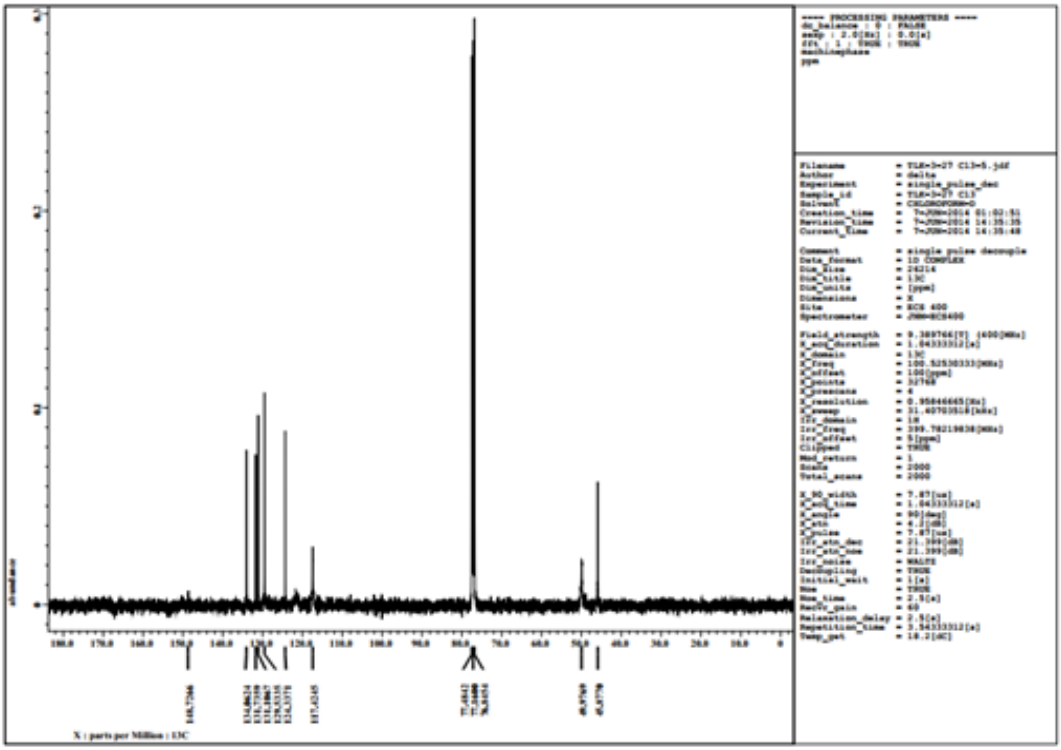

^{13}C-NMR of compound VS-3

(1-((4-chloro-2,5-dimethylphenyl)sulfonyl)-4-phenylpiperazine) VS-4

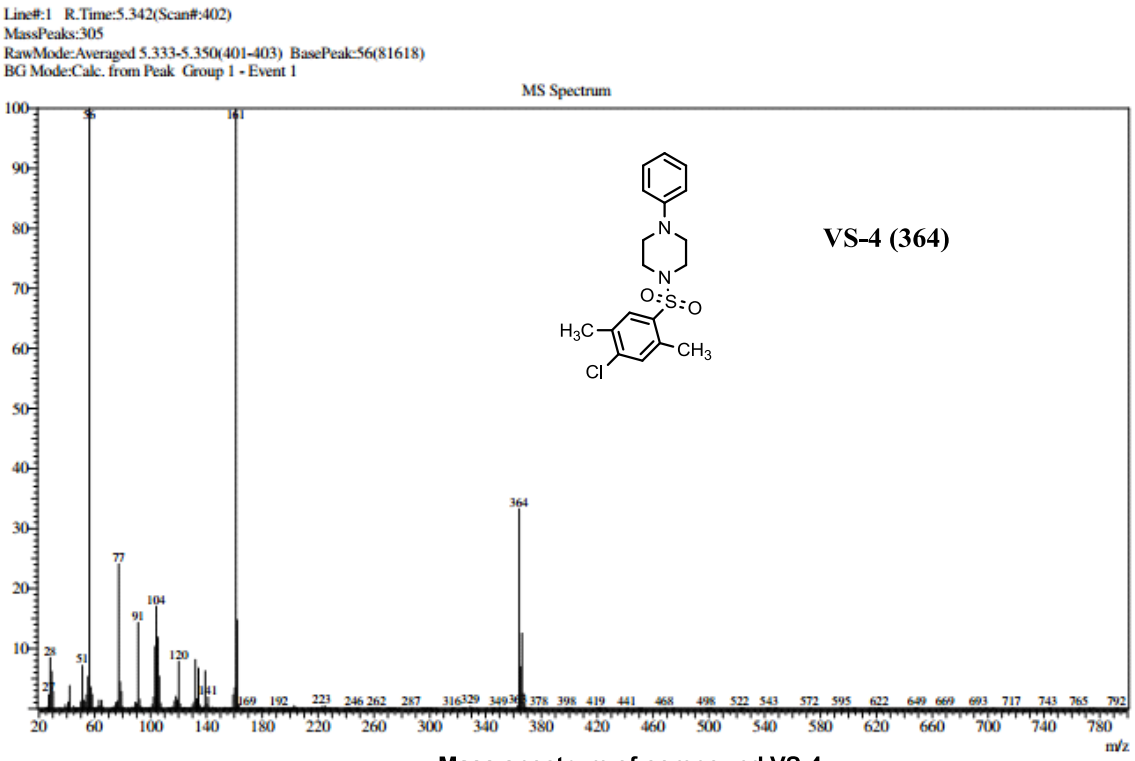

Mass spectrum of compound VS-4

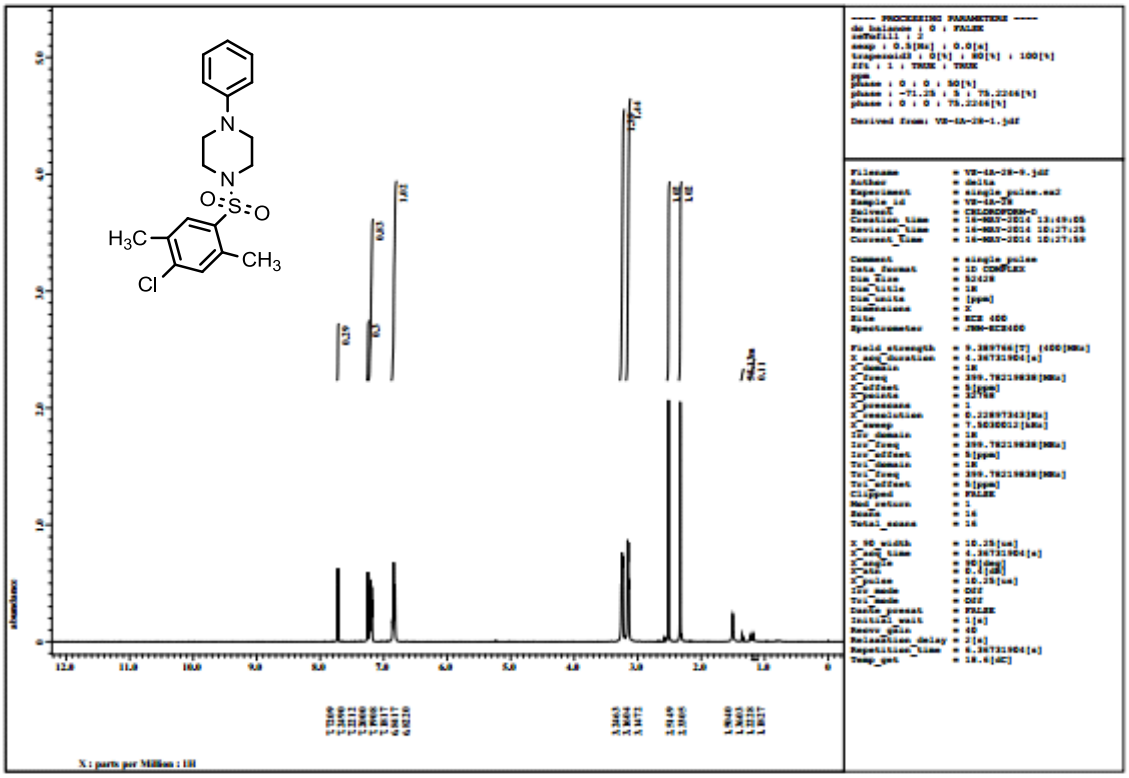

^{1}H-NMR of compound VS-4

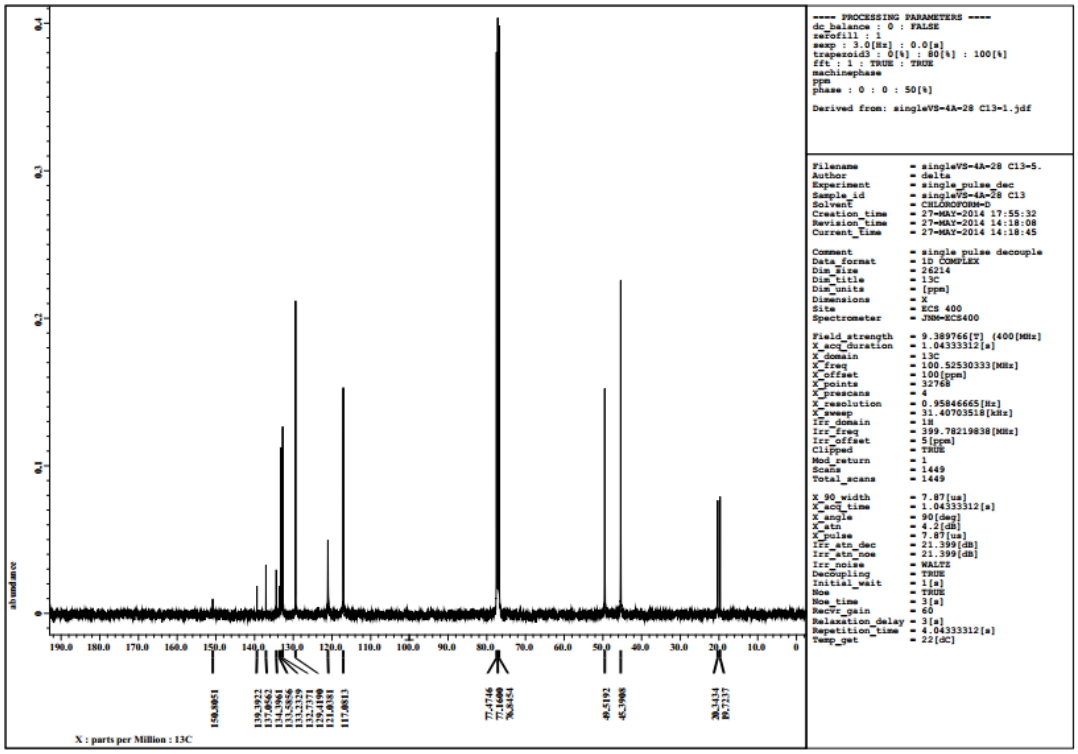

^{13}C-NMR of compound VS-4

(1-((4-(tert-butyl)phenyl)sulfonyl)-4-phenylpiperazine) VS-5

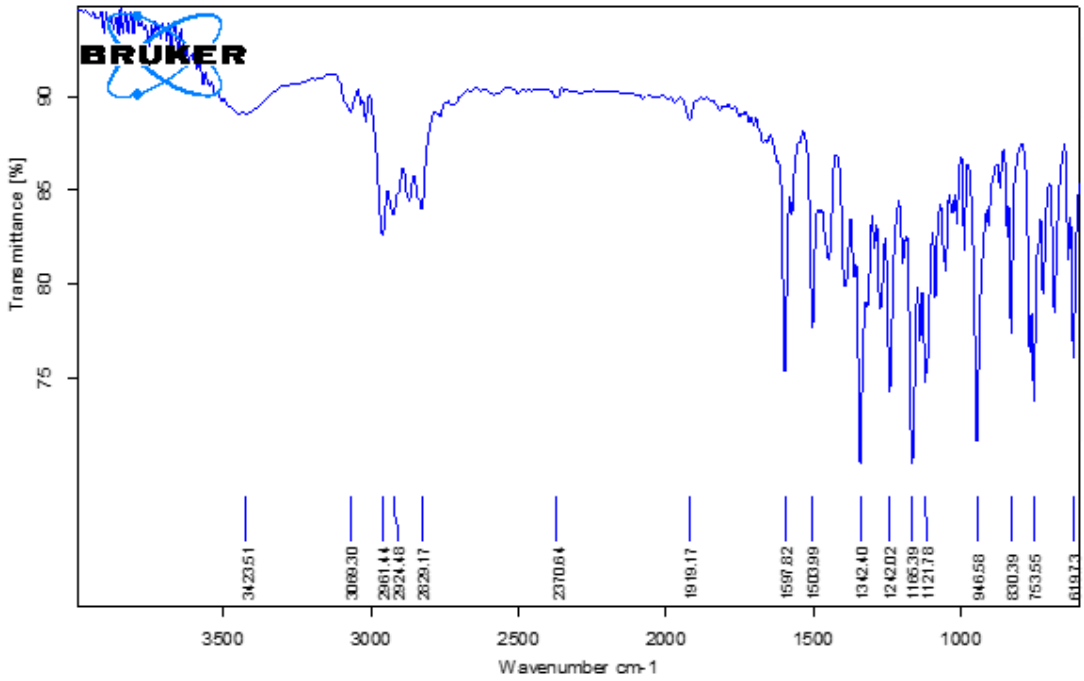

IR spectra of compound VS-5

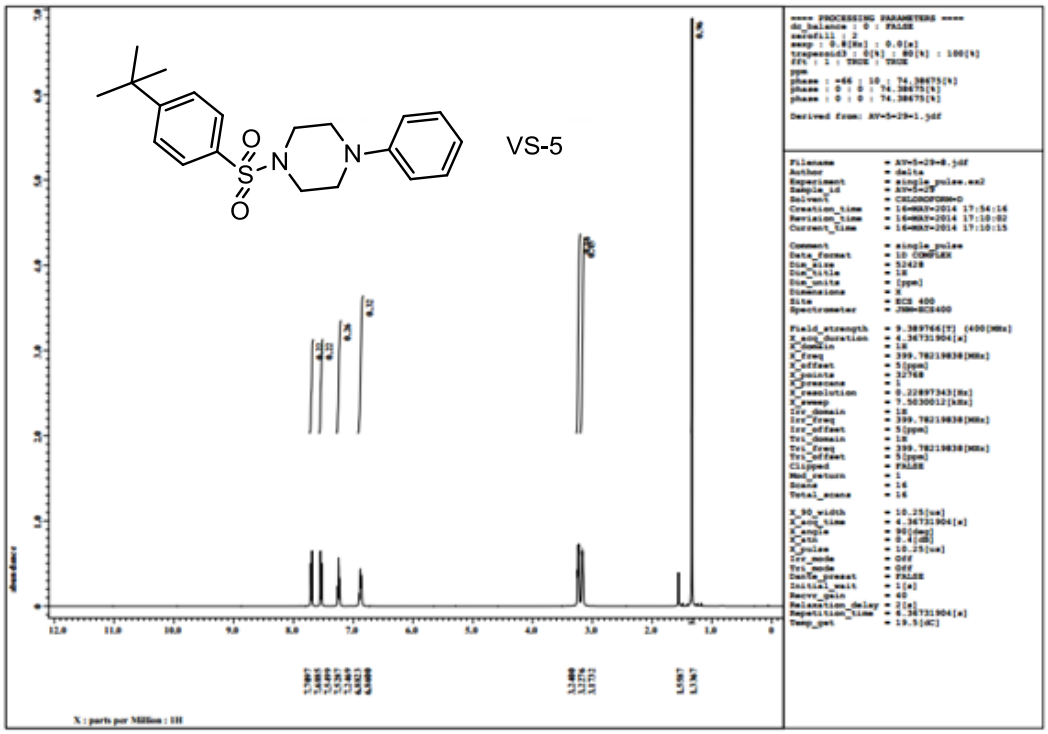

^{1}H-NMR of compound VS-5

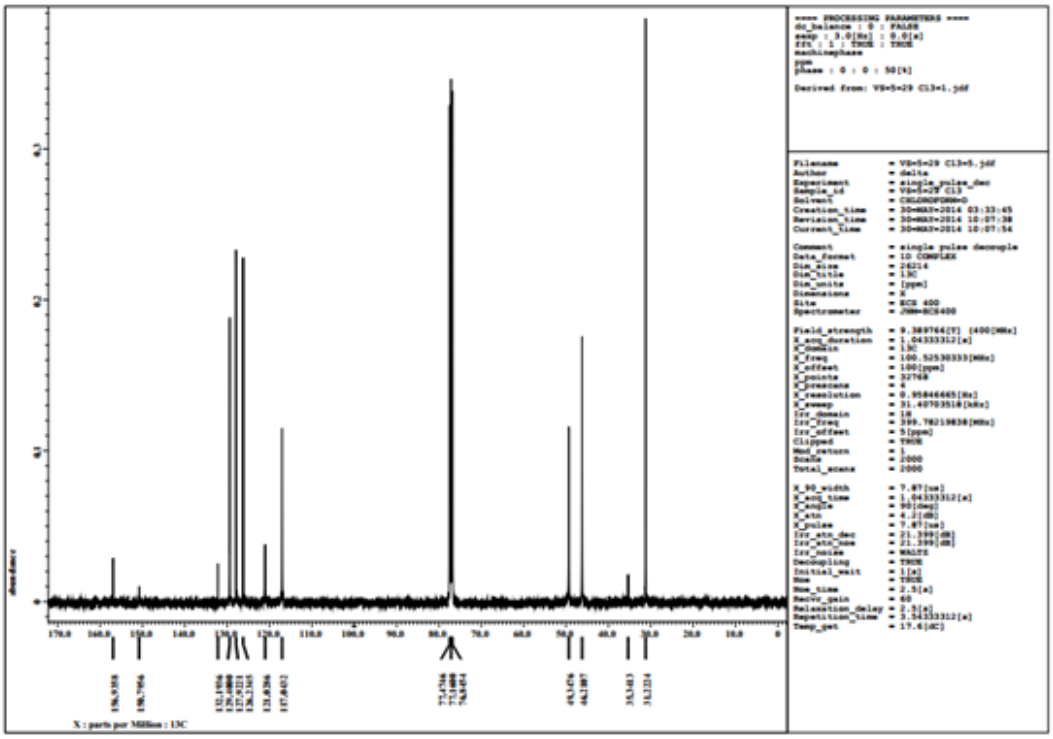

^{13}C-NMR of compound VS-5

(1,4-diphenylpiperazine) VS-6

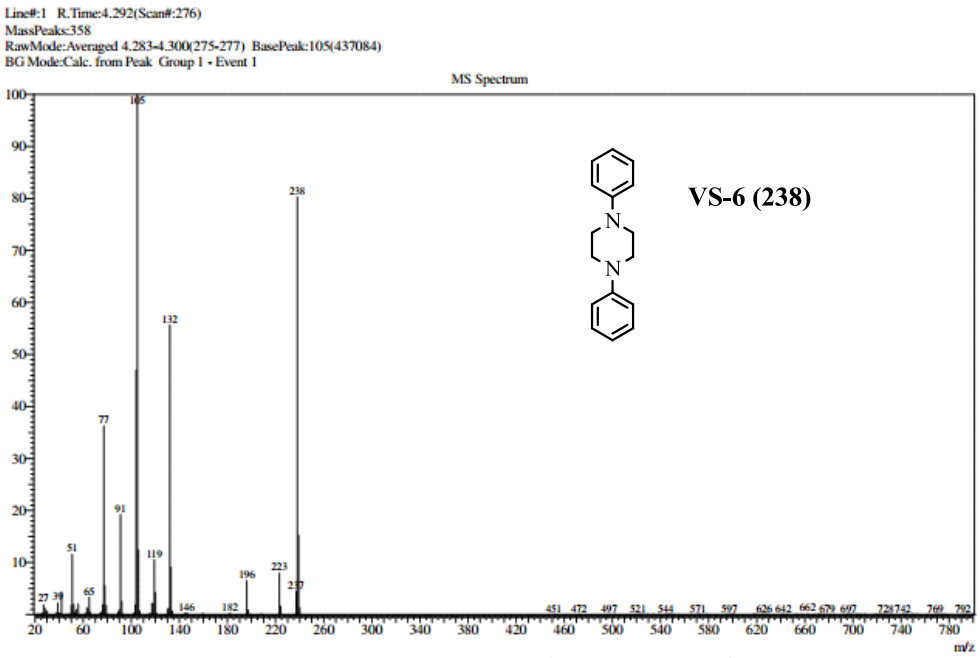

Mass spectrum of compound VS-6

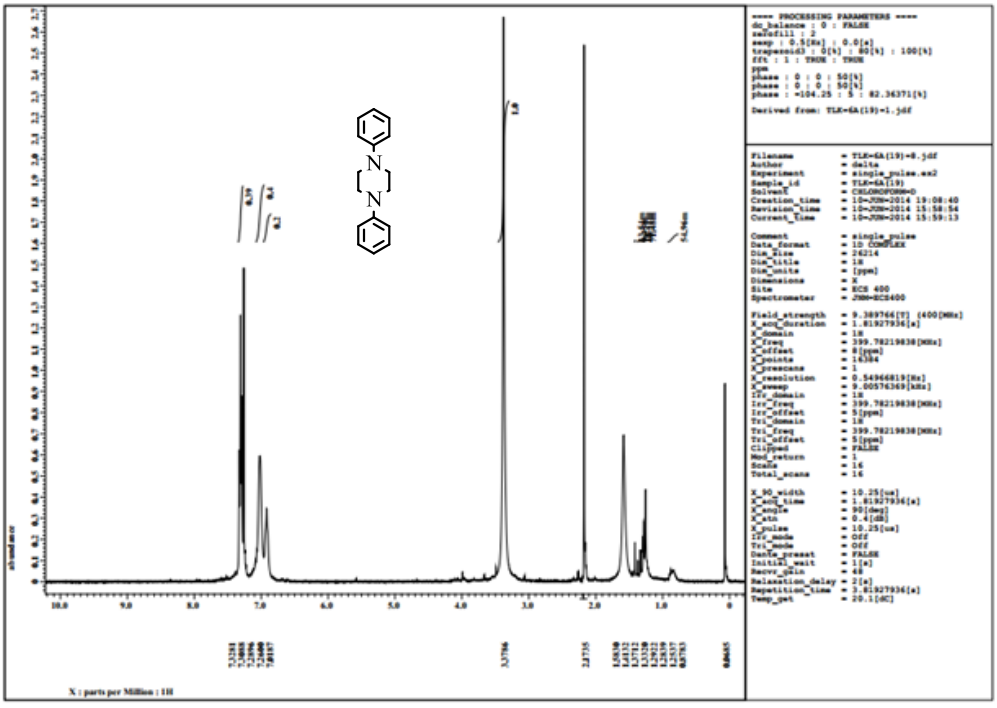

^{1}H-NMR of compound VS-5

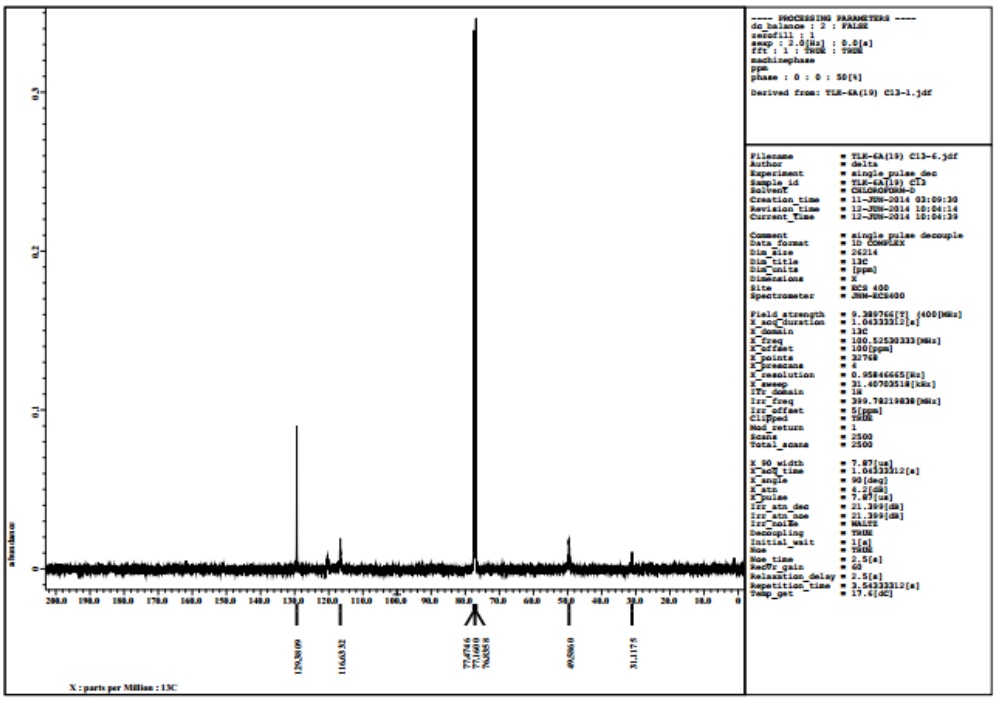

^{13}C-NMR of compound VS-6

(3-(4-phenylpiperazin-1-yl)quinolone)VS-7

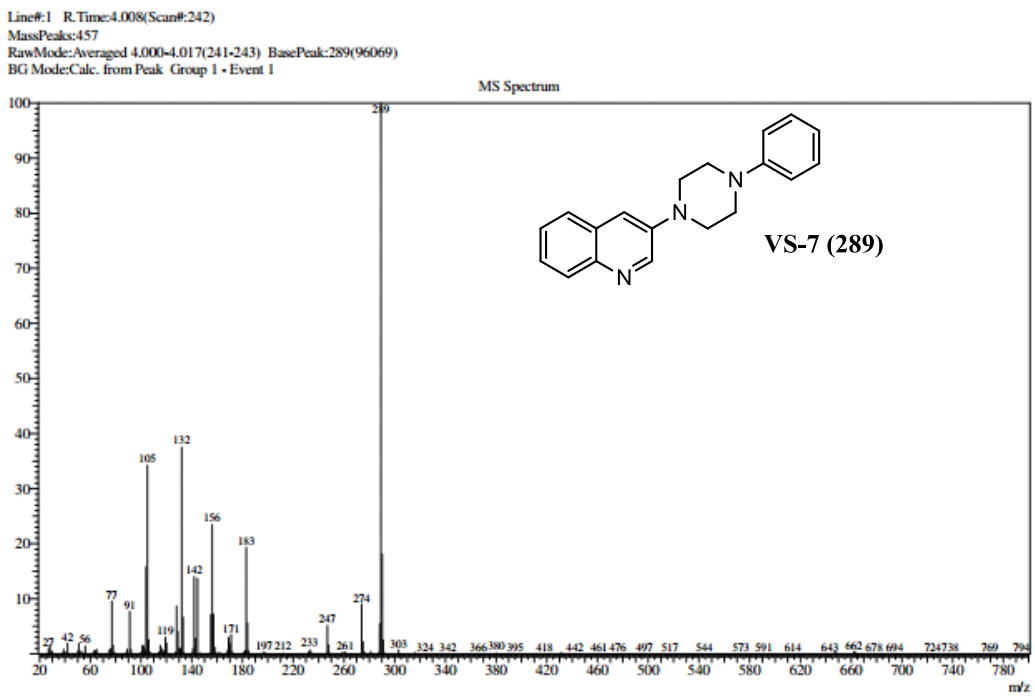

Mass spectrum of compound VS-7

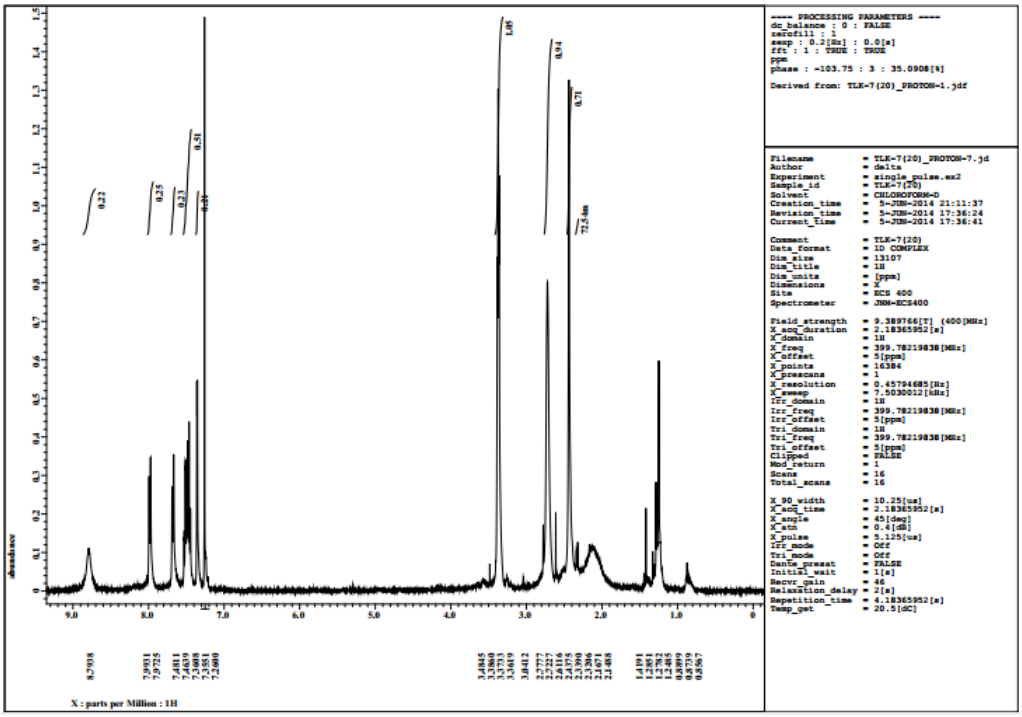

^{1}H-NMR of compound VS-7

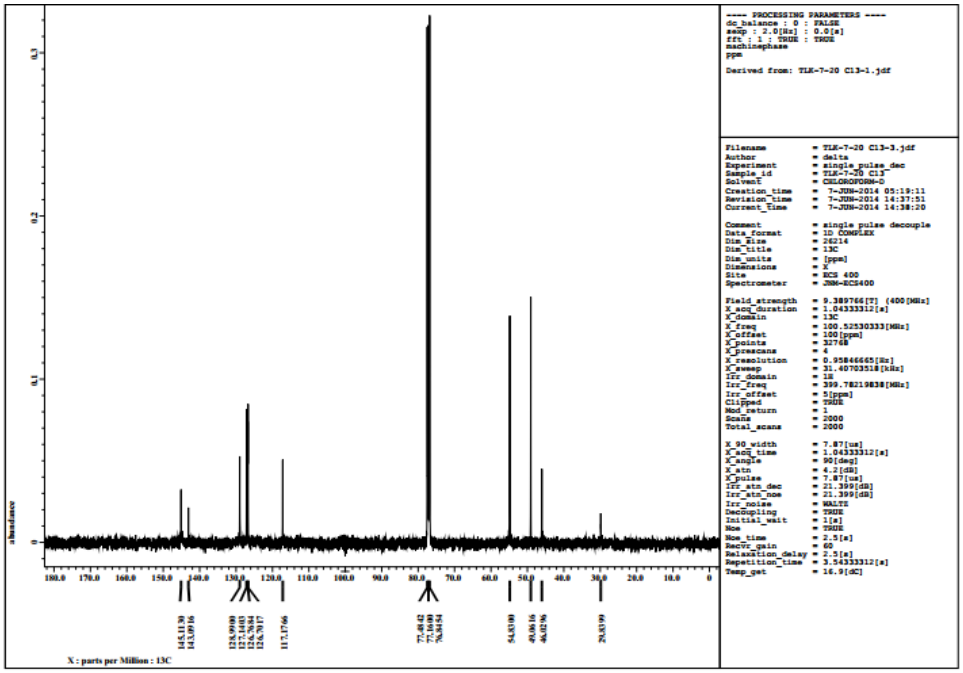

^{13}C-NMR of compound VS-7

((4-phenylpiperazin-1-yl)(p-tolyl)methanone) VS-8

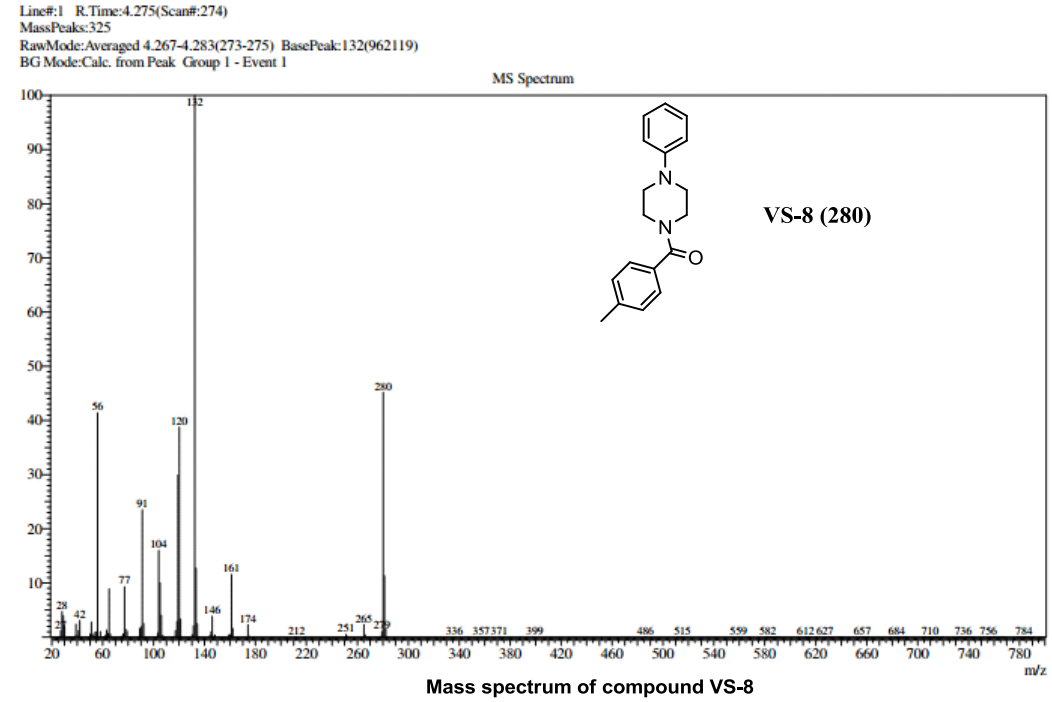

Mass spectrum of compound VS-8

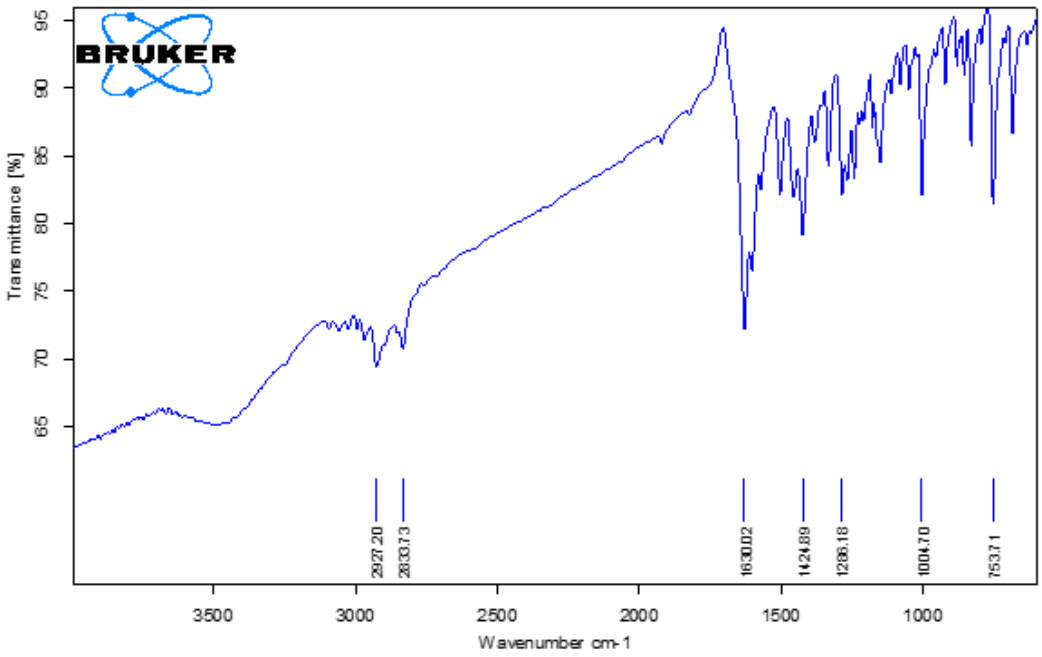

IR spectraof compound VS-8

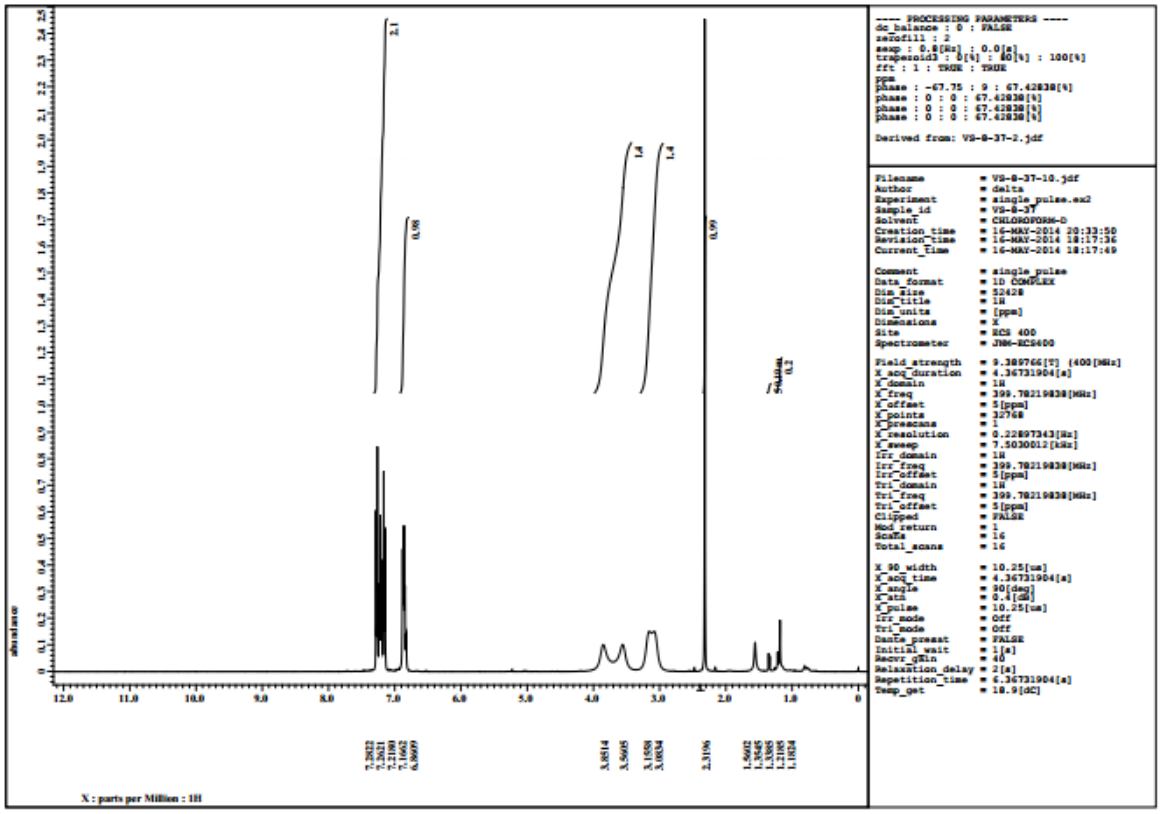

^{1}H-NMR of compound VS-8

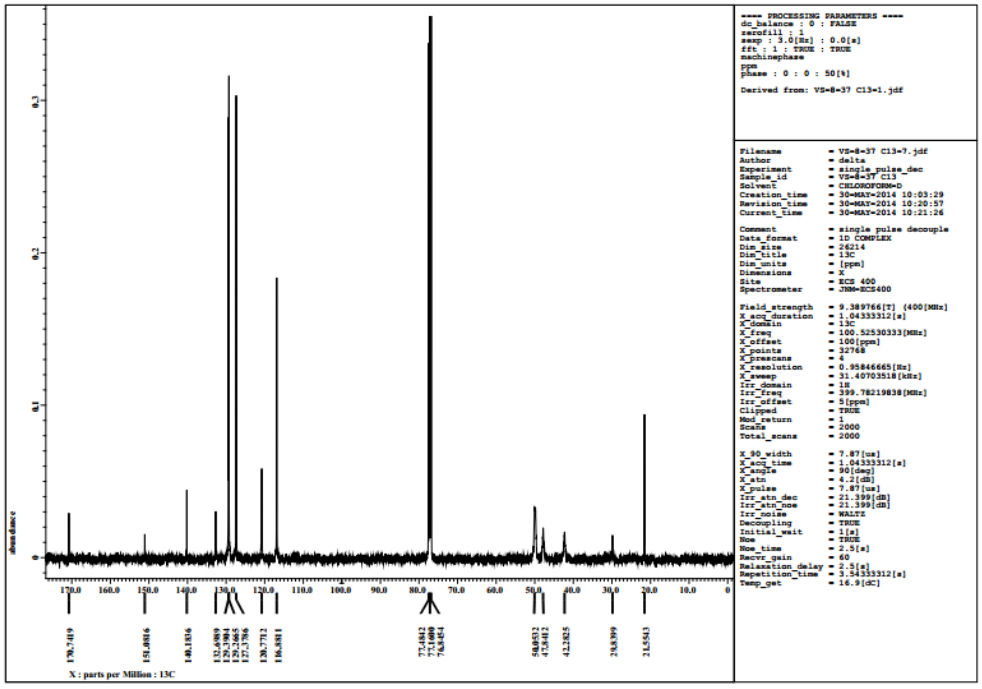

^{13}C-NMR of compound VS-8

(1-(naphthalen-1-yl)-4-phenylpiperazine) VS-9

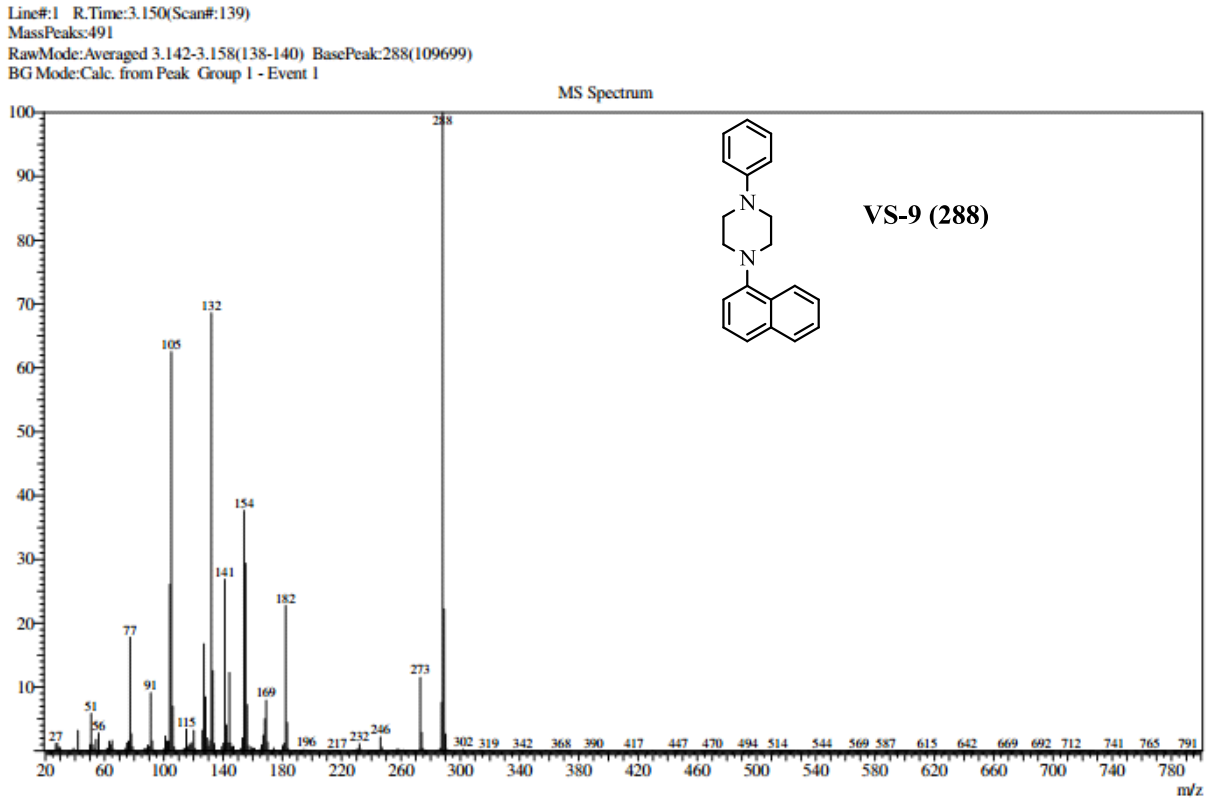

Mass spectrum of compound VS-9

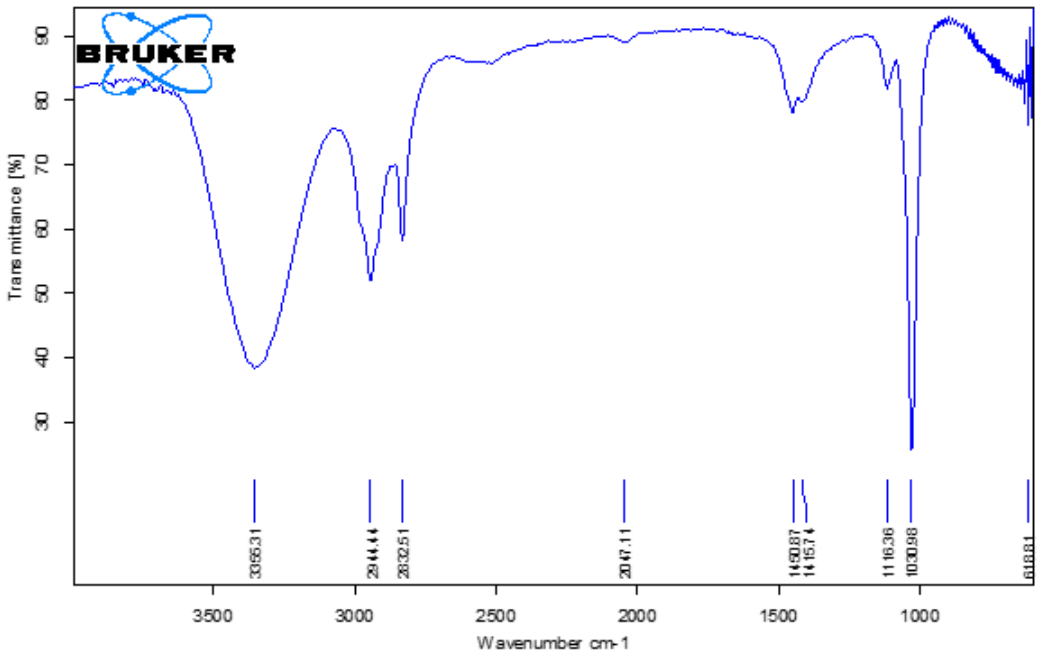

IR spectraof compound VS-9

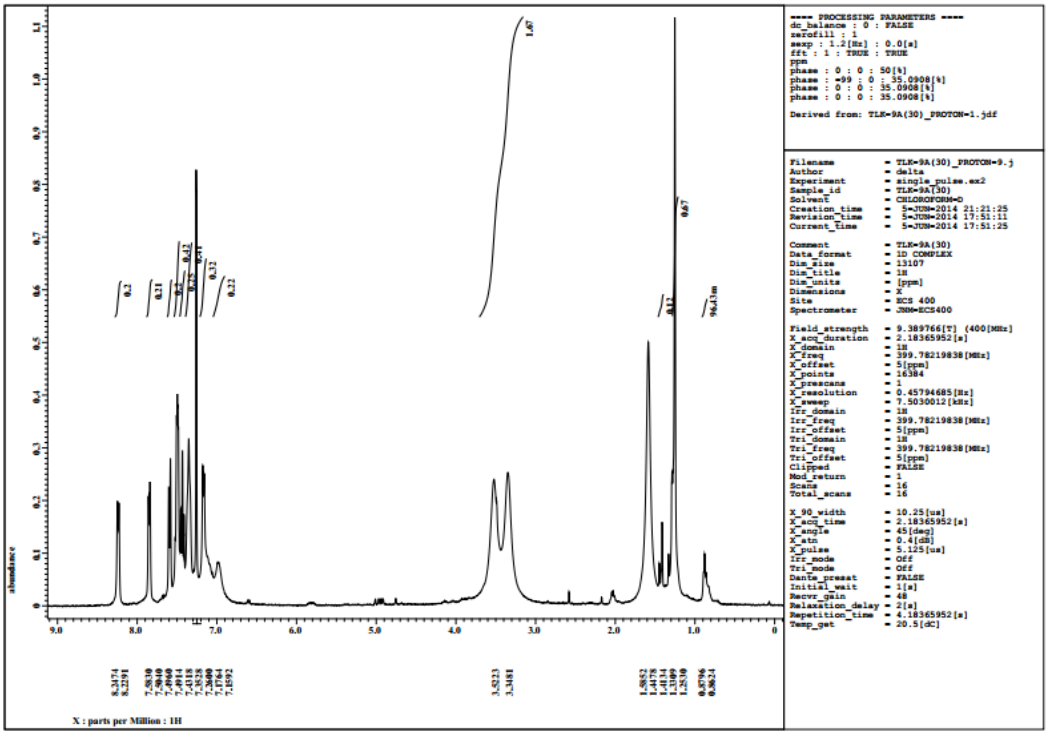

^{1}H-NMR of compound VS-9

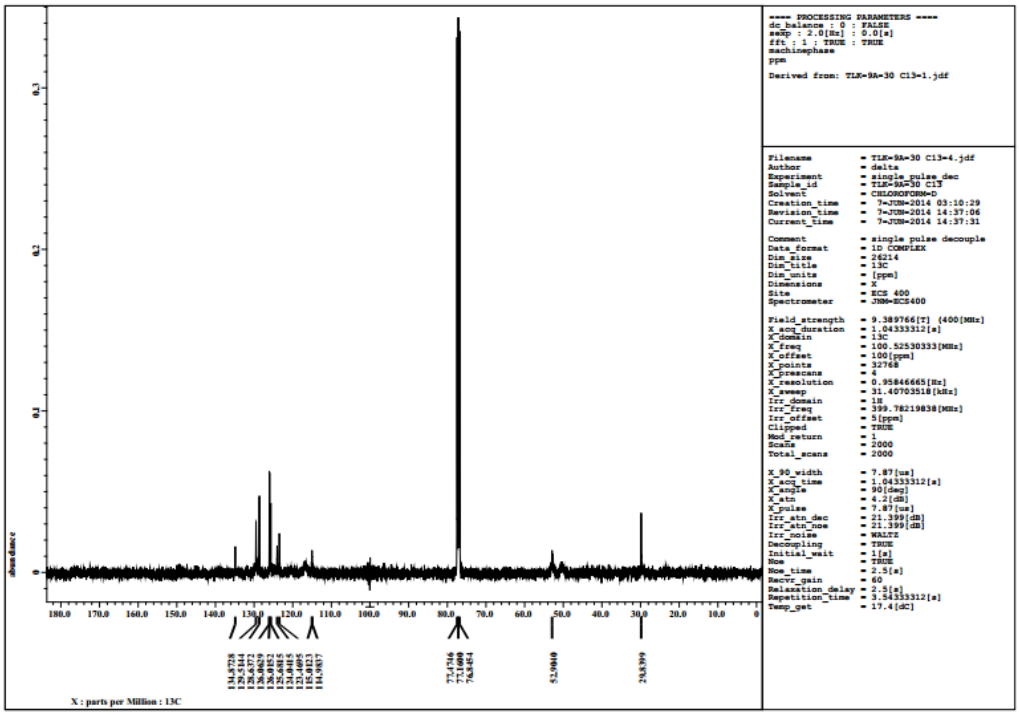

^{13}C-NMR of compound VS-9

(1-(anthracen-9-yl)-4-phenylpiperazine) VS-10

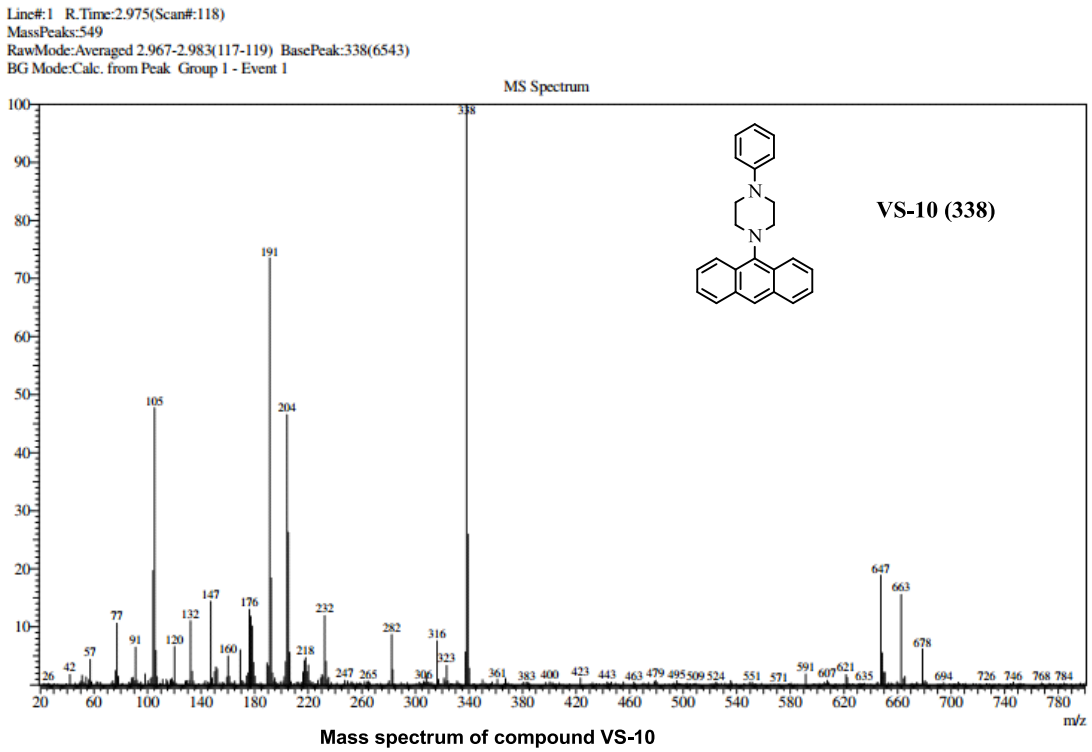

Mass spectrum of compound VS-10

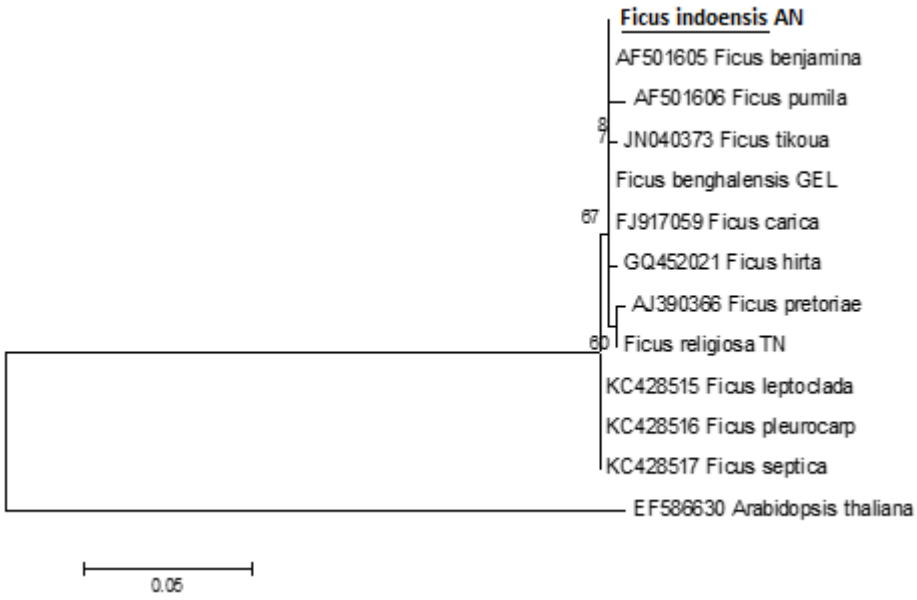

Fig. 26: Molecular phylogenetic analysis of *Ficus* using trnL by Maximum Likelihood method based on the Tamura 3-parameter model (LnL=-910.7407). The percentage of trees in which the associated taxa clustered together is shown next to the branches. Initial tree(s) for the heuristic search were obtained automatically by applying Neighbor-Joining and BioNJ algorithms to a matrix of pairwise distances estimated using the MCL approach, and then selecting the topology with superior log likelihood value. The tree is drawn to scale, with branch lengths measured in the number of substitutions per site. The analysis involved 13 nucleotide sequences. All positions with less than 95% site coverage were eliminated. That is, fewer than 5% alignment gaps, missing data, and ambiguous bases were allowed at any position. There were a total of 387 positions in the final dataset.

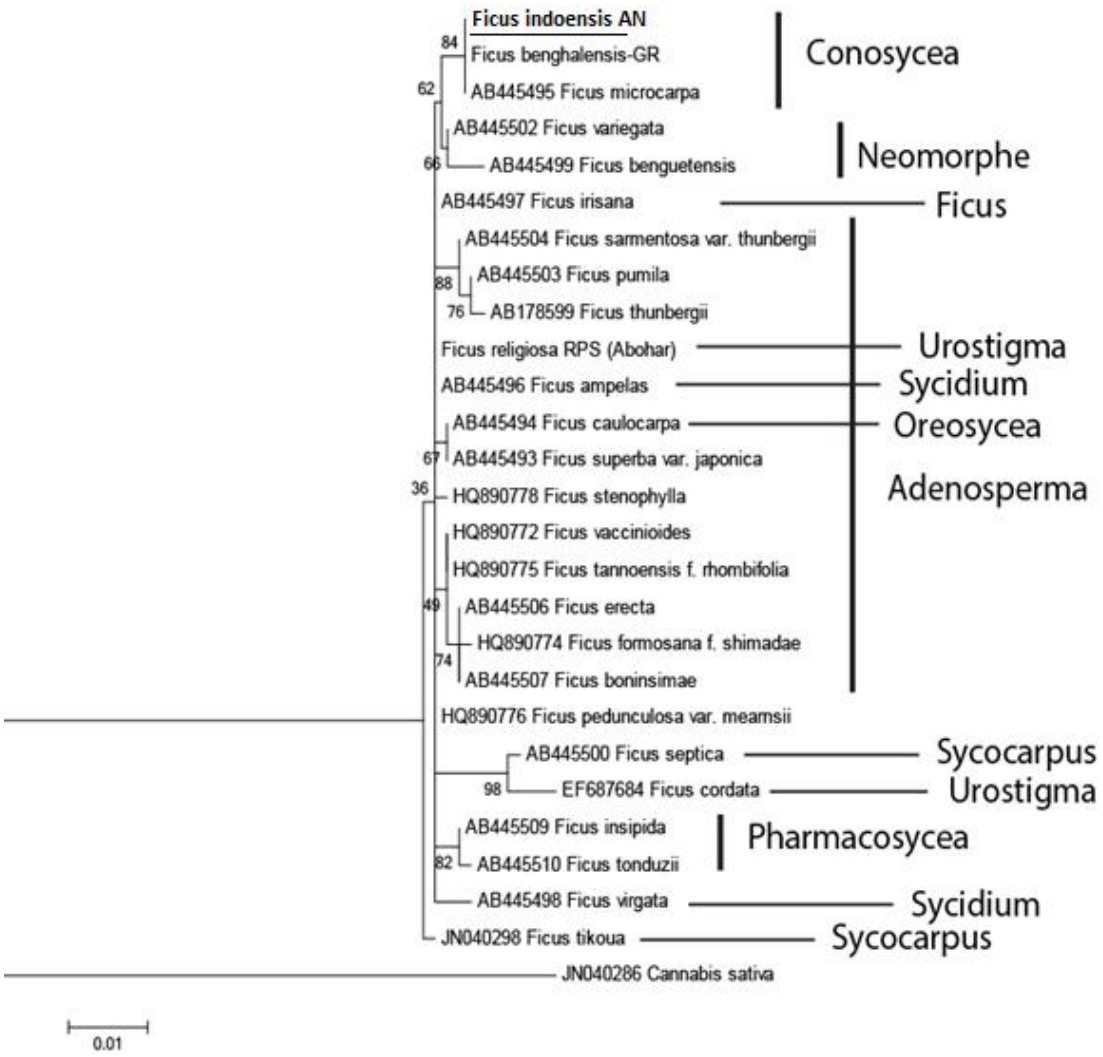

Fig. 27: Molecular phylogenetic analysis of *Ficus* using RPS16-intron by Maximum Likelihood method based on the Tamura 3-parameter (LnL=-1415.0850). The percentage of trees in which the associated taxa clustered together is shown next to the branches. Initial tree(s) for the heuristic search were obtained automatically by applying Neighbor-Joining and BioNJ algorithms to a matrix of pairwise distances estimated using the MCL approach, and then selecting the topology with superior log likelihood value. The tree is drawn to scale, with branch lengths measured in the number of substitutions per site. The analysis involved 27 nucleotide sequences. All positions with less than 95% site coverage were eliminated. That is, fewer than 5% alignment gaps, missing data, and ambiguous bases were allowed at any position. There were a total of 661 positions in the final dataset.

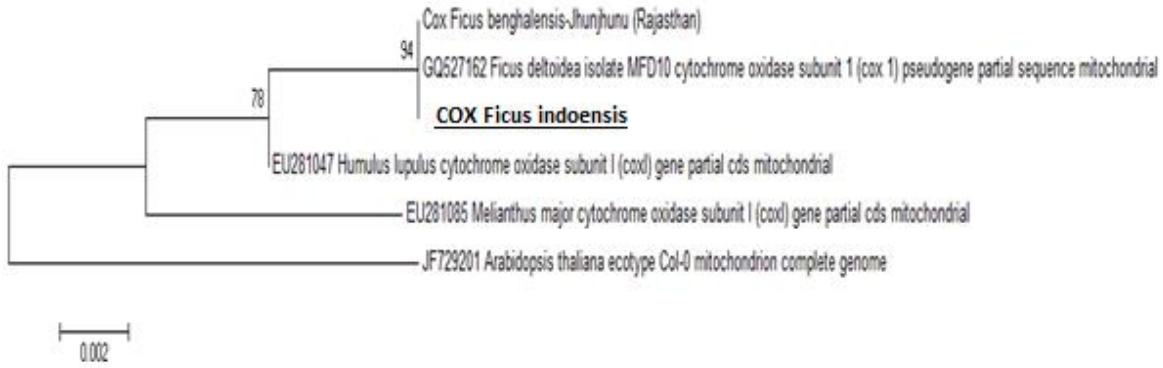

Fig. 28: Molecular phylogenetic analysis of *Ficus* using *COX1* gene by Maximum Likelihood method based on the Hasegawa-Kishino-Yano model (LnL=-1462.4365). The percentage of trees in which the associated taxa clustered together is shown next to the branches. Initial tree(s) for the heuristic search were obtained automatically by applying Neighbor-Joining and BioNJ algorithms to a matrix of pairwise distances estimated using the MCL approach, and then selecting the topology with superior log likelihood value. The tree is drawn to scale, with branch lengths measured in the number of substitutions per site. The analysis involved 6 nucleotide sequences. All positions with less than 95% site coverage were eliminated. That is, fewer than 5% alignment gaps, missing data, and ambiguous bases were allowed at any position. There were a total of 940 positions in the final dataset.

4.6. Morphological study of *F. indoensis* Sp. Nov. leaves and fruits: Different morphological characteristics was observed (Figure 29) in leaves of *F. indoensis* Sp. Nov. when morphological comparison was done in case of both species, than unique characters like leaf shape, apical tail length and texture of leaf was noticeably remarkable (Figure 29). Accuminate leaf shape, rough leaf texture, short axial tail was noticed in newly identified species, whereas, truncate leaf shape, shiny leaf texture and long axial end tail was found in *F. religiosa* (Figure 29). Fruits (commonly called as figs) of this novel species was compared with *F. religiosa* fruits (Figure 30). There was not more difference in both fruits but noticeable character was its colour. Figs of *F. religiosa* are of green colour and changes to red/purple with maturity but in case of *F. indoensis* Sp. Nov. figs are of green colour throughout its life.

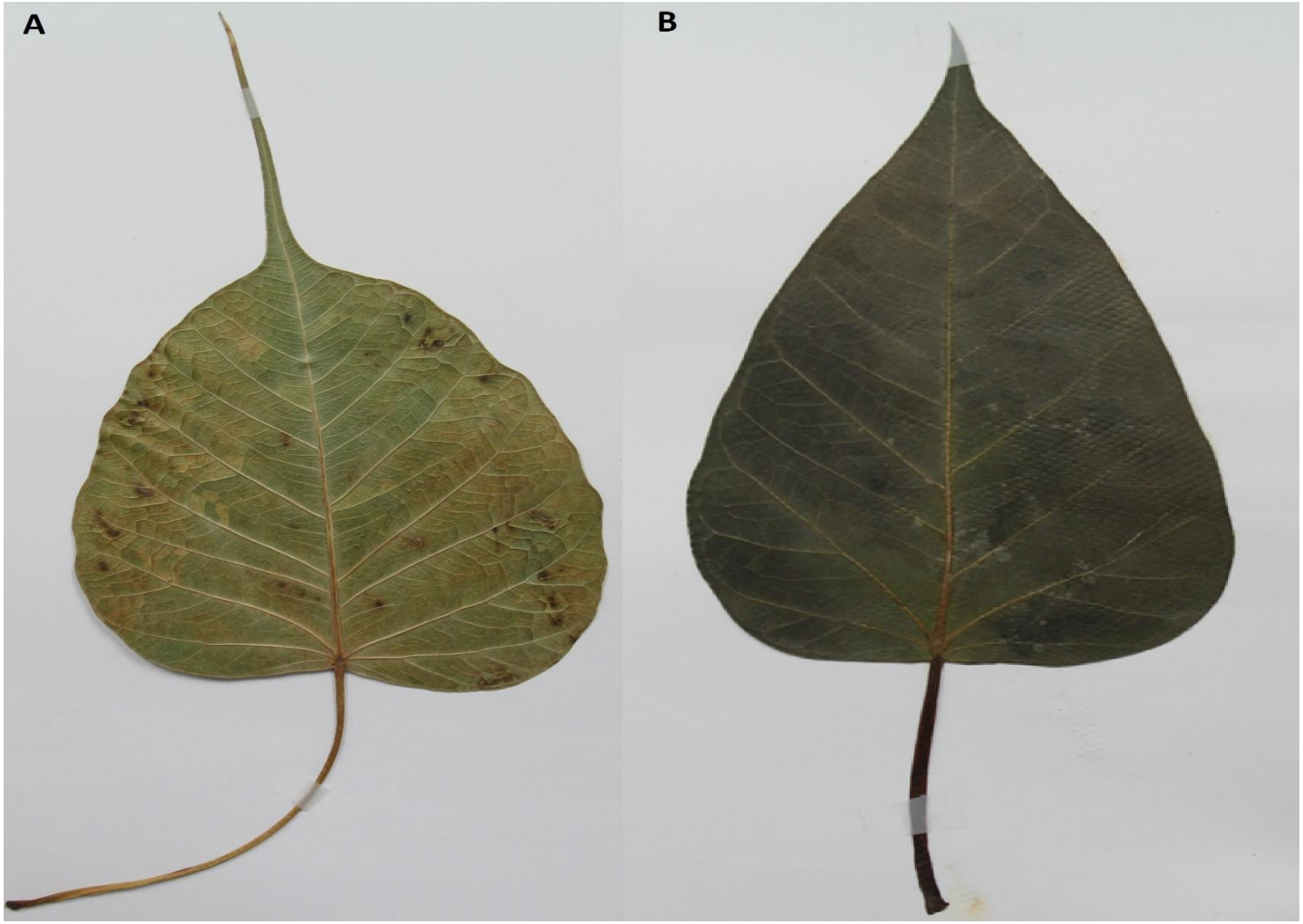

Fig. 29: Picture of leaf, A- *F. religiosa* from city campus of Central University of Punjab, B- *F. indoensis* Sp. Nov. from Nicobar Island

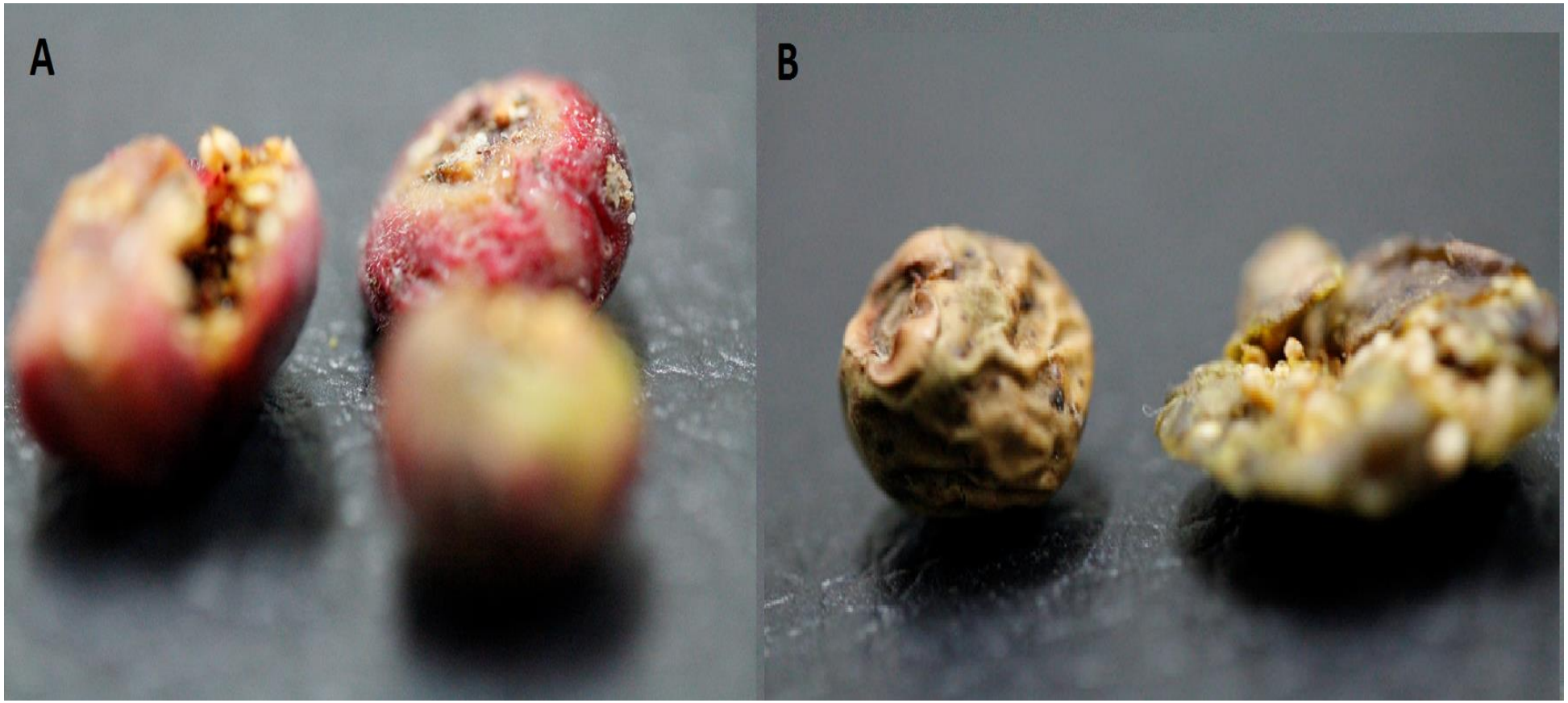

Fig. 30: Picture of fruits, A- *F. religiosa* from city campus of Central University of Punjab, B- *F. indoensis* Sp. Nov. from Nicobar Island

CHAPTER 5

DISCUSSION

The main aim of this study was to investigate sequence-based phylogeography of *F. benghalensis* and *F. religiosa* in Indian subcontinent. This study generated sequence information of *F. religiosa* and *F. benghalensis* at ITS, trnL, RPS16-intron and COX loci. Out of these, the RPS16-intron and COX spacer were sequenced for these species for the first time in the world. This is for the first time that DNA Barcoding was used to assess these species from India. Total of 22 sequences were generated each for ITS, trnL, RPS16-intron loci for *F. benghalensis*. Similarly, 33 sequences each were generated for ITS, trnL, RPS16-intron loci for *F. religiosa*. New specific primer was designed for amplifying COX gene specific to genus *Ficus*. Amplicons were used in multilocal molecular assessment study.

Multilocal phylogenetic analyses were congruent to reveal very low rate of evolution of *F. benghalensis* in Indian subcontinent. In phylograms of *F. benghalensis* (Figure 13-16) no consistent clade was formed at three loci. This inconsistency can be attributed to low genetic diversity of this species in Indian subcontinent. In 2006, a cyclone destroyed original trunk of the “big banyan” tree at Adyar, Chennai, Tamil Nadu, however, in a matter of years the tree have resurrected from the surrounding prop roots. Phylogenetic analysis using samples collected from the colony of Adyar big banyan tree confirmed that these were indeed clonal colonies with 100% similarity in sequences.

Most significant conclusion of the present dissertation is the existence of cryptic speciation within *F. religiosa* (Peepal). Samples collected from throughout its range in the subcontinent clustered within two strongly supported clades in all of the phylogenetic analyses at three loci (ITS, trnL and RPS16, Figure 17-20). These results were congruent with present study morphometric investigations, which revealed distinct leaf axil shape, leaf texture and seed color for the newly revealed cryptic species. Cryptic diversity is believed to be a potentially important factor influencing future conservation decisions. The proportion of cryptic species is almost evenly distributed among major metazoan taxa and biogeographical regions-a conclusion of potentially profound impact on biodiversity assessment and

conservation. The consistent novel clade reveals its possibility to be a novel species and the name *Ficus indoensis* Sp. Nov. is proposed. Furthermore, molecular phylogeny study of *Ficus* genus using dense taxon sampling (N=312) to identify evolutionary affinities of *F. indoensis* Sp. Nov. also revealed the possibility of *F. indoensis* Sp. Nov. as a novel species. Present study morphometric analyses also revealed distinct synapomorphic characters. Seeds of *F. religiosa* are of green colour and changes to red/purple with maturity (Figure 30) but in case of *F. indoensis* Sp. Nov., seeds changes its colour from green to brown towards maturity. Among other distinct, unique characteristics of *Ficus indoensis* Sp. Nov. are accuminate axil shape (Figure 29), rough leaf texture and truncate leaf shape (Table 15).

Ficus genus have been subjected to molecular phylogenetic assessment only once previously (Ronsted *et. al.* 2005) but that had several short comings. First, the study was based only on nuclear ITS1 sequences. The study included only 146 species of *Ficus*, thereby obscuring fine phylogenetic structures within this plant genus. However, the present study included 312 taxa (Figure 25) at ITS dataset. The present study also included trnL (Figure 26), RPS16-intron (Figure 27) and COX (Figure 28) datasets of *Ficus* which represents by far the most comprehensive phylogenetic assessment of *Ficus* till date. In the phylogenetic tree generated by Ronsted *et al.* subgenus Sycomorus was not monophyletic. In this study, section Urostigma and Conosycea showed polyphyly. The molecular phylogeny revealed that the novel species *F. indoensis* was showing affinity with section Conosycea to which *F. benghalensis* belongs rather than showing affinity to section Urostigma to which *F. religiosa* belongs, which evidently supports *F. indoensis* Sp. Nov. as a novel species. This clade include samples from Nicobar Island, Gujrat, Assam and Havelock Island, Andaman.

SUMMARY

Principal conclusion of the present dissertation is revelation of the existence of cryptic speciation within *Ficus religiosa* populations in the Indian subcontinent, with a novel clade "*indoensis*" showing affinity with section Conosycea to which *F. benghalensis* belongs. Phylograms of all three independent loci, as well as the concatenated “supermatrix”, strongly supported this clade. In addition, at least three synapomorphic characters of this clade was also revealed in this morphometric analyses, including leaf shape and texture, and seed color. Phylogenetic and morphological analyses were congruent to an extant to describe the novel clade as a novel species, for which the binomen *Ficus indoensis* Sp. Nov. is proposed. *F. religiosa* sensu Linnaeus was part of section Urostigma, while newly discovered cryptic species was part of the section Conosycea. Analyses did not reveal any phylogeographic structures, either for *F. benghalensis* or for *F. religiosa*, in Indian subcontinent. *Ficus benghalensis* populations in the subcontinent showed very low genetic diversity at all 4 genetic loci examined. Most of the previous studies on molecular phylogeny of figs was done in relation with investigations to reveal its co-evolution with fig wasps. There is only one study till date that included comprehensive molecular systematics of this genus (Ronsted *et. al.* 2005). That study included 146 *Ficus* species, while this included 312 *Ficus* species, at ITS dataset. While the earlier study was based only on one locus, (ITS), this study is based on four loci (ITS, COX, RPS16 and trnL), making this the most comprehensive molecular systematic assessment of genus *Ficus* till date. In addition, this study generated 330 DNA Barcodes of isolates from India overall (none existed prior to this study). This study generated sequence information of *F. religiosa* and *F. benghalensis* at RPS16-intron and *COX1-2* spacer for first time in the world. It is hoped that results revealed in this dissertation will be useful to future research endeavours in this important tree genus.

REFERENCES

Amel, S. H. Mokhtar, T. Salwa, Z. Jihène, H. Messaoud, M. Abdelmajid, R. and Mohamed, M. (2004). Inter-simple sequence repeat fingerprints to assess genetic diversity in Tunisian fig (*Ficus carica* L.) germplasm. *Genetic Resources and Crop Evolution* **51**(3): 269-275.

Arbogast, B. S. Edwards, S. V. Wakeley, J. Beerli, P. and Slowinski, J. B. (2002). Estimating divergence times from molecular data on phylogenetic and population genetic timescales. *Annual Review of Ecology and Systematics* **33**(1): 707-740.

Asmussen, C. B. Dransfield, J. Deickmann, V. Barfod, A. S. PINTAUD, J. C. and Baker, William J. (2006). A new subfamily classification of the palm family (Arecaceae): evidence from plastid DNA phylogeny. *Botanical Journal of the linnean Society* **151**(1): 15-38.

Avise, J. C. (1998a). The history and purview of phylogeography: a personal reflection. *Molecular Ecology* **7**(4): 371-379.

Avise, J. C. (1998b). Pleistocene phylogeographic effects on avian populations and the speciation process. *Proceedings of the Royal Society of London. Series B: Biological Sciences* **265**(1395): 457-463.

Avise, J. C. (2009). Phylogeography: retrospect and prospect. *Journal of Biogeography* **36**(1): 3-15.

Avise, J. C. Arnold, J. B. Martin, R. Bermingham, E. L. Trip, N. Joseph, E. S. and Nancy, C. (1987). Intraspecific phylogeography: the mitochondrial DNA bridge between population genetics and systematics. *Annual review of ecology and systematics* **18**(1): 489-522.

Avise, J. C. Davidson G. Cecilia, L. Joshua, P. John, C. L. and Robert A. (1979). Mitochondrial DNA clones and matriarchal phylogeny within and among geographic populations of the pocket gopher, Geomys pinetis. *Proceedings of the National Academy of Sciences* **76**(12): 6694-6698.

Avise, J. C. Hubbell, S. P. and Ayala, F. J. (2008). In the light of evolution II: Biodiversity and extinction. *Proceedings of the National Academy of Sciences* **105**(Supplement 1): 11453-11457.

Bahulikar, R. A. Lagu, M. D. Kulkarni, B. G. Pandit, S. S. Suresh, H. S. Rao, M. K. V. and Gupta, V. S. (2004). Genetic diversity among spatially isolated populations of Eurya nitida Korth (Theaceae) based on inter-simple sequence repeats. *Current Science-Bangalore* **86**(6): 824-831.

Baker, W. J. Hedderson, T. A. and Dransfield, J. (2000). Molecular Phylogenetics of Subfamily Calamoideae (Palmae) Based on nrDNA ITS and cpDNA RPS16-intron Sequence Data. *Molecular phylogenetics and evolution* **14**(2): 195-217.

Baldwin, B. G. (1992). Phylogenetic utility of the internal transcribed spacers of nuclear ribosomal DNA in plants: an example from the Compositae. *Molecular phylogenetics and evolution* **1**(1): 3-16.

Baldwin, B. G. Sanderson, M. J. Porter, J. M. Wojciechowski, M. F. Campbell, C. S. and Donoghue, M. J. (1995). The ITS region of nuclear ribosomal DNA: a valuable source of evidence on angiosperm phylogeny. *Annals of the Missouri Botanical Garden*: 247-277.

Baraket, G. A. Ahmed B. Saddoud, O. Chatti, K. M. Messaoud, T. M. and Hannachi, S. A. (2010). Molecular polymorphism of cytoplasmic DNA in *Ficus carica* L.: Insights from non-coding regions of chloroplast DNA. *Scientia horticulturae* **125**(3): 512-517.

Baraket, G. A. Abdelkrim, B. Ahmed B. Messaoud, T. M. and Hannachi S. A. (2011). Cyto-nuclear discordance in the genetic relationships among Tunisian fig cultivars (*Ficus carica* L.): Evidence from non coding trnL–trnF and ITS regions of chloroplast and ribosomal DNAs. *Scientia Horticulturae* **130**(1): 203-210.

Baraket, G. A. Chatti, K. Saddoud, O. Abdelkarim, B. Ahmed B. Messaoud, T. M. and Hannachi, S. A. (2011). Comparative assessment of SSR and AFLP markers for evaluation of genetic diversity and conservation of fig, *Ficus carica* L., genetic resources in Tunisia. *Plant molecular biology reporter* **29**(1): 171-184.

Baraket, G. A. Chatti, K. Saddoud, O. Messaoud, T. M. Mokhtar, M. and Hannachi, S. A. (2009). Genetic analysis of Tunisian fig (*Ficus carica* L.) cultivars using amplified fragment length polymorphism (AFLP) markers. *Scientia Horticulturae* **120**(4): 487-492.

Baraket, G. A. Chatti, K. Saddoud, O. Messaoud, T. M. Mokhtar, M. and Hannachi, S. A. (2008). Chloroplast DNA analysis in Tunisian fig cultivars (*Ficus carica* L.): Sequence variations of the trnL-trnF intergenic spacer. *Biochemical Systematics and Ecology* **36**(11): 828-835.

Baraket, G. A. Chatti, K. Saddoud, O. Messaoud, T. M. Mokhtar, M. and Hannachi, S. A. (2009). Sequence analysis of the internal transcribed spacers (ITSs) region of the nuclear ribosomal DNA (nrDNA) in fig cultivars (*Ficus carica* L.). *Scientia Horticulturae* **120**(1): 34-40.

Baral, N. Timilsina, N. and Tamang, B. (2003). Status of Bengal florican *Houbaropsis benghalensis* in Nepal. *Forktail*: 51-56.

Bast, F. (2014). Ancestors of Land Plants with Rich Diversity. *Resonance*.

Beheregaray, L. B. (2008). Twenty years of phylogeography: the state of the field and the challenges for the Southern Hemisphere. *Molecular Ecology* **17**(17): 3754-3774.

Berg, C. C. (1989). Classification and distribution of *Ficus*. *Experientia* **45**(7): 605-611.

Bermingham, E. and Moritz, C. (1998). Comparative phylogeography: concepts and applications. *Molecular Ecology* **7**(4): 367-369.

Bernatchez, L. and Wilson, C. C. (1998). Comparative phylogeography of Nearctic and Palearctic fishes. *Molecular Ecology* **7**(4): 431-452.

Brack, D. Gray, K. and Hayman, G. (2002). Controlling the international trade in illegally logged timber and wood products. *Sustainable Development Programme, Royal Institute of International Affairs. London*.

Brito, P. H. and Edwards, and S. V. (2009). Multilocus phylogeography and phylogenetics using sequence-based markers. *Genetica* **135**(3): 439-455.

Brown, J. H. (1984). On the relationship between abundance and distribution of species. *American naturalist*: 255-279.

Cabrita, L. F. Aksoy, U. Hepaksoy, S. and Leitão, J. M. (2001). Suitability of isozyme, RAPD and AFLP markers to assess genetic differences and relatedness among fig (*Ficus carica* L.) clones. *Scientia Horticulturae,* **87**(4): 261-273.

Chase, M. W. Salamin, N. Wilkinson, M. Dunwell, J. M. Kesanakurthi, R. P. Haidar, N. and Savolainen, V. (2005). Land plants and DNA barcodes: short-term and long-term goals. *Philosophical Transactions of the Royal Society B: Biological Sciences* **360**(1462): 1889-1895.

Chatti, K. Saddoud, O. Hannachi, S. A. Messaoud, M. M. Mohamed, T. M. (2007). Analysis of genetic diversity and relationships in a Tunisian fig (*Ficus carica*) germplasm collection by random amplified microsatellite polymorphisms. *Journal of Integrative Plant Biology* **49**(3): 386-391.

Clement, W. L. and Weiblen, G. D. (2009). Morphological evolution in the mulberry family (Moraceae). *Systematic Botany* **34**(3): 530-552.

Cook, J. M. and Rasplus, J. Y. (2003). Mutualists with attitude: coevolving fig wasps and figs. *Trends in Ecology and Evolution* **18**(5): 241-248.

Corner, E. J. H. (1940). Wayside trees of Malaya, Vols. I and II. *Wayside trees of Malaya, Vols. I and II*.

Corner, E. J. H. (1985). *Ficus* (Moraceae) and Hymenoptera (Chalcidoidea): figs and their pollinators. *Biological Journal of the Linnean Society* **25**(2): 187-195.

Datwyler, S. L. and Weiblen, G. D. (2004). On the origin of the fig: phylogenetic relationships of Moraceae from ndhF sequences. *American Journal of Botany* **91**(5): 767-777.

Ghani, A. Monier, M. and Khalik, A. K. N. (2006). Floristic Diversity and Phytogeography of the Gebel Elba National Park, South-East Egypt. *Turkish Journal of Botany* **30**(2): 398-405.

Groot, D. G. Arjen, D. Heinjo, J. Maas, J. W. Schneider, H. Vogel, J. C. and Erkens, R. H. J. (2011). Use of rbcL and trnL-F as a two-locus DNA barcode for identification of NW-European ferns: an ecological perspective. *PLoS one* **6**(1): 16371-16380.

Domyati, F. M. Y. Rania A. A. Edris, S. Mansour, A. Sabir, G. and Bahieldin, A. (2011). Molecular markers associated with genetic diversity of some medicinal plants in Sinai. *Journal of Medicinal plants Research* **5**(2): 200-210.

Downie, S. R. and Palmer, J. D. (1992). Use of chloroplast DNA rearrangements in reconstructing plant phylogeny *Molecular systematics of plants Springer* 14-35.

Ellstrand, N. C, and Roose, M. L. (1987). Patterns of genotypic diversity in clonal plant species. *American Journal of Botany* 123-131.

Feliner, G. N. and Rosselló, J. A. (2007). Better the devil you know? Guidelines for insightful utilization of nrDNA ITS in species-level evolutionary studies in plants. *Molecular phylogenetics and evolution* **44**(2): 911-919.

Felsenstein, J. (1988). Phylogenies from molecular sequences: inference and reliability. *Annual review of genetics* **22**(1): 521-565.

Forrest, I. Burg, K. and Klumpp, R. (2008). Genetic markers: tools for identifying and characterising Scots pine populations. *Forest Systems* **9**(3): 67-88.

Frézal, L. and Leblois, R. (2008). Four years of DNA barcoding: current advances and prospects. *Infection, Genetics and Evolution* **8**(5): 727-736.

Gao, T. Yao, H. Song, J. Liu, C. Zhu, Y. Xinye, M. and Chen, S. (2010). Identification of medicinal plants in the family Fabaceae using a potential DNA barcode ITS2. *Journal of ethnopharmacology* **130**(1): 116-121.

Gathier, G. Niet, T. Peelen, T. Vugt, R. R. Eurlings, M. and Gravendeel, B. (2013). Forensic Identification of CITES Protected Slimming Cactus (Hoodia) Using DNA Barcoding. *Journal of forensic sciences* **58**(6): 1467-1471.

Gaut, B. S. Muse, S. V. and Clegg, M. T. (1993). Relative rates of nucleotide substitution in the chloroplast genome. *Molecular Phylogenetics and Evolution* **2**(2): 89-96.

Ghada, B. Ahmed, B. Abdelkrim, K. C. Saddoud, O. Messaoud, M. Mokhtar, T. and Hannachi, S. A. (2010). Molecular evolution of chloroplast DNA in fig (*Ficus carica* L.): Footprints of sweep selection and recent expansion. *Biochemical Systematics and Ecology* **38**(4): 563-575.

Ghada, B. Ahmed, B. Chatti, K. Saddoud, O. Messaoud, T.M. Mokhtar M. and Hannachi, S. A. (2013). Genetic diversity and molecular evolution of the internal transcribed spacer (ITSs) of nuclear ribosomal DNA in the Tunisian fig cultivars (*Ficus carica* L.; Moracea). *Biochemical Systematics and Ecology* **48**: 20-33.

Giaimo, M. S. (1987). Deforestation in Brazil: domestic political imperative-global ecological disaster. *Envtl. L.* **18**: 537-538.

Gimaret, C. Clémentine, P. Raphaël, P. Pierre, J. and Houllier, F. (1998). Sampling strategies for the assessment of tree species diversity. *Journal of Vegetation Science* **9**(2): 161-172.

Gonzalez, M. A. Baraloto, C. Engel, J. Mori, S. A. Pétronelli, P. Riéra, B. Chave, J. (2009). Identification of Amazonian trees with DNA barcodes. *PLoS one* **4**(10): 7483-7509.

Gottlieb, L. D. (1977). Electrophoretic evidence and plant systematics. *Annals of the Missouri Botanical Garden*: 161-180.

Hajibabaei, M. S. Gregory, A. C. Hebert, P. D. N. and Hickey, D. A. (2007). DNA barcoding: How it complements taxonomy, molecular phylogenetics and population genetics. *TRENDS in Genetics* **23**(4: 167-172.

Hamrick, J. L. and Godt, M. J. W. (1996). Effects of life history traits on genetic diversity in plant species. *Philosophical Transactions of the Royal Society of London. Series B: Biological Sciences* **351**(1345): 1291-1298.

Hamrick, J. L. Godt, M. J. W. and Broyles, S. Susan, L. (1992). Factors influencing levels of genetic diversity in woody plant species *Population genetics of forest trees* Springer 95-124.

Hamrick, J. L. Mitton, J. B. and Linhart, Y. B. (1981). Levels of genetic variation in trees: influence of life history characteristics. *Isozymes of north American forest trees and forest insects* 35-41.

Hewitt, G. M. (2004). The structure of biodiversity–insights from molecular phylogeography. *Frontiers in Zoology* **1**(4): 1-16.

Hollingsworth, P. M. (2011). Refining the DNA barcode for land plants. *Proceedings of the National Academy of Sciences* **108**(49) 19451-19452.

Hollingsworth, P. M. Forrest, L. L. Spouge, J. L. Hajibabaei, M. Ratnasingham, S. Michelle, F. Aron, J. (2009). A DNA barcode for land plants. *Proceedings of the National Academy of Sciences* **106**(31): 12794-12797.

Hollingsworth, P. M. Graham, S. W. and Little, D. P. (2011). Choosing and using a plant DNA barcode. *PLoS one* **6**(5): 19254-19290.

Ikegami, H. Nogata, H. Hirashima, K. Awamura, M. and Nakahara, T. (2009). Analysis of genetic diversity among European and Asian fig varieties (*Ficus carica* L.) using ISSR, RAPD, and SSR markers. *Genetic resources and crop evolution* **56**(2): 201-209.

Iqbal, Z. Khalid, N. Q. Khan, M. N. Akhtar, M. S. and Waraich, F. N. (2001). In vitro anthelmintic activity of Allium sativum, Zingiber officinale, Curcurbita mexicana and *Ficus religiosa*. *International Journal of Agriculture and Biology* **3**(4): 454-457.

Jebara, M. Mhamdi, R. Aouani, M. E. Ghrir, R. and Mars, M. (2001). Genetic diversity of Sinorhizobium populations recovered from different Medicago varieties cultivated in Tunisian soils. *Canadian journal of microbiology* **47**(2): 139-147.

Joseph, B. and Raj, S. J. (2011). An overview-*Ficus benghalensis* linn. *International Journal of Pharmaceutical Sciences Review and Research* **6**(1).

Jousselin, E. Rasplus, J. Y. and Kjellberg, F. (2003). Convergence and coevolution in a mutualism: evidence from a molecular phylogeny of *Ficus*. *Evolution* **57**(6): 1255-1269.

Keller and Barbara E. M. (2000). Genetic variation among and within populations of Phragmites australis in the Charles River watershed. *Aquatic Botany* **66**(3): 195-208.

Kester, D. R. Duedall, I. W. Connors, D. N. and Pytkowicz, R. M. (1967). Preparation of artificial seawater. *Limnol. Oceanogr* **12**(1) 176-179.

Khadari, B. Grout, C. Santoni, S. and Kjellberg, F. (2005). Contrasted genetic diversity and differentiation among Mediterranean populations of *Ficus carica* L.: a study using mtDNA RFLP. *Genetic resources and crop evolution* **52**(1): 97-109.

Khadari, B. Roger, J. P. Ater, M. Achtak, H. Oukabli, A. and Kjellberg, F. (2005). *Moroccan fig presents specific genetic resources: a high potential of local selection.* Paper presented at the III International Symposium on Fig: 798.

Khan, S. Qurainy, A. F. Nadeem, M. and Tarroum, M. (2012). Development of genetic markers for *Ochradenus arabicus* (Resedaceae), an endemic medicinal plant of Saudi Arabia. *Genetics and Molecular Research* **11**(2): 1300-1308.

Khedr, A. H. Marc, W. Keblawy, E. A. and Doust, L. J. (2002). Phylogenetic diversity and ecological features in the Egyptian flora. *Biodiversity and Conservation* **11**(10): 1809-1824.

Kinloch, B. B. Westfall, R. D. and Forrest, G. I. (1986). Caledonian Scots pine: origins and genetic structure. *New Phytologist* **104**(4): 703-729.

Knowles, L. L. (2009). Statistical phylogeography. *Annual Review of Ecology, Evolution, and Systematics* **40**: 593-612.

Knowles, L L. and Maddison, W. P. (2002). Statistical phylogeography. *Molecular Ecology* **11**(12): 2623-2635.

Knowles, L. L. (2004). The burgeoning field of statistical phylogeography. *Journal of evolutionary biology* **17**(1): 1-10.

Kress, W. J. and Erickson, D. L. (2007). A two-locus global DNA barcode for land plants: the coding rbcL gene complements the non-coding trnH-psbA spacer region. *PLoS one* **2**(6): 508-530.

Kress, W. J. Wurdack, K. J. Zimmer, E. A. Weigt, L. A. and Janzen, D. H. (2005). Use of DNA barcodes to identify flowering plants. *Proceedings of the National Academy of Sciences of the United States of America* **102**(23): 8369-8374.

Kunwar, R. M. and Bussmann, R. W. (2006). *Ficus* (Fig) species in Nepal: a review of diversity and indigenous uses. *Lyonia* **11**(1): 85-97.

Kuroiwa, T. (1991). The replication, differentiation, and inheritance of plastids with emphasis on the concept of organelle nuclei. *Int Rev Cytol* **128**: 1-62.

Kusumi, J. Azuma, H. Tzeng, H. Chou, L. S. Peng, Y. Q. Nakamura, K. and Su, Z. H. (2012). Phylogenetic analyses suggest a hybrid origin of the figs (Moraceae:*Ficus*) that are endemic to the Ogasawara (Bonin) Islands, Japan. *Molecular phylogenetics and evolution* **63**(1): 168-179.

Lahaye, R. VanderBank, M. Bogarin, D. Warner, J. Pupulin, F. Gigot, G. Savolainen, V. (2008). DNA barcoding the floras of biodiversity hotspots. *Proceedings of the National Academy of Sciences* **105**(8): 2923-2928.

Laiou, A., Mandolini, L. A. Piredda, R. Bellarosa, R. and Simeone, M. C. (2013). DNA barcoding as a complementary tool for conservation and valorisation of forest resources. *ZooKeys* **8**(365): 197-230.

Lidén, M. Fukuhara, T. Rylander, J. and Oxelman, B. (1997). Phylogeny and classification ofFumariaceae, with emphasis onDicentra sl, based on the plastid geneRPS16 intron. *Plant Systematics and Evolution* **206**(1-4): 411-420.

Li, De-Zhu, Gao, Lian-Ming, Li, Hong-Tao, Wang, Hong, Ge, Xue-Jun, Liu, Jian-Quan, Yang, Jun-Bo. (2011). Comparative analysis of a large dataset indicates that internal transcribed spacer (ITS) should be incorporated into the core barcode for seed plants. *Proceedings of the National Academy of Sciences* **108**(49): 19641-19646.

LI, H-Q, CHEN, J-Y, Wang, S, and XIONG, S-Z. (2012). Evaluation of six candidate DNA barcoding loci in *Ficus* (Moraceae) of China. *Molecular ecology resources* **12**(5): 783-790.

LI, Hong-Qing, Wang, Shuang, CHEN, Ji-Yun, and Gui, Ping. (2012). Molecular phylogeny of *Ficus* section *Ficus* in China based on four DNA regions. *Journal of Systematics and Evolution* **50**(5): 422-432.

Linhart, Y. B. and Grant, M. C. (1996). Evolutionary significance of local genetic differentiation in plants. *Annual Review of Ecology and Systematics* **27**(1): 237-277.

Linnaeus, C. (1753). *Species plantarum* (Vol. 4): Impensis GC Nauk.

Liston, A. Robinson, W. A. Oliphant, J. M. Buylla, A. and Elena, R. (1996). Length variation in the nuclear ribosomal DNA internal transcribed spacer region of non-flowering seed plants. *Systematic Botany* 21-34.

Loveless, M. D. and Hamrick, J. L. (1984). Ecological determinants of genetic structure in plant populations. *Annual review of ecology and systematics* 65-95.

Makhija, I. K. Sharma, I. P. and Khamar, D. (2010). Phytochemistry and Pharmacological properties of *Ficus religiosa*: An overview. *Annals of Biological Research* **1**(4): 435-459.

Meng-Meng, Lu, Xiu-Qin, CI, Guo-Ping, YANG, and Jie, LI. DNA Barcoding of Subtropical Forest Trees-A Study from Ailao Mountains Nature Reserve, Yunnan, China.

Meyer, C. P. and Paulay, G. (2005). DNA barcoding: error rates based on comprehensive sampling. *PLoS biology* **3**(12): 422-439.

Mitchell-Olds, T. and Schmitt, J. (2006). Genetic mechanisms and evolutionary significance of natural variation in Arabidopsis. *Nature* **441**(7096): 947-952.

Navarro, S. P. Jurado, R. José, A. Gómez, Z. Jesús, L. Christopher, H. C. and Vogler, A. P. (2010). DNA profiling of host–herbivore interactions in tropical forests. *Ecological Entomology* **35**(s1): 18-32.

Nepal, M. P. and Ferguson, C. J. (2012). Phylogenetics of *Morus* (Moraceae) inferred from ITS and trnL-trnF sequence data. *Systematic Botany* **37**(2): 442-450.

Newton, A. C. Allnutt, T. R. Gillies, A. C. M. Lowe, A. J. and Ennos, R. A. (1999). Molecular phylogeography, intraspecific variation and the conservation of tree species. *Trends in Ecology and Evolutio,* **14**(4): 140-145.

Nybom, H. (2004). Comparison of different nuclear DNA markers for estimating intraspecific genetic diversity in plants. *Molecular ecology* **13**(5): 1143-1155.

Oxelman, B. Lidén, M. and Berglund, D. (1997). Chloroplast RPS16 intron phylogeny of the tribe Sileneae (Caryophyllaceae). *Plant Systematics and Evolution* **206**(1-4): 393-410.

Packer, L. Gibbs, J. Sheffield, C. and Hanner, R. (2009). DNA barcoding and the mediocrity of morphology. *Molecular Ecology Resources* **9**(s1) 42-50.

Paliwal, D. Prelimi (1987). pharmacological profile of *Ficus religiosa* l.: a overview.

Palmer, J. D. (1992). Mitochondrial DNA in plant systematics: applications and limitations *Molecular systematics of plants Springer* 36-49.

Parker, M. Thompson, J. N. and Weller, S. G. (2001). The population biology of invasive species. *Annu. Rev. Ecol. Syst* **32:** 305-332.

Parrish, T. L. Koelewijn, H. P. and Van D. Peter, J. (2004). Identification of a male-specific AFLP marker in a functionally dioecious fig, *Ficus fulva* Reinw. ex Bl.(Moraceae). *Sexual Plant Reproduction* **17**(1): 17-22.

Petit, R. J. Duminil, J. Fineschi, S. Hampe, A. Salvini, D. and Vendramin, G. G. (2005). Invited review: Comparative organization of chloroplast, mitochondrial and nuclear diversity in plant populations. *Molecular Ecology* **14**(3): 689-701.

Poeaim, A. Poeaim, S. Soytong, K. and Krajangvuthi, T. (2008). Genetic Diversity of *Ficus carica* L. Based on Non-Coding Regions of Chloroplast DNA. *The 8th International Symposium on Biocontrol and Biotechnology* **2**(47): 295-300.

Ponoy, B. (1993). Genetic variability in Douglas-fir based on molecular genetic markers and morphological traits. University of British Columbia 1-175.

Rakshith, D. Santosh, P. and Satish, S. (2013). Isolation and characterization of antimicrobial metabolite producing endophytic Phomopsis sp. from *Ficus pumila* Linn.(Moraceae). *International Journal of Chemical and Analytical Science* **4**(3): 156-160.

Ronquist, F. (1997). Dispersal-vicariance analysis: a new approach to the quantification of historical biogeography. *Systematic Biology* **46**(1): 195-203.

Ronquist, F. and Huelsenbeck, J. P. (2003). MrBayes 3: Bayesian phylogenetic inference under mixed models. *Bioinformatic* **19**(12): 1572-1574.

Ronsted, N. Weiblen, G. D. Clement, W. L. Zerega, N. J. C. and Savolainen, V. (2008). Reconstructing the phylogeny of figs (*Ficus*, Moraceae) to reveal the history of the fig pollination mutualism. *Symbiosis (Rehovot)* **45**(1): 45.

Rønsted, N. Yektaei, K. E. Turk, K. Clarkson, J. M. and Chase, M. W. (2006). Species-level phylogenetics of large genera: prospects of studying co-evolution and polyploidy. *Reconstructing the tree of life: taxonomy and systematics of species rich taxa* **72**.

Rønsted, N. Salvo, G. and Savolainen, V. (2007a). Biogeographical and phylogenetic origins of African fig species (*Ficus* section *Galoglychia*). *Molecular phylogenetics and evolution* **43**(1): 190-201.

Rønsted, N. Salvo, G. and Savolainen, V. (2007b). Biogeographical and phylogenetic origins of African fig species (*Ficus* section Galoglychia). *Molecular phylogenetics and evolution* **43**(1): 190-201.

Rønsted, N. Weiblen, G. D. Cook, J. M. Salamin, N. Machado, C. A. and Savolainen, V. (2005). 60 million years of co-divergence in the fig–wasp symbiosis. *Proceedings of the Royal Society B: Biological Sciences* **272**(1581): 2593-2599.

Rønsted, N. Weiblen, G. D. Savolainen, V. and Cook, J. M. (2008a). Phylogeny, biogeography, and ecology of *Ficus* section Malvanthera (Moraceae). *Molecular Phylogenetics and Evolution* **48**(1): 12-22.

Rønsted, N. Weiblen, G. D. Savolainen, V. and Cook, J. M. (2008b). Phylogeny, biogeography, and ecology of *Ficus* section Malvanthera(Moraceae). *Molecular Phylogenetics and Evolution* **48**(1): 12-22.

Rout, G. R. and Aparajita, S. (2009). Genetic relationships among 23 *Ficus* accessions using inter-simple sequence repeat markers. *Journal of Crop Science and Biotechnology* **12**(2): 91-96.

Roy, S. Tyagi, A. Shukla, V. Kumar, A. Singh, U. M. Chaudhary, L. B. Nair, N. K. (2010). Universal plant DNA barcode loci may not work in complex groups: a case study with Indian *Berberis* species. *PLoS One* **5**(10): 13674-13689.

Saravanan, P. and Chandramohan, G. (2011). Dyeing of Silk with Ecofriendly Natural Dye obtained from Barks of *Ficus religiosa*. L. *Universal Journal of Environmental Research and Technology* **1**(3).

Sanchez, P. M. Virginia, C. Yangrae, M. Jeffrey, P. Alverson, A. J. and Palmer, J. D. (2008). Frequent, phylogenetically local horizontal transfer of the cox1 group I intron in flowering plant mitochondria. *Molecular biology and evolution* **25**(8): 1762-1777.

Sharma, A. Kumari, M. and Jagannadham, M. V. (2009). Benghalensin, a highly stable serine protease from the latex of medicinal plant *Ficus benghalensis*. *Journal of agricultural and food chemistry* **57**(23): 11120-11126.

Sharma, S. Chaturvedi, M. Edwin, E. Shukla, S. and Sagrawat, H. (2007). Evaluation of the phytochemicals and antidiabetic activity of *Ficus benghalensis*. *International journal of diabetes in developing countries,* **27**(2): 234-256.

Sinclair, W. T. Morman, J. D. and Ennos, R. A. (1998). Multiple origins for Scots pine (*Pinus sylvestris* L.) in Scotland: evidence from mitochondrial DNA variation. *Heredity* **80**(2): 233-240.

Sinclair, W. T. Morman, J. D. and Ennos, R. A. (1999). The postglacial history of Scots pine (*Pinus sylvestris* L.) in western Europe: evidence from mitochondrial DNA variation. *Molecular Ecology* **8**(1): 83-88.

Soininen, E. M. Valentini, A. Coissac, E. Miquel, C. Gielly, L. Brochmann, C. and Yoccoz, N. G. (2009). Analysing diet of small herbivores: the efficiency of DNA barcoding coupled with high-throughput pyrosequencing for deciphering the composition of complex plant mixtures. *Frontiers in Zoology* **6**(1): 16.

Soltis, D. E. Gitzendanner, M. A. Strenge, D. D. and Soltis, P. S. (1997). Chloroplast DNA intraspecific phylogeography of plants from the Pacific Northwest of North America. *Plant Systematics and Evolution* **206**(1-4) 353-373.

Sugiura, M. (1989). The chloroplast chromosomes in land plants. *Annual Review of Cell Biology* **5**(1): 51-70.

Summerell, B. A. Laurence, M. H. Liew, E. C. Y. and Leslie, J. F. (2010). Biogeography and phylogeography of Fusarium: a review. *Fungal Diversity* **44**(1): 3-13.

Taberlet, P. Coissac, E. Pompanon, F. Gielly, L. Miquel, C. Valentini, A. and Willerslev, E. (2007). Power and limitations of the chloroplast trnL (UAA) intron for plant DNA barcoding. *Nucleic Acids Research* **35**(3): 14-34.

Templeton, A. R. (2004). Statistical phylogeography: methods of evaluating and minimizing inference errors. *Molecular Ecology* **13**(4): 789-809.

Thompson, J. D. Higgins, D. G. and Gibson, T. J. (1994). CLUSTAL W: improving the sensitivity of progressive multiple sequence alignment through sequence

weighting, position-specific gap penalties and weight matrix choice. *Nucleic acids research* **22**(22): 4673-4680.

Tous, J. and Ferguson, L. (1996). Mediterranean fruits. *Progress in new crops* 416-430.

Tripathi, A. M. Tyagi, A. Kumar, A. Singh, A. Singh, S. Chaudhary, L. B. and Roy, Sribash. (2013). The Internal Transcribed Spacer (ITS) Region and trnhH-psbA Are Suitable Candidate Loci for DNA Barcoding of Tropical Tree Species of India. *PloS one* **8**(2): 57934-57946.

Tsai, Li-Chin, Yu, Yung-Chien, Hsieh, Hsing-Mei, Wang, Jenn-Che, Linacre, Adrian, and Lee, James Chun-I. (2006). Species identification using sequences of the trnL intron and the trnL-trnF IGS of chloroplast genome among popular plants in Taiwan. *Forensic science international* **164**(2): 193-200.

Uma, B. Prabhakar, K. and Rajendran, S. (2009). Invitro antimicrobial activity and phytochemical analysis of *Ficus religiosa* L. and *Ficus benghalensis* L. against Diarrhoeal Enterotoxigenic *E. coli*. *Ethnobotanical leaflets* **2009**(4): 7.

Uzun, A. Yesiloglu, T. Polat, I. Aka, K. Y. Gulsen, O. Yildirim, B. Sahin, A. (2011). Evaluation of genetic diversity in lemons and some of their relatives based on SRAP and SSR markers. *Plant Molecular Biology Reporter* **29**(3): 693-701.

Valentini, A. Miquel, C. Nawaz, M. A. Bellemain, E. V. A. Coissac, E. Pompanon, F. Wincker, P. (2009). New perspectives in diet analysis based on DNA barcoding and parallel pyrosequencing: the trnL approach. *Molecular Ecology Resources* **9**(1): 51-60.

Wares, J. P. and Cunningham, C. W. (2001). Phylogeography and historical ecology of the North Atlantic intertidal. *Evolution* **55**(12): 2455-2469.

Weiblen, G. D. (2000). Phylogenetic relationships of functionally dioecious *Ficus* (Moraceae) based on ribosomal DNA sequences and morphology. *American Journal of Botany* **87**(9): 1342-1357.

Weiblen, G. D. (2001). Phylogenetic relationships of fig wasps pollinating functionally dioecious *Ficus* based on mitochondrial DNA sequences and morphology. *Systematic Biology* **50**(2): 243-267.

Xu, L. Harrison, R. D. Yang, P. and YANG, D. R. (2011). New insight into the phylogenetic and biogeographic history of genus *Ficus*: Vicariance played a

relatively minor role compared with ecological opportunity and dispersal. *Journal of Systematics and Evolution* **49**(6): 546-557.

Yao, H. Song, J. Liu, C. Luo, K. Han, J. Li, Y. Xiao, P. (2010). Use of ITS2 region as the universal DNA barcode for plants and animals. *PloS one* **5**(10): 13102-13111.

Yu, H. and Nason, J. D. (2013). Nuclear and chloroplast DNA phylogeography of *Ficus hirta*: obligate pollination mutualism and constraints on range expansion in response to climate change. *New Phytologist* **197**(1): 276-289.

Yu, H. Nason, J. D. Xuejun, G. and Zeng, J. (2010). Slatkin's Paradox: When direct observation and realized gene flow disagree. A case study in *Ficus*. *Molecular ecology* **19**(20): 4441-4453.

Yuhua, W. Wei, W. Wei, T. and Weiguo, Z. (2013). Analysis of chloroplast ribosomal subunit S16 (RPS16) intron sequences in *Morus* (Urticales: Moraceae). *African Journal of Biotechnology* **10**(77): 17695-17699.

Zink, R. M. Kessen, A. E. Line, T. V. and Rago, B. Rachelle C. (2001). Comparative phylogeography of some aridland bird species. *The Condor* **103**(1): 1-10.

Zoghlami, N. Chrita, I. Bouamama, B. Gargouri, M. Zemni, H. Ghorbel, A. and Mliki, A. (2007). Molecular based assessment of genetic diversity within Barbary fig (*Opuntia Ficus indica* (L.) Mill.) in Tunisia. *Scientia horticulturae* **113**(2): 134-141.

APPENDIX A

Pairwise distances calculated using MEGA

Table 21: Pairwise distances between *F. benghalensis* using ITS datasets

Andhra Pradesh (Mahbubnagar)		0.000	0.000	0.000	0.004	0.000	0.008	0.000	0.000	0.000	0.000	0.000	0.000	0.000	0.000	0.000	0.000	0.000	0.007	0.000	0.000
Jammu (Bantalab)	0.000		0.000	0.000	0.004	0.000	0.008	0.000	0.000	0.000	0.000	0.000	0.000	0.000	0.000	0.000	0.000	0.000	0.007	0.000	0.000
Punjab (Abohar)	0.000	0.000		0.000	0.004	0.000	0.008	0.000	0.000	0.000	0.000	0.000	0.000	0.000	0.000	0.000	0.000	0.000	0.007	0.000	0.000
Maharashtra (Viman Nagar)	0.000	0.000	0.000		0.004	0.000	0.008	0.000	0.000	0.000	0.000	0.000	0.000	0.000	0.000	0.000	0.000	0.000	0.007	0.000	0.000
Rajasthan (NRC)	0.004	0.004	0.004	0.004		0.004	0.009	0.004	0.004	0.004	0.004	0.004	0.004	0.004	0.004	0.004	0.004	0.004	0.006	0.004	0.004
Tamil Nadu (Murugunagar)	0.000	0.000	0.000	0.000	0.004		0.008	0.000	0.000	0.000	0.000	0.000	0.000	0.000	0.000	0.000	0.000	0.000	0.007	0.000	0.000
Assam (Bokajan)	0.014	0.014	0.014	0.014	0.019	0.014		0.008	0.008	0.008	0.008	0.008	0.008	0.008	0.008	0.008	0.008	0.008	0.011	0.008	0.008
Tamil Nadu (Adyar Gate Extreme Left)	0.000	0.000	0.000	0.000	0.004	0.000	0.014		0.000	0.000	0.000	0.000	0.000	0.000	0.000	0.000	0.000	0.000	0.007	0.000	0.000
Andhra Pradesh (Hydrabad)	0.000	0.000	0.000	0.000	0.004	0.000	0.014	0.000		0.000	0.000	0.000	0.000	0.000	0.000	0.000	0.000	0.000	0.007	0.000	0.000
Bihar (Sheikhpura)	0.000	0.000	0.000	0.000	0.004	0.000	0.014	0.000	0.000		0.000	0.000	0.000	0.000	0.000	0.000	0.000	0.000	0.007	0.000	0.000
Tamil Nadu (Adyar Gate Left)	0.000	0.000	0.000	0.000	0.004	0.000	0.014	0.000	0.000	0.000		0.000	0.000	0.000	0.000	0.000	0.000	0.000	0.007	0.000	0.000
Gujarat (Chandkheda)	0.000	0.000	0.000	0.000	0.004	0.000	0.014	0.000	0.000	0.000	0.000		0.000	0.000	0.000	0.000	0.000	0.000	0.007	0.000	0.000
Jharkand (Palamu)	0.000	0.000	0.000	0.000	0.004	0.000	0.014	0.000	0.000	0.000	0.000	0.000		0.000	0.000	0.000	0.000	0.000	0.007	0.000	0.000
Tamil Nadu (Adyar Gate Right)	0.000	0.000	0.000	0.000	0.004	0.000	0.014	0.000	0.000	0.000	0.000	0.000	0.000		0.000	0.000	0.000	0.000	0.007	0.000	0.000
Himachal Pradesh (Gandhi Nagar)	0.000	0.000	0.000	0.000	0.004	0.000	0.014	0.000	0.000	0.000	0.000	0.000	0.000	0.000		0.000	0.000	0.000	0.007	0.000	0.000
Madhya Pradesh (Bina Junction)	0.000	0.000	0.000	0.000	0.004	0.000	0.014	0.000	0.000	0.000	0.000	0.000	0.000	0.000	0.000		0.000	0.000	0.007	0.000	0.000
Punjab (CUPB)	0.000	0.000	0.000	0.000	0.004	0.000	0.014	0.000	0.000	0.000	0.000	0.000	0.000	0.000	0.000	0.000		0.000	0.007	0.000	0.000
Kerala (Pyannur)	0.000	0.000	0.000	0.000	0.004	0.000	0.014	0.000	0.000	0.000	0.000	0.000	0.000	0.000	0.000	0.000	0.000		0.007	0.000	0.000
Haryana (Palri)	0.013	0.013	0.013	0.013	0.009	0.013	0.029	0.013	0.013	0.013	0.013	0.013	0.013	0.013	0.013	0.013	0.013	0.013		0.007	0.007
Rajasthan (Jhunjhunu)	0.000	0.000	0.000	0.000	0.004	0.000	0.015	0.000	0.000	0.000	0.000	0.000	0.000	0.000	0.000	0.000	0.000	0.000	0.013		0.000
Delhi	0.000	0.000	0.000	0.000	0.004	0.000	0.014	0.000	0.000	0.000	0.000	0.000	0.000	0.000	0.000	0.000	0.000	0.000	0.013	0.000	

Table 22: Pairwise distances between *F. benghalensis* using trnL datasets.

Assam (Bokajan)		0.004	0.000	0.003	0.005	0.003	0.000	0.003	0.005	0.003	0.000	0.003	0.000	0.003	0.005	0.005	0.000	0.003	0.003	0.003	0.003	0.003	0.000
Jharkand (Palamu)	0.004		0.002	0.002	0.002	0.002	0.004	0.002	0.003	0.002	0.003	0.002	0.003	0.002	0.002	0.003	0.005	0.002	0.002	0.002	0.002	0.002	0.002
Rajasthan (Jhunjhunu)	0.000	0.002		0.000	0.002	0.000	0.000	0.000	0.002	0.000	0.002	0.000	0.000	0.000	0.002	0.003	0.004	0.000	0.002	0.000	0.000	0.000	0.000
F. benjamina	0.003	0.005	0.000		0.001	0.000	0.003	0.000	0.003	0.000	0.001	0.000	0.002	0.000	0.001	0.003	0.004	0.000	0.001	0.000	0.000	0.000	0.000
Punjab (CUPB)	0.007	0.003	0.002	0.001		0.001	0.003	0.001	0.002	0.001	0.002	0.001	0.003	0.002	0.000	0.002	0.005	0.001	0.000	0.001	0.001	0.001	0.001
Karnataka (Mysore)	0.003	0.005	0.000	0.000	0.001		0.003	0.000	0.003	0.000	0.001	0.000	0.002	0.000	0.001	0.003	0.004	0.000	0.001	0.000	0.000	0.000	0.000
Tamil Nadu (Adyar Gate Left)	0.000	0.008	0.000	0.004	0.006	0.004		0.003	0.004	0.003	0.003	0.003	0.003	0.000	0.003	0.004	0.005	0.003	0.003	0.003	0.003	0.003	0.003
Andhra Pradesh (Mahbubnagar)	0.003	0.005	0.000	0.000	0.001	0.000	0.004		0.003	0.000	0.001	0.000	0.002	0.000	0.001	0.003	0.004	0.000	0.001	0.000	0.000	0.000	0.000
Punjab (Abohar)	0.007	0.010	0.002	0.007	0.006	0.007	0.012	0.007		0.003	0.003	0.003	0.004	0.002	0.002	0.003	0.005	0.003	0.002	0.003	0.003	0.003	0.003
Kerala (Pyannur)	0.003	0.005	0.000	0.000	0.001	0.000	0.004	0.000	0.007		0.001	0.000	0.002	0.000	0.001	0.003	0.004	0.000	0.001	0.000	0.000	0.000	0.000
Madhya Pradesh (Bina Junction)	0.000	0.003	0.002	0.002	0.003	0.002	0.006	0.002	0.009	0.002		0.001	0.003	0.002	0.002	0.003	0.004	0.001	0.002	0.001	0.001	0.001	0.001
Gujarat (Chandkheda)	0.003	0.005	0.000	0.000	0.001	0.000	0.004	0.000	0.007	0.000	0.002		0.002	0.000	0.001	0.003	0.004	0.000	0.001	0.000	0.000	0.000	0.000
Rajasthan (NRC)	0.000	0.005	0.000	0.003	0.005	0.003	0.005	0.003	0.011	0.003	0.005	0.003		0.000	0.003	0.003	0.006	0.002	0.003	0.002	0.002	0.002	0.002
Maharashtra (Viman Nagar)	0.003	0.002	0.000	0.000	0.002	0.000	0.000	0.000	0.002	0.000	0.002	0.000	0.000		0.002	0.002	0.004	0.000	0.002	0.000	0.000	0.000	0.000
Haryana (Palri)	0.007	0.003	0.002	0.001	0.000	0.001	0.006	0.001	0.006	0.001	0.003	0.001	0.005	0.002		0.002	0.005	0.001	0.000	0.001	0.001	0.001	0.001
Bihar (Sheikhpura)	0.007	0.008	0.004	0.006	0.004	0.006	0.010	0.006	0.010	0.006	0.008	0.006	0.006	0.002	0.004		0.006	0.003	0.002	0.003	0.003	0.003	0.003
Delhi	0.000	0.010	0.006	0.008	0.010	0.008	0.014	0.008	0.014	0.008	0.008	0.008	0.014	0.006	0.010	0.018		0.004	0.005	0.004	0.004	0.004	0.004
Tamil Nadu (Murugunagar)	0.003	0.005	0.000	0.000	0.001	0.000	0.004	0.000	0.007	0.000	0.002	0.000	0.003	0.000	0.001	0.006	0.008		0.001	0.000	0.000	0.000	0.000
Himachal Pradesh (Gandhi Nagar)	0.003	0.003	0.002	0.001	0.000	0.001	0.006	0.001	0.006	0.001	0.003	0.001	0.005	0.002	0.000	0.004	0.010	0.001		0.001	0.001	0.001	0.001
Tamil Nadu (Adyar Gate Extreme Left)	0.003	0.005	0.000	0.000	0.001	0.000	0.004	0.000	0.007	0.000	0.002	0.000	0.003	0.000	0.001	0.006	0.008	0.000	0.001		0.000	0.000	0.000
Jammu (Bantalab)	0.003	0.005	0.000	0.000	0.001	0.000	0.004	0.000	0.007	0.000	0.002	0.000	0.003	0.000	0.001	0.006	0.008	0.000	0.001	0.000		0.000	0.000
Andhra Pradesh (Hydrabad)	0.003	0.005	0.000	0.000	0.001	0.000	0.004	0.000	0.007	0.000	0.002	0.000	0.003	0.000	0.001	0.006	0.008	0.000	0.001	0.000	0.000		0.000
Tamil Nadu (Adyar Gate Right)	0.000	0.005	0.000	0.000	0.001	0.000	0.004	0.000	0.007	0.000	0.002	0.000	0.003	0.000	0.001	0.006	0.008	0.000	0.001	0.000	0.000	0.000	

Table 23: Pairwise distances between *F. benghalensis* using RPS16 datasets.

Delhi		0.006	0.005	0.005	0.005	0.006	0.007	0.005	0.005	0.005	0.003	0.005	0.005	0.006	0.005	0.005	0.005	0.006	0.005	0.005	0.013	0.011
Haryana (Palri)	0.023		0.004	0.004	0.004	0.004	0.003	0.004	0.004	0.005	0.003	0.004	0.004	0.004	0.004	0.006	0.004	0.005	0.005	0.004	0.015	0.012
Gujarat (Chandkheda)	0.022	0.017		0.005	0.005	0.005	0.003	0.005	0.005	0.005	0.002	0.005	0.005	0.005	0.005	0.006	0.005	0.007	0.005	0.005	0.013	0.011
Tamil Nadu (Adyar Gate Extreme Left)	0.021	0.014	0.028		0.000	0.000	0.003	0.004	0.003	0.003	0.002	0.004	0.004	0.004	0.004	0.005	0.004	0.006	0.004	0.004	0.013	0.010
Andhra Pradesh (Hyderabad)	0.024	0.015	0.035	0.000		0.000	0.003	0.004	0.003	0.004	0.002	0.004	0.004	0.004	0.004	0.005	0.004	0.007	0.004	0.004	0.013	0.010
Tamil Nadu (Adyar Gate Right)	0.022	0.014	0.031	0.000	0.000		0.003	0.004	0.003	0.003	0.002	0.004	0.004	0.004	0.004	0.005	0.004	0.006	0.004	0.004	0.013	0.010
Bihar (Sheikhpura)	0.012	0.004	0.004	0.004	0.004	0.004		0.003	0.003	0.004	0.003	0.003	0.003	0.003	0.003	0.003	0.003	0.003	0.006	0.005	0.029	0.032
Jharkand (Palamu)	0.024	0.015	0.033	0.011	0.016	0.014	0.004		0.003	0.001	0.000	0.002	0.002	0.003	0.002	0.003	0.002	0.006	0.004	0.002	0.012	0.010
Tamil Nadu (Adyar Gate Left)	0.020	0.015	0.029	0.005	0.009	0.006	0.004	0.011		0.003	0.000	0.003	0.003	0.004	0.004	0.004	0.004	0.006	0.005	0.004	0.012	0.010
Punjab (CUPB)	0.028	0.017	0.035	0.013	0.016	0.014	0.007	0.003	0.014		0.001	0.002	0.002	0.003	0.002	0.003	0.002	0.006	0.004	0.002	0.012	0.010
Jammu (Bantalab)	0.007	0.005	0.003	0.003	0.003	0.003	0.004	0.000	0.000	0.002		0.000	0.000	0.000	0.002	0.002	0.002	0.002	0.003	0.002	0.015	0.012
Maharashtra (Viman Nagar)	0.025	0.015	0.031	0.014	0.018	0.015	0.004	0.004	0.013	0.005	0.000		0.000	0.002	0.001	0.002	0.001	0.005	0.003	0.002	0.012	0.009
Himachal Pradesh (Gandhi Nagar)	0.024	0.015	0.031	0.014	0.018	0.015	0.004	0.003	0.013	0.005	0.000	0.000		0.002	0.001	0.002	0.001	0.005	0.003	0.002	0.012	0.009
Rajasthan (NRC)	0.029	0.015	0.038	0.011	0.014	0.013	0.004	0.006	0.016	0.008	0.000	0.004	0.004		0.002	0.003	0.002	0.006	0.003	0.003	0.012	0.009
Tamil Nadu (Adyar)	0.021	0.014	0.030	0.013	0.016	0.014	0.004	0.004	0.014	0.006	0.003	0.001	0.001	0.005		0.003	0.000	0.005	0.003	0.001	0.012	0.009
Kerala (Pyannur)	0.029	0.021	0.035	0.018	0.021	0.019	0.004	0.006	0.016	0.009	0.003	0.004	0.004	0.008	0.005		0.003	0.005	0.004	0.003	0.012	0.010
Andhra Pradesh (Mahbubnagar)	0.021	0.014	0.030	0.013	0.016	0.014	0.004	0.004	0.014	0.006	0.003	0.001	0.001	0.005	0.000	0.005		0.005	0.003	0.001	0.012	0.009
Punjab (Abohar)	0.034	0.021	0.047	0.033	0.037	0.034	0.004	0.023	0.033	0.027	0.003	0.020	0.020	0.025	0.019	0.021	0.019		0.006	0.005	0.013	0.012
Assam (Bokajan)	0.028	0.021	0.036	0.017	0.020	0.018	0.015	0.013	0.023	0.014	0.008	0.010	0.010	0.009	0.009	0.014	0.009	0.027		0.003	0.013	0.010
Tamil Nadu (Murugunagar)	0.023	0.015	0.033	0.013	0.018	0.015	0.007	0.005	0.015	0.006	0.003	0.003	0.003	0.006	0.001	0.005	0.001	0.020	0.011		0.012	0.009
Karnataka (Mysore)	0.160	0.181	0.173	0.151	0.155	0.153	0.404	0.147	0.156	0.147	0.181	0.145	0.143	0.141	0.140	0.147	0.140	0.160	0.137	0.143		0.011
Rajasthan (Jhunjhunu)	0.091	0.101	0.103	0.082	0.086	0.083	0.262	0.077	0.089	0.079	0.093	0.075	0.075	0.073	0.073	0.079	0.073	0.093	0.071	0.075	0.092	

Table 24: Pairwise distances between *F. religiosa* using ITS datasets.

Tamil Nadu (Villupuram)		0.000	0.000	0.000	0.003	0.000	0.000	0.000	0.003	0.002	0.003	0.004	0.002	0.000	0.000	0.000	0.000	0.000	0.002	0.000	0.002	0.002	0.002	0.000	0.000	0.003	0.000	0.010	0.010	0.010
Tamil Nadu (Nilgiri)	0.000		0.000	0.000	0.003	0.000	0.000	0.000	0.003	0.002	0.003	0.004	0.002	0.000	0.000	0.000	0.000	0.000	0.002	0.000	0.002	0.002	0.002	0.000	0.000	0.003	0.000	0.010	0.011	0.010
Haryana (Palri)	0.000	0.000		0.000	0.003	0.000	0.000	0.000	0.003	0.002	0.003	0.004	0.002	0.000	0.000	0.000	0.000	0.000	0.002	0.000	0.002	0.002	0.002	0.000	0.000	0.003	0.000	0.010	0.011	0.010
Uttar Pradesh (Noida)	0.000	0.000	0.000		0.003	0.000	0.000	0.000	0.003	0.002	0.003	0.004	0.002	0.000	0.000	0.000	0.000	0.000	0.002	0.000	0.002	0.002	0.002	0.000	0.000	0.003	0.000	0.010	0.010	0.010
Punjab (CUPB)	0.004	0.004	0.004	0.004		0.003	0.003	0.003	0.004	0.002	0.002	0.003	0.004	0.003	0.003	0.003	0.003	0.003	0.002	0.002	0.002	0.002	0.002	0.003	0.003	0.002	0.003	0.010	0.011	0.010
Tamil Nadu (Dharampuri)	0.000	0.000	0.000	0.000	0.004		0.000	0.000	0.002	0.002	0.003	0.004	0.002	0.000	0.000	0.000	0.000	0.000	0.002	0.000	0.002	0.002	0.002	0.000	0.000	0.004	0.000	0.010	0.010	0.010
Tamil Nadu (Murugunagar)	0.000	0.000	0.000	0.000	0.004	0.000		0.000	0.003	0.002	0.003	0.004	0.002	0.000	0.000	0.000	0.000	0.000	0.002	0.000	0.002	0.002	0.002	0.000	0.000	0.003	0.000	0.010	0.010	0.010
Punjab (Abohar)	0.000	0.000	0.000	0.000	0.004	0.000	0.000		0.003	0.002	0.003	0.004	0.002	0.000	0.000	0.000	0.000	0.000	0.002	0.000	0.002	0.002	0.002	0.000	0.000	0.004	0.000	0.011	0.011	0.010
Orissa (keonjhar)	0.007	0.007	0.007	0.007	0.011	0.002	0.007	0.008		0.004	0.005	0.005	0.004	0.003	0.003	0.003	0.003	0.003	0.004	0.003	0.004	0.004	0.004	0.003	0.003	0.005	0.004	0.011	0.011	0.010
Rajasthan (Jhunjhunu)	0.002	0.002	0.002	0.002	0.002	0.002	0.002	0.002	0.009		0.002	0.003	0.003	0.002	0.002	0.002	0.002	0.002	0.000	0.000	0.000	0.000	0.000	0.002	0.002	0.002	0.002	0.010	0.010	0.010
Delhi	0.006	0.006	0.006	0.006	0.002	0.006	0.006	0.006	0.013	0.004		0.003	0.004	0.003	0.003	0.003	0.003	0.003	0.002	0.002	0.002	0.002	0.002	0.003	0.003	0.002	0.004	0.011	0.011	0.010
Jammu (Miran Sahib)	0.009	0.009	0.009	0.009	0.006	0.010	0.009	0.010	0.017	0.007	0.004		0.004	0.004	0.004	0.004	0.004	0.004	0.003	0.003	0.003	0.003	0.003	0.004	0.004	0.003	0.004	0.011	0.011	0.010
Tamil Nadu (Kanyakumari)	0.004	0.004	0.004	0.004	0.007	0.004	0.004	0.004	0.011	0.006	0.009	0.013		0.002	0.002	0.002	0.002	0.002	0.003	0.002	0.003	0.003	0.003	0.002	0.002	0.004	0.003	0.011	0.011	0.010
Rajasthan (NRC)	0.000	0.000	0.000	0.000	0.004	0.000	0.000	0.000	0.007	0.002	0.006	0.009	0.004		0.000	0.000	0.000	0.000	0.002	0.000	0.002	0.002	0.002	0.000	0.000	0.003	0.000	0.010	0.010	0.010
Kerala (Payannur)	0.000	0.000	0.000	0.000	0.004	0.000	0.000	0.000	0.007	0.002	0.006	0.009	0.004	0.000		0.000	0.000	0.000	0.002	0.000	0.002	0.002	0.002	0.000	0.000	0.003	0.000	0.010	0.010	0.010
Maharashtra (Viman Nagar)	0.000	0.000	0.000	0.000	0.004	0.000	0.000	0.000	0.007	0.002	0.006	0.009	0.004	0.000	0.000		0.000	0.000	0.002	0.000	0.002	0.002	0.002	0.000	0.000	0.003	0.000	0.010	0.010	0.010
Chandigarh-17	0.000	0.000	0.000	0.000	0.004	0.000	0.000	0.000	0.007	0.002	0.006	0.009	0.004	0.000	0.000	0.000		0.000	0.002	0.000	0.002	0.002	0.002	0.000	0.000	0.003	0.000	0.010	0.010	0.010
Tamil Nadu (Thiruvannamalai)	0.000	0.000	0.000	0.000	0.004	0.000	0.000	0.000	0.007	0.002	0.006	0.009	0.004	0.000	0.000	0.000	0.000		0.002	0.000	0.002	0.002	0.002	0.000	0.000	0.003	0.000	0.010	0.010	0.010
Madhya Pradesh (Bina Junction)	0.002	0.002	0.002	0.002	0.002	0.002	0.002	0.002	0.009	0.000	0.004	0.007	0.006	0.002	0.002	0.002	0.002	0.002		0.000	0.000	0.000	0.000	0.002	0.002	0.002	0.002	0.010	0.011	0.010
Andaman and Nicobar Island (Port Blair)	0.000	0.000	0.000	0.000	0.002	0.000	0.000	0.000	0.007	0.000	0.004	0.007	0.004	0.000	0.000	0.000	0.000	0.000	0.000		0.000	0.000	0.000	0.000	0.000	0.002	0.000	0.010	0.010	0.010
Jharkand (Palamu)	0.002	0.002	0.002	0.002	0.002	0.002	0.002	0.002	0.009	0.000	0.004	0.007	0.006	0.002	0.002	0.002	0.002	0.002	0.000	0.000		0.000	0.000	0.002	0.002	0.002	0.002	0.010	0.011	0.010
Tamil Nadu (Namakkal)	0.002	0.002	0.002	0.002	0.002	0.002	0.002	0.002	0.009	0.000	0.004	0.007	0.006	0.002	0.002	0.002	0.002	0.002	0.000	0.000	0.000		0.000	0.002	0.002	0.002	0.002	0.010	0.011	0.010
Karnataka (Mysore)	0.002	0.002	0.002	0.002	0.002	0.002	0.002	0.002	0.009	0.000	0.004	0.007	0.006	0.002	0.002	0.002	0.002	0.002	0.000	0.000	0.000	0.000		0.002	0.002	0.002	0.002	0.010	0.011	0.010
Punjab (CUPB-Wavy)	0.000	0.000	0.000	0.000	0.004	0.000	0.000	0.000	0.007	0.002	0.006	0.009	0.004	0.000	0.000	0.000	0.000	0.000	0.002	0.000	0.002	0.002	0.002		0.000	0.003	0.000	0.010	0.010	0.010
Bihar (Sheikhpura)	0.000	0.000	0.000	0.000	0.004	0.000	0.000	0.000	0.007	0.002	0.006	0.009	0.004	0.000	0.000	0.000	0.000	0.000	0.002	0.000	0.002	0.002	0.002	0.000		0.003	0.000	0.010	0.010	0.010
Uttar Pradesh (Bulandshahr)	0.006	0.006	0.006	0.006	0.002	0.006	0.006	0.006	0.013	0.004	0.002	0.006	0.009	0.006	0.006	0.006	0.006	0.006	0.004	0.004	0.004	0.004	0.004	0.006	0.006		0.003	0.010	0.011	0.010
Andhra Pradesh (Mahbubnagar)	0.000	0.000	0.000	0.000	0.004	0.000	0.000	0.000	0.007	0.002	0.007	0.011	0.004	0.000	0.000	0.000	0.000	0.000	0.002	0.000	0.002	0.002	0.002	0.000	0.000	0.004		0.011	0.011	0.010
Assam	0.065	0.065	0.063	0.065	0.068	0.060	0.065	0.067	0.068	0.065	0.070	0.074	0.068	0.065	0.065	0.065	0.065	0.065	0.066	0.065	0.067	0.066	0.066	0.065	0.065	0.067	0.057		0.003	0.002
Andaman and Nicobar Island (Nicobar)	0.061	0.062	0.059	0.061	0.065	0.057	0.061	0.063	0.065	0.061	0.067	0.070	0.065	0.061	0.061	0.061	0.061	0.061	0.063	0.061	0.063	0.063	0.063	0.061	0.061	0.063	0.057	0.004		0.003
Andaman and Ncobar Island (Havelock)	0.063	0.063	0.061	0.063	0.066	0.058	0.063	0.065	0.067	0.063	0.068	0.072	0.066	0.063	0.063	0.063	0.063	0.063	0.065	0.063	0.065	0.065	0.065	0.063	0.063	0.065	0.055	0.002	0.006	

Table 25: Pairwise distances between *F. religiosa* using trnL datasets.

Gujrat (Chandkheda)		0.000	0.004	0.004	0.004	0.004	0.000	0.004	0.004	0.004	0.004	0.004	0.004	0.004	0.004	0.004	0.004	0.004	0.005	0.005	0.004	0.004	0.004	0.004	0.000	0.004	0.004
Andaman and Nicobar Island (Nicobar)	0.000		0.004	0.004	0.004	0.004	0.000	0.004	0.004	0.004	0.004	0.004	0.004	0.004	0.004	0.004	0.004	0.004	0.005	0.005	0.004	0.004	0.004	0.004	0.000	0.004	0.004
Kerala (Payannur)	0.010	0.010		0.000	0.000	0.000	0.005	0.000	0.000	0.000	0.000	0.000	0.000	0.000	0.000	0.000	0.000	0.000	0.003	0.003	0.000	0.000	0.000	0.000	0.004	0.000	0.000
Tamil Nadu (Villupuram)	0.009	0.009	0.000		0.000	0.000	0.004	0.000	0.000	0.000	0.000	0.000	0.000	0.000	0.000	0.000	0.000	0.000	0.003	0.003	0.000	0.000	0.000	0.000	0.004	0.000	0.000
Delhi	0.009	0.009	0.000	0.000		0.000	0.004	0.000	0.000	0.000	0.000	0.000	0.000	0.000	0.000	0.000	0.000	0.000	0.003	0.003	0.000	0.000	0.000	0.000	0.004	0.000	0.000
Orissa (keonjhar)	0.009	0.009	0.000	0.000	0.000		0.004	0.000	0.000	0.000	0.000	0.000	0.000	0.000	0.000	0.000	0.000	0.000	0.003	0.003	0.000	0.000	0.000	0.000	0.004	0.000	0.000
Assam (Bokajan)	0.000	0.000	0.011	0.010	0.010	0.010		0.004	0.004	0.004	0.004	0.004	0.004	0.004	0.004	0.004	0.004	0.004	0.005	0.005	0.004	0.004	0.004	0.004	0.000	0.004	0.004
Karnataka (Mysore)	0.009	0.009	0.000	0.000	0.000	0.000	0.010		0.000	0.000	0.000	0.000	0.000	0.000	0.000	0.000	0.000	0.000	0.003	0.003	0.000	0.000	0.000	0.000	0.004	0.000	0.000
Bihar (Sheikhpura)	0.009	0.009	0.000	0.000	0.000	0.000	0.010	0.000		0.000	0.000	0.000	0.000	0.000	0.000	0.000	0.000	0.000	0.003	0.003	0.000	0.000	0.000	0.000	0.004	0.000	0.000
Himachal Pradesh (Gandhi Nagar)	0.009	0.009	0.000	0.000	0.000	0.000	0.010	0.000	0.000		0.000	0.000	0.000	0.000	0.000	0.000	0.000	0.000	0.003	0.003	0.000	0.000	0.000	0.000	0.004	0.000	0.000
Jammu (Miran Sahib)	0.009	0.009	0.000	0.000	0.000	0.000	0.010	0.000	0.000	0.000		0.000	0.000	0.000	0.000	0.000	0.000	0.000	0.003	0.003	0.000	0.000	0.000	0.000	0.004	0.000	0.000
Haryana (Palri)	0.009	0.009	0.000	0.000	0.000	0.000	0.010	0.000	0.000	0.000	0.000		0.000	0.000	0.000	0.000	0.000	0.000	0.003	0.003	0.000	0.000	0.000	0.000	0.004	0.000	0.000
Rajasthan (NRC)	0.009	0.009	0.000	0.000	0.000	0.000	0.010	0.000	0.000	0.000	0.000	0.000		0.000	0.000	0.000	0.000	0.000	0.003	0.003	0.000	0.000	0.000	0.000	0.004	0.000	0.000
Andaman and Nicobar Island (Port Blair)	0.009	0.009	0.000	0.000	0.000	0.000	0.010	0.000	0.000	0.000	0.000	0.000	0.000		0.000	0.000	0.000	0.000	0.003	0.003	0.000	0.000	0.000	0.000	0.004	0.000	0.000
Maharashtra (Viman Nagar)	0.009	0.009	0.000	0.000	0.000	0.000	0.010	0.000	0.000	0.000	0.000	0.000	0.000	0.000		0.000	0.000	0.000	0.003	0.003	0.000	0.000	0.000	0.000	0.004	0.000	0.000
Chandigarh-17	0.009	0.009	0.000	0.000	0.000	0.000	0.010	0.000	0.000	0.000	0.000	0.000	0.000	0.000	0.000		0.000	0.000	0.003	0.003	0.000	0.000	0.000	0.000	0.004	0.000	0.000
Punjab (Abohar)	0.009	0.009	0.000	0.000	0.000	0.000	0.010	0.000	0.000	0.000	0.000	0.000	0.000	0.000	0.000	0.000		0.003	0.003	0.003	0.000	0.000	0.000	0.000	0.004	0.000	0.000
Tamil Nadu (Kanyakumari)	0.011	0.011	0.003	0.003	0.003	0.003	0.013	0.003	0.003	0.003	0.003	0.003	0.003	0.003	0.003	0.003	0.003		0.000	0.003	0.003	0.003	0.003	0.005	0.003	0.003
Tamil Nadu (Nilgiri)	0.011	0.011	0.003	0.003	0.003	0.003	0.013	0.003	0.003	0.003	0.003	0.003	0.003	0.003	0.003	0.003	0.003	0.000		0.003	0.003	0.003	0.003	0.005	0.003	0.003
Tamil Nadu (Nammakkal)	0.009	0.009	0.000	0.000	0.000	0.000	0.010	0.000	0.000	0.000	0.000	0.000	0.000	0.000	0.000	0.000	0.000	0.003	0.003		0.000	0.000	0.000	0.004	0.000	0.000
Uttar Pradesh (Bulandshahr)	0.009	0.009	0.000	0.000	0.000	0.000	0.010	0.000	0.000	0.000	0.000	0.000	0.000	0.000	0.000	0.000	0.000	0.003	0.003	0.000		0.000	0.000	0.004	0.000	0.000
Uttar Pradesh (Noida)	0.009	0.009	0.000	0.000	0.000	0.000	0.010	0.000	0.000	0.000	0.000	0.000	0.000	0.000	0.000	0.000	0.000	0.003	0.003	0.000	0.000		0.000	0.004	0.000	0.000
Jharkhand (Palamu)	0.009	0.009	0.000	0.000	0.000	0.000	0.010	0.000	0.000	0.000	0.000	0.000	0.000	0.000	0.000	0.000	0.000	0.003	0.003	0.000	0.000	0.000		0.004	0.000	0.000
Andaman and Nicobar Island (Havelock)	0.000	0.000	0.010	0.009	0.009	0.009	0.000	0.009	0.009	0.009	0.009	0.009	0.009	0.009	0.009	0.009	0.009	0.011	0.011	0.009	0.009	0.009	0.009		0.004	0.004
Tamil Nadu (Thiruvannamalai)	0.009	0.009	0.000	0.000	0.000	0.000	0.010	0.000	0.000	0.000	0.000	0.000	0.000	0.000	0.000	0.000	0.000	0.003	0.003	0.000	0.000	0.000	0.000	0.009		0.000
Punjab (CUPB)	0.009	0.009	0.000	0.000	0.000	0.000	0.010	0.000	0.000	0.000	0.000	0.000	0.000	0.000	0.000	0.000	0.000	0.003	0.003	0.000	0.000	0.000	0.000	0.009	0.000	

Table 26: Pairwise distances between *F. religiosa* using RPS16 datasets.

Punjab (Wavy CUPB)		0.000	0.000	0.000	0.000	0.002	0.000	0.000	0.002	0.000	0.000	0.002	0.000	0.000	0.000	0.000	0.000	0.002	0.000	0.000	0.000	0.000	0.000	0.000	0.000	0.000	0.000
Chandigarh-17	0.000		0.000	0.000	0.000	0.002	0.000	0.000	0.002	0.000	0.000	0.002	0.000	0.000	0.000	0.000	0.000	0.002	0.000	0.000	0.000	0.000	0.000	0.000	0.000	0.000	0.000
Karnataka (Mysore)	0.000	0.000		0.000	0.000	0.002	0.000	0.000	0.002	0.000	0.000	0.002	0.000	0.000	0.000	0.000	0.000	0.002	0.000	0.000	0.000	0.000	0.000	0.000	0.000	0.000	0.000
Orissa (Keonjhar)	0.000	0.000	0.000		0.000	0.002	0.000	0.000	0.002	0.000	0.000	0.002	0.000	0.000	0.000	0.000	0.000	0.002	0.000	0.000	0.000	0.000	0.000	0.000	0.000	0.000	0.000
Tamil Nadu (Villupuram)	0.000	0.000	0.000	0.000		0.002	0.000	0.000	0.002	0.000	0.000	0.002	0.000	0.000	0.000	0.000	0.000	0.002	0.000	0.000	0.000	0.000	0.000	0.000	0.000	0.000	0.000
Assam (Bokajan)	0.003	0.003	0.003	0.003	0.003		0.002	0.002	0.000	0.002	0.002	0.000	0.002	0.002	0.002	0.002	0.002	0.000	0.002	0.002	0.002	0.002	0.002	0.002	0.002	0.003	0.002
Jammu (Bantalab)	0.000	0.000	0.000	0.000	0.000	0.003		0.000	0.002	0.000	0.000	0.002	0.000	0.000	0.000	0.000	0.000	0.002	0.000	0.000	0.000	0.000	0.000	0.000	0.000	0.000	0.000
Bihar (Sheikhpura)	0.000	0.000	0.000	0.000	0.000	0.003	0.000		0.002	0.000	0.000	0.002	0.000	0.000	0.000	0.000	0.000	0.002	0.000	0.000	0.000	0.000	0.000	0.000	0.000	0.000	0.000
Andaman and Nicobar Island (Havelock)	0.003	0.003	0.003	0.003	0.003	0.000	0.003	0.003		0.002	0.002	0.000	0.002	0.002	0.002	0.002	0.002	0.000	0.002	0.002	0.002	0.002	0.002	0.002	0.002	0.002	0.002
Andaman and Nicobar Island (Port Blair)	0.000	0.000	0.000	0.000	0.000	0.003	0.000	0.000	0.003		0.000	0.002	0.000	0.000	0.000	0.000	0.000	0.002	0.000	0.000	0.000	0.000	0.000	0.000	0.000	0.000	0.000
Rajasthan (Jhunjhunu)	0.000	0.000	0.000	0.000	0.000	0.003	0.000	0.000	0.003	0.000		0.002	0.000	0.000	0.000	0.000	0.000	0.002	0.000	0.000	0.000	0.000	0.000	0.000	0.000	0.000	0.000
Gujrat (Chandkheda)	0.003	0.003	0.003	0.003	0.003	0.000	0.003	0.003	0.000	0.003	0.003		0.002	0.002	0.002	0.002	0.002	0.000	0.002	0.002	0.002	0.002	0.002	0.002	0.002	0.002	0.002
Haryana (Palri)	0.000	0.000	0.000	0.000	0.000	0.003	0.000	0.000	0.003	0.000	0.000	0.003		0.000	0.000	0.000	0.000	0.002	0.000	0.000	0.000	0.000	0.000	0.000	0.000	0.000	0.000
Tamil Nadu (Nammakkal)	0.000	0.000	0.000	0.000	0.000	0.003	0.000	0.000	0.003	0.000	0.000	0.003	0.000		0.000	0.000	0.000	0.002	0.000	0.000	0.000	0.000	0.000	0.000	0.000	0.000	0.000
Delhi	0.000	0.000	0.000	0.000	0.000	0.003	0.000	0.000	0.003	0.000	0.000	0.003	0.000	0.000		0.000	0.000	0.002	0.000	0.000	0.000	0.000	0.000	0.000	0.000	0.000	0.000
Madhya Pradesh (Bina Junction)	0.000	0.000	0.000	0.000	0.000	0.003	0.000	0.000	0.003	0.000	0.000	0.003	0.000	0.000	0.000		0.000	0.002	0.000	0.000	0.000	0.000	0.000	0.000	0.000	0.000	0.000
Uttar Pradesh (Bulandshahr)	0.000	0.000	0.000	0.000	0.000	0.003	0.000	0.000	0.003	0.000	0.000	0.003	0.000	0.000	0.000	0.000		0.002	0.000	0.000	0.000	0.000	0.000	0.000	0.000	0.000	0.000
Andaman and Nicobar Island (Nicobar))	0.003	0.003	0.003	0.003	0.003	0.000	0.003	0.003	0.000	0.003	0.003	0.000	0.003	0.003	0.003	0.003	0.003		0.002	0.002	0.002	0.002	0.002	0.002	0.002	0.002	0.002
Rajasthan (NRC)	0.000	0.000	0.000	0.000	0.000	0.003	0.000	0.000	0.003	0.000	0.000	0.003	0.000	0.000	0.000	0.000	0.000	0.003		0.000	0.000	0.000	0.000	0.000	0.000	0.000	0.000
Tamil Nadu (Murugunagar)	0.000	0.000	0.000	0.000	0.000	0.003	0.000	0.000	0.003	0.000	0.000	0.003	0.000	0.000	0.000	0.000	0.000	0.003	0.000		0.000	0.000	0.000	0.000	0.000	0.000	0.000
Himachal Pradesh (Gandhi Nagar)	0.000	0.000	0.000	0.000	0.000	0.003	0.000	0.000	0.003	0.000	0.000	0.003	0.000	0.000	0.000	0.000	0.000	0.003	0.000	0.000		0.000	0.000	0.000	0.000	0.000	0.000
Maharashtra (Viman Nagar)	0.000	0.000	0.000	0.000	0.000	0.003	0.000	0.000	0.003	0.000	0.000	0.003	0.000	0.000	0.000	0.000	0.000	0.003	0.000	0.000	0.000		0.000	0.000	0.000	0.000	0.000
Tamil Nadu (Nilgiri)	0.000	0.000	0.000	0.000	0.000	0.003	0.000	0.000	0.003	0.000	0.000	0.003	0.000	0.000	0.000	0.000	0.000	0.003	0.000	0.000	0.000	0.000		0.000	0.000	0.000	0.000
Uttar Pradesh (Noida)	0.000	0.000	0.000	0.000	0.000	0.003	0.000	0.000	0.003	0.000	0.000	0.003	0.000	0.000	0.000	0.000	0.000	0.003	0.000	0.000	0.000	0.000	0.000		0.000	0.000	0.000
Punjab (Abohar)	0.000	0.000	0.000	0.000	0.000	0.003	0.000	0.000	0.003	0.000	0.000	0.003	0.000	0.000	0.000	0.000	0.000	0.003	0.000	0.000	0.000	0.000	0.000	0.000		0.000	0.000
Tamil Nadu (Dharampuri)	0.000	0.000	0.000	0.000	0.000	0.003	0.000	0.000	0.003	0.000	0.000	0.003	0.000	0.000	0.000	0.000	0.000	0.003	0.000	0.000	0.000	0.000	0.000	0.000	0.000		0.000
Jharkand (Palamu)	0.000	0.000	0.000	0.000	0.000	0.003	0.000	0.000	0.003	0.000	0.000	0.003	0.000	0.000	0.000	0.000	0.000	0.003	0.000	0.000	0.000	0.000	0.000	0.000	0.000	0.000	


Sect. Adenosperma
Sect. Rhizocladus
Sect. Eriosycea
Sect. Sycidium
Sect. Ficus
Sect. Urostigma
Sect. Oreosycea
Sect. Neomorphe/ Adenosperma
Sect. Sycomorus
Sect. Sycocarpus
Sect. Pharmacosycea
Sect. Malvanthera
Sect. Conosycea
Sect. Galoglychia
Sect. Americana
Sect. Galoglychia
0.2